

Description of $e^-e^+ \rightarrow \gamma\gamma, Z\gamma, ZZ$ in SM and MSSM[†]

G.J. Gounaris^a, J. Layssac^b and F.M. Renard^b

^aDepartment of Theoretical Physics, Aristotle University of Thessaloniki,
Gr-54124, Thessaloniki, Greece.

^bPhysique Mathématique et Théorique, UMR 5825
Université Montpellier II, F-34095 Montpellier Cedex 5.

Abstract

We present a complete analysis of the one loop electroweak corrections to $e^-e^+ \rightarrow \gamma\gamma, Z\gamma, ZZ$ in the Standard (SM) and the Minimal Supersymmetric Standard Model (MSSM). Analytic expressions are written for the contributions to the helicity amplitudes. Several observables accessible for polarized or unpolarized beams and transverse, longitudinal or unpolarized final states are computed. We show that in the few hundred GeV region, these observables provide a test of the various SM or MSSM components. For the dominant TT amplitude at high energy, the sensitivity to the details of the various sectors disappears, but the energy dependence fixed by leading logarithmic contributions, provides a model independent signature discriminating SM from MSSM. Subdominant TL or LL amplitudes though, remain sensitive to the details of the SM or MSSM sectors. Numerical illustrations are given for energies up to several TeV. The analysis may also be used to search for new physics characterized by anomalously strong interactions among the neutral gauge bosons.

PACS 12.15.-y, 12.15.Lk, 14.70.-e

[†]Programme d'Actions Intégrées Franco-Hellenique, Platon 04100 UM

1 Introduction

The search for new physics (NP) beyond the Standard Model (SM) has strongly motivated projects of high energy e^-e^+ colliders (LC, CLIC) [1, 2]. This NP search should proceed either in a direct way (production of new particles), or in an indirect way (observation of departures from SM predictions in processes where the external particles are standard, and NP effects only arise from virtual exchanges).

In this paper we are addressing the indirect way. The experimental accuracy that should be available at the high luminosity e^-e^+ machines is expected to be very high; better than the percent level. This means that the SM predictions, from which departures will be searched, should be made with a comparable high accuracy, requiring computations of high order effects of electroweak interactions.

One already knows that the electroweak radiative corrections to several standard processes strongly increase with the energy. This arises due to the presence already at the 1-loop level, of large double (DL) and single (SL) logarithm terms behaving like¹ $(\alpha/\pi) \ln^2 s$, $(\alpha/\pi) \ln s$, [4, 5, 6, 7]. In the TeV range such terms reach the several percent level, which renders them observable at the future colliders. Alternatively, these large logarithmic effects may also be viewed as large background contributions to possible NP signals. It will therefore be essential to have a full control on them, and to analyse precisely the various virtual contributions they get from each dynamical sector.

The relevance of these large logarithmic effects at high energy colliders, has been stressed recently for the process $e^+e^- \rightarrow f\bar{f}$ in the SM [6] and MSSM [8] cases, and for the process $e^+e^- \rightarrow \tilde{f}\tilde{f}^*$ [9]. As these 1-loop effects are known to reach the 10% level at the multi-TeV range, the need for a two loop computation and even a resummation of the higher order leading effects arises; attempts in this direction have already started [9, 10].

A very important property of these large logarithms is that they offer a striking signature for studying the underlying dynamics [11]. Depending on the interaction sector (gauge, Yukawa) from which they originate, these large logarithmic terms may be isotropic and universal with well defined relative coefficients, or they may present very specific angular dependencies [11]. This has allowed a classification of all such log-terms and their possible physical origins [11]. In particular, the logarithmic behaviour of the $e^-e^+ \rightarrow f\bar{f}$, $\tilde{f}\tilde{f}^*$ cross sections at high energy reflects in an observable way the gauge and Higgs structures of the interactions, and even differentiates between SM and MSSM, in a way which is largely independent of the specific values of the MSSM parameters [12].

Similar properties for the leading logarithmic SM and MSSM contributions at high energies are also expected in $\gamma\gamma \rightarrow f\bar{f}$ [13], which should be measurable at photon-photon colliders [14].

The inverse process $e^+e^- \rightarrow \gamma\gamma$ and well as the neutral gauge boson production ones $e^+e^- \rightarrow \gamma Z$, ZZ have been calculated in SM a long time ago [15], and received recently considerable theoretical [16, 17] and experimental [18] interest motivated by the search for

¹In process like $\gamma\gamma \rightarrow \gamma\gamma$, $Z\gamma$, ZZ , which do not contain any Born contribution, only single logarithm terms caused by the imaginary part of DL contributions remain; the rest is canceled [3].

anomalous neutral gauge boson self couplings (NAGC). At tree level, there is no NAGC coupling among three neutral gauge bosons (γ or Z) in SM or MSSM; *i.e.* no contribution of the type $e^+e^- \rightarrow (\gamma, Z) \rightarrow \gamma Z, ZZ$; (real $\gamma\gamma$ final states are forbidden).

Non vanishing NAGC couplings first arise at one loop, through fermionic triangles involving leptons and quarks in SM, and additional chargino and neutralino triangles in MSSM [17]. Additional contributions may also come from NP forms containing *e.g.* heavier fermions, non perturbative structures, or even direct neutral boson couplings. Since such NP effects may be rather small, a complete and accurate computation of the high order SM and MSSM contributions is needed, in order to identify them.

The aim of this paper is to discuss these various points. Thus, we analyze the content of the complete 1-loop contributions to the $e^+e^- \rightarrow \gamma\gamma, \gamma Z, ZZ$ amplitudes, firstly within SM, and secondly within the MSSM. Since the exact 1-loop formulae are rather complicated, the study of the high energy behaviour of the amplitudes, helps supplying a clear intuitive picture. We therefore study in detail the relative importance of each type of asymptotic and non asymptotic contributions (double log (DL), single log (SL), angular independent and angular dependent terms) in the gauge, Higgs and particle and sparticle sectors, indicating how these sectors conspire, to produce the correct high energy behaviour. This should also be instructive for the discussion of possible modifications due to NP.

As in the fermion and sfermion production cases mentioned above [6, 8, 9], the numerical value of the SL coefficient may serve as signature discriminating between SM and MSSM, in way which is largely independent of the specific values of the MSSM parameters. In other words, the dependence on the specific values of the MSSM parameters largely disappears, once the MSSM thresholds are overpassed². These discussions are done in parallel for the three neutral processes $e^+e^- \rightarrow \gamma\gamma, \gamma Z, ZZ$. Many numerical illustrations are also given. An asymptotic energy treatment for the SM case of such amplitudes has also recently appeared in [7]; we have checked that our results agree with those of this reference.

We then concentrate on the role of the NAGC couplings in $e^+e^- \rightarrow \gamma Z, ZZ$ and compare their effect to the one of the other sectors of electroweak corrections, as well as to possible new additional NP contributions.

Finally, we discuss the role of longitudinal Z_L production. The production of this state is strongly depressed at the high energy. Moreover, for $Z_L Z_L$ production above 1TeV, the Born contribution is found to be negligible compared to the 1-loop one. Such effects render the above processes very sensitive to virtual contributions and provide interesting checks of possible anomalous NP contribution arising, for example, from a strongly interacting Higgs sector. We make this study at various energies, showing the road to asymptopia, from the LEP2 energy range to the LC and to the CLIC one.

The paper is organized as follows. Section 2 contains the kinematics for the three considered processes. The one loop electroweak contributions to the amplitudes are written in

²Only a dependence in the overall MSSM scale may remain in some cases.

Section 3; renormalized Born, triangle and box contributions. Section 4 is devoted to the asymptotic properties. Numerical applications are given in Section 5, while the physics issues and conclusions are presented in Section 6. Useful technical details are given in several Appendices; details on kinematics in Appendix A; the chargino and neutralino mixing matrices in Appendix B; the gauge and electron self-energies and renormalization constants in Appendix C; details of triangle contributions in Appendix D; asymptotic self-energy and triangle contributions in Appendix E and Box ones in Appendix F.

2 Kinematics and Observable quantities

We consider the process

$$e^-(\lambda, l) + e^+(\lambda', l') \rightarrow V(e, p) + V'(e', p') \quad , \quad (1)$$

where (l, l') are the incoming electron and positron momenta, and (λ, λ') their corresponding helicities. Since the electron mass is throughout neglected, we have $\lambda' = -\lambda = \pm 1/2$.

Correspondingly, V and V' denote the outgoing neutral gauge bosons Z or γ , whose momenta are described as (p, p') respectively, while (e, e') denote the complex conjugate of their polarization vectors and (μ, μ') the corresponding helicities. We also define

$$\begin{aligned} q &= l - p = p' - l' \quad , \quad q' = l - p' = p - l' \\ s &= (l + l')^2 = (p + p')^2 \quad , \quad t = q^2 \quad , \quad u = q'^2 \quad . \end{aligned}$$

The c.m. scattering angle between \vec{l} and \vec{p} is denoted by θ . The helicity amplitude of the above process (1) is written as

$$\begin{aligned} F_{\lambda, \mu, \mu'} &\equiv F[e^-(\lambda, l) e^+(\lambda' = -\lambda, l') \rightarrow V(e(\mu), p) V'(e'(\mu'), p')] \\ &= \sum_{j=1,9} \bar{v}(\lambda', l') I_j N_j(s, t, u, \lambda) u(\lambda, l) \quad , \end{aligned} \quad (2)$$

in terms of nine Lorentz invariant forms I_j , ($j = 1, 9$) defined in Appendix A. Their coefficients may then be split, according to the electron-helicity, as

$$N_j(s, t, u, \lambda) \equiv N_j^L(s, t, u) P_L + N_j^R(s, t, u) P_R \quad , \quad (3)$$

where

$$P_L = \frac{1}{2} - \lambda \quad , \quad P_R = \frac{1}{2} + \lambda \quad , \quad (4)$$

while $N_j^{L,R}(s, t, u)$ are scalar functions.

Observables

The polarized angular distribution is obtained in terms of the helicity amplitudes as:

$$\frac{d\sigma(\lambda, \mu, \mu')}{d \cos \theta} = \frac{\beta}{32\pi s} C_{stat} |F_{\lambda, \mu, \mu'}|^2 \quad , \quad (5)$$

with $C_{stat} = 1/2, 1/2, 1$ for $\gamma\gamma, ZZ, \gamma Z$, respectively. The corresponding integrated cross sections are

$$\sigma(\lambda, \mu, \mu') = \int_{-c}^c d\cos\theta \frac{d\sigma(\lambda, \mu, \mu')}{d\cos\theta} , \quad (6)$$

where $c \equiv \cos\theta_{min}$ is an angular cut (fixed at $\theta_{min} = 30^\circ$ in the numerical applications).

The cross section for unpolarized e^\pm beams is

$$\sigma(\mu, \mu')_{\text{unp}} = \frac{1}{4} \sum_{\lambda=\pm 1/2} \sigma(\lambda, \mu, \mu') , \quad (7)$$

while we refer to final transverse (T) or longitudinal (L) gauge bosons by taking $\mu = \pm 1, (\mu' = \pm 1)$ or $\mu = 0, (\mu' = 0)$, respectively.

For longitudinally polarized e^\pm beams, the Left-Right polarization asymmetry is defined as:

$$A_{LR}(\mu, \mu') = \frac{\sigma(-\frac{1}{2}, \mu, \mu') - \sigma(+\frac{1}{2}, \mu, \mu')}{\sigma(-\frac{1}{2}, \mu, \mu') + \sigma(+\frac{1}{2}, \mu, \mu')} . \quad (8)$$

In the numerical examples below, we only consider the Left-Right asymmetry A_{LR} , where all possible final gauge boson polarizations are summed over.

3 The Born and 1-loop Amplitudes

3.1 The Born terms

These are due to electron exchange in the t and u channels. In terms of the invariant functions defined in (3) and in Appendix A, they are written as

$$N_j^{\text{Born}} = N_j^{\text{Born, t}} + N_j^{\text{Born, u}} , \quad (9)$$

which give:

- $e^-e^+ \rightarrow \gamma\gamma$.

$$\begin{aligned} N_1^{\text{Born, t}} = N_2^{\text{Born, t}} = N_4^{\text{Born, t}} &= -\frac{e_L^2}{t}P_L - \frac{e_R^2}{t}P_R , \\ N_1^{\text{Born, u}} = N_2^{\text{Born, u}} = -N_4^{\text{Born, u}} &= -\frac{e_L^2}{u}P_L - \frac{e_R^2}{u}P_R , \end{aligned} \quad (10)$$

with

$$e_L = e_R = -e ; \quad (11)$$

- $e^-e^+ \rightarrow ZZ$.

$$N_1^{\text{Born, t}} = N_2^{\text{Born, t}} = N_4^{\text{Born, t}} = -\frac{s}{t - m_Z^2} N_5^{\text{Born, t}} = -\frac{s}{2} N_6^{\text{Born, t}}$$

$$\begin{aligned}
&= -\frac{s}{s-t+m_Z^2} N_7^{\text{Born, t}} = \frac{s}{2} N_8^{\text{Born, t}} = -\frac{g_{ZL}^2}{t} - \frac{g_{ZR}^2}{t}, \\
N_1^{\text{Born, u}} &= N_2^{\text{Born, u}} = -N_4^{\text{Born, u}} = \frac{-s}{s-u+m_Z^2} N_5^{\text{Born, u}} \\
&= \frac{-s}{2} N_6^{\text{Born, u}} = \frac{-s}{u-m_Z^2} N_7^{\text{Born, u}} = \frac{s}{2} N_8^{\text{Born, u}} = -\frac{g_{ZL}^2}{u} - \frac{g_{ZR}^2}{u}, \tag{12}
\end{aligned}$$

with

$$g_{ZL} = e \frac{(2s_W^2 - 1)}{2s_W c_W} \quad g_{ZR} = e \frac{s_W}{c_W} ; \tag{13}$$

- $e^-e^+ \rightarrow Z\gamma$.

$$\begin{aligned}
\frac{s}{s-m_Z^2} N_1^{\text{Born, t}} &= \frac{s}{s+m_Z^2} N_2^{\text{Born, t}} = N_4^{\text{Born, t}} \\
&= -\frac{s}{t-m_Z^2} N_5^{\text{Born, t}} = -\frac{s}{2} N_6^{\text{Born, t}} = -\frac{e_L g_{ZL}}{t} P_L - \frac{e_R g_{ZR}}{t} P_R, \\
\left(\frac{s}{s-m_Z^2}\right) N_1^{\text{Born, u}} &= \left(\frac{s}{s+m_Z^2}\right) N_2^{\text{Born, u}} = -N_4^{\text{Born, u}} \\
&= \left(\frac{-s}{s-u}\right) N_5^{\text{Born, u}} = \frac{-s}{2} N_6^{\text{Born, u}} = -\frac{e_L g_{ZL}}{u} P_L - \frac{e_R g_{ZR}}{u} P_R. \tag{14}
\end{aligned}$$

Note that for all processes

$$N_{3,9}^{\text{Born, t}} = N_{3,9}^{\text{Born, u}} = 0. \tag{15}$$

In the following Sections, the complete $e^-e^+ \rightarrow VV'$ amplitudes at one loop are obtained applying the usual renormalization program in the on-shell scheme [19]. The renormalized Lagrangian is obtained from the unrenormalized one by the substitution

$$\psi_{eL} \rightarrow \sqrt{Z_{eL}} \psi_{eL}, \quad \psi_{eR} \rightarrow \sqrt{Z_{eR}} \psi_{eR}, \tag{16}$$

$$B_\mu \rightarrow \sqrt{Z_B} B_\mu, \quad \vec{W}_\mu \rightarrow \sqrt{Z_W} \vec{W}_\mu \tag{17}$$

$$g' \rightarrow \frac{1}{\sqrt{Z_B}} g', \quad g \rightarrow \frac{\tilde{Z}_2}{\sqrt{Z_W}} g, \tag{18}$$

where (16, 17) describe the wave function renormalization for the electron and the gauge-bosons. Eqs.(18) supply the renormalization of the gauge couplings, taking into account that the $U(1)_Y$ Ward identity guarantees that g' does not need any additional renormalization, at least, at the 1-loop level [19]. Contrary to these, the $SU(2)$ coupling g does need the additional renormalization described by \tilde{Z}_2 , which in the 'tHooft-Feynman gauge is determined by the W and Goldstone loop contributions to the γZ mixed self-energy.

The SM and MSSM contributions to the various renormalization constants are given in Sect.3.2 and Appendix C. The explicit expressions of the 1-loop amplitudes are given in terms of N_j -functions containing the contributions from the renormalized Born terms, the triangle and the box diagrams according to

$$N_j(s, t, u) = N_j^{\text{ren+Born}} + N_j^{\text{Tri}} + N_j^{\text{Box}}, \tag{19}$$

which are computed in the subsequent subsections.

3.2 The renormalized Born contribution

The on-shell renormalization procedure [19] uses as input the electric charge $e(0) \equiv \sqrt{4\pi\alpha(0)}$, the physical masses m_W , m_Z , and the Weinberg angle defined³ by $c_W^2 = 1 - s_W^2 = m_W^2/m_Z^2$. The renormalization introduces modifications to the Born amplitude induced by the substitutions (16, 17, 18), and the self-energies given in Appendix C.

We separate the finite renormalized self-energy contributions denoted with a "hat", from the divergent ones. The former are absorbed in $N_j^{\text{ren+Born}}$; while the later are put in N_j^{Tri} , together with the divergent triangle contributions presented in Sect.3.3. Thus, both $N_j^{\text{ren+Born}}$ and N_j^{Tri} are finite.

The finite hat-quantities entering $N_j^{\text{ren+Born}}$ stem from the renormalized electron self energy, and the renormalized Z self energy and γZ mixing on the Z -mass shell [19].

In analogy to (9), we write

$$N_j^{\text{ren+Born}} = N_j^{\text{ren+Born, t}} + N_j^{\text{ren+Born, u}} \quad , \quad (20)$$

where the two terms in the r.h.s. arise from electron exchanges in the t - and u -channel respectively.

- $e^-e^+ \rightarrow \gamma\gamma$.

According to the aforementioned conventions, $N_j^{\text{ren+Born}}$ are obtained from (10,11) by the replacement

$$\begin{aligned} e_L^2 &\Longrightarrow \hat{e}_L^2(x) \equiv 4\pi\alpha(0)[1 - \hat{\Sigma}_{Le}(x)] \quad , \\ e_R^2 &\Longrightarrow \hat{e}_R^2(x) \equiv 4\pi\alpha(0)[1 - \hat{\Sigma}_{Re}(x)] \quad , \end{aligned} \quad (21)$$

where x stands for t or u . The counter terms for the gauge boson-electron vertices which could contribute to (21) through the divergent factors

$$[1 + 2\delta Z_{Le} + \delta\tilde{Z}_2] \quad , \quad [1 + 2\delta Z_{Re}] \quad , \quad (22)$$

for e_L^2 , e_R^2 respectively, are (as said above) absorbed in the triangle contributions N_j^{Tri} ; see (28).

- $e^-e^+ \rightarrow ZZ$.

The replacement to be made now in (12,13) is:

$$g_{ZL}^2 \Longrightarrow \hat{g}_{ZL}^2(x) \equiv \frac{4\pi\alpha(0)(1 - 2s_W^2)^2}{4s_W^2c_W^2} \left[1 - \hat{\Sigma}_{Le}(x) - \hat{\Sigma}'_{ZZ}(m_Z^2) + \frac{4s_Wc_W\hat{\Sigma}_{\gamma Z}(m_Z^2)}{(2s_W^2 - 1)m_Z^2} \right] \quad ,$$

³We follow the usual convention $W_\mu^3 = c_W Z_\mu + s_W A_\mu$ and $B_\mu = -s_W Z_\mu + c_W A_\mu$, which has a sign difference compared to the one in [19].

$$g_{ZR}^2 \implies \widehat{g}_{ZR}^2(x) \equiv \frac{4\pi\alpha(0)s_W^2}{c_W^2} \left[1 - \widehat{\Sigma}_{Re}(x) - \widehat{\Sigma}'_{ZZ}(m_Z^2) + \frac{2c_W \widehat{\Sigma}_{\gamma Z}(m_Z^2)}{s_W m_Z^2} \right], \quad (23)$$

while the Zee counter terms which would contribute through the additional factors

$$\left[1 + 2\delta Z_{Le} + \frac{2c_W^2}{(1-2s_W^2)} \delta \tilde{Z}_2 \right], \quad [1 + 2\delta Z_{Re}], \quad (24)$$

will be put together with the triangle contributions, in order to make finite quantities; see (41).

- $e^-e^+ \rightarrow Z\gamma$.

The replacement in (14) is now

$$\begin{aligned} e_{LgZL} &\implies \widehat{e_{LgZL}}(x) \equiv \frac{4\pi\alpha(0)(1-2s_W^2)}{2s_W c_W} \left[1 - \widehat{\Sigma}_{Le}(x) - \frac{\widehat{\Sigma}'_{ZZ}(m_Z^2)}{2} + \frac{2s_W c_W \widehat{\Sigma}_{\gamma Z}(m_Z^2)}{(2s_W^2-1)m_Z^2} \right], \\ e_{RgZR} &\implies \widehat{e_{RgZR}}(x) \equiv -\frac{4\pi\alpha(0)s_W}{c_W} \left[1 - \widehat{\Sigma}_{Re}(x) - \frac{\widehat{\Sigma}'_{ZZ}(m_Z^2)}{2} + \frac{c_W \widehat{\Sigma}_{\gamma Z}(m_Z^2)}{s_W m_Z^2} \right], \end{aligned} \quad (25)$$

while the additional divergent factors

$$\left[1 + 2\delta Z_{Le} + \frac{(3-4s_W^2)}{2(1-2s_W^2)} \delta \tilde{Z}_2 \right], \quad [1 + 2\delta Z_{Re}] \quad (26)$$

generated by the counter terms, will again be put together with the triangle contributions in (57).

The complete expressions of the various self-energy functions and counter terms are given in Appendix C.

3.3 Triangle contributions

These arise from triangle diagrams of the type depicted in Fig.1d, 1e and from the diagrams in Fig.1f which induce "anomalous neutral gauge couplings" NAGC [16]. Below and in Appendix D, we give the complete expressions for these contributions, while in Appendix E we quote their dominant leading logarithmic contribution when s , t , u are all much larger than all internal and external masses. As already said, these "Triangle" contributions to the various N_j^{Tri} amplitudes, also include the counter term factors in (22, 24, 26), which guarantee their finiteness. This has been checked using the expressions in Appendix D.

- $e^-e^+ \rightarrow \gamma\gamma$

In this case, the diagram of the type Fig.1d gives the SM contributions generated by loops involving the particle-strings

$$(abc) \equiv (\gamma ee), \quad (Zee), \quad (\nu_e WW) \quad ,$$

while the MSSM contributions involve

$$(abc) \equiv (\tilde{\nu}_e \tilde{\chi}_i^+ \tilde{\chi}_j^+), \quad (\tilde{\chi}_i^0 \tilde{e} \tilde{e}) .$$

The generic diagram Fig.1e only induces an SM contribution involving the particle-strings

$$(abc) \equiv (\nu_e WW) ,$$

containing the 4-leg $WW\gamma\gamma$ coupling. There is no NAGC contribution from Fig.1f, for two on-shell final photons.

The resulting contributions to the N_j^{Tri} functions are

$$\begin{aligned} N_1^{Tri} &= N_2^{Tri} = \alpha^2 \left[\frac{2T_t^\gamma + T_t'^\gamma}{t} + \frac{2T_u^\gamma + T_u'^\gamma}{u} + N_1''^\gamma P_L \right] \\ N_3^{Tri} &= 0 , \\ N_4^{Tri} &= \alpha^2 \left[\frac{2T_t^\gamma}{t} - \frac{2T_u^\gamma}{u} \right] . \end{aligned} \quad (27)$$

Separating the L, R parts of T terms in (27), and adding the divergent counter term corrections generated from (22), we write

$$T^\gamma \equiv [T^{\gamma L} + \delta^{\gamma L}] P_L + [T^{\gamma R} + \delta^{\gamma R}] P_R , \quad (28)$$

with

$$\delta^{\gamma L} = -\frac{4\pi}{\alpha} [\delta Z_{Le} + \frac{1}{2} \delta \tilde{Z}_2] , \quad (29)$$

$$\delta^{\gamma R} = -\frac{4\pi}{\alpha} \delta Z_{Re} \quad (30)$$

obtained from (22), and

$$T'^\gamma \equiv T'^{\gamma L} P_L + T'^{\gamma R} P_R . \quad (31)$$

The SM contributions arising from the triangles involving γ , Z , W exchanges are then written as

$$T_t^{\gamma L \text{ SM}} = b_\gamma^L(t) + \frac{(2s_W^2 - 1)^2}{4s_W^2 c_W^2} b_Z^L(t) + \frac{1}{2s_W^2} b_W^L(t) , \quad (32)$$

$$T_t^{\gamma R \text{ SM}} = b_\gamma^R(t) + \frac{s_W^2}{c_W^2} b_Z^R(t) , \quad (33)$$

$$T_t'^{\gamma L \text{ SM}} = a_\gamma^L(t) + \frac{(2s_W^2 - 1)^2}{4s_W^2 c_W^2} a_Z^L(t) + \frac{1}{2s_W^2} a_W^L(t) , \quad (34)$$

$$T_t'^{\gamma R \text{ SM}} = a_\gamma^R(t) + \frac{s_W^2}{c_W^2} a_Z^R(t) , \quad (35)$$

while the MSSM contributions due to triangles involving chargino or neutralino exchanges are

$$T_t^{\gamma L \text{ MSSM}} = -\frac{1}{s_W^2} b_{2\tilde{\chi}}^L(t) - \frac{1}{s_W^2 c_W^2} b_{1\tilde{\chi}}^L(t), \quad (36)$$

$$T_t^{\gamma R \text{ MSSM}} = -\frac{4}{c_W^2} b_{1\tilde{\chi}}^R(t), \quad (37)$$

$$T_t^{\prime\gamma L \text{ MSSM}} = -\frac{1}{s_W^2} a_{2\tilde{\chi}}^L(t) - \frac{1}{s_W^2 c_W^2} a_{1\tilde{\chi}}^L(t), \quad (38)$$

$$T_t^{\prime\gamma R \text{ MSSM}} = -\frac{4}{c_W^2} a_{1\tilde{\chi}}^R(t), \quad (39)$$

where $a_i^{L,R}$, $b_i^{L,R}$ and $N_1^{\prime\prime\gamma}$ corresponding to each triangle diagram are given in (D.1, D.2) in terms of Passarino-Veltman functions [20], in which the internal propagator masses are determined by the particle-strings mentioned above. The analogous u -channel expressions are obtained correspondingly.

The results for the asymptotic regime where s , t , u are much larger than all internal propagator masses, are given in Appendix E.

- $e^-e^+ \rightarrow ZZ$

The diagrams of the type of Fig.1d supply the SM contributions due to the particle-strings

$$(abc) \equiv (\gamma ee), \quad (Zee), \quad (W\nu_e\nu_e), \quad (\nu_e WW),$$

and the MSSM ones through

$$(abc) \equiv (\tilde{\nu}_e\tilde{\chi}_i^+\tilde{\chi}_j^+), \quad (\tilde{e}\tilde{\chi}_i^0\tilde{\chi}_j^0), \quad (\tilde{\chi}_i^+\tilde{\nu}_e\tilde{\nu}_e), \quad (\tilde{\chi}_i^0\tilde{e}\tilde{e}).$$

The diagram of Fig.1e induces just an SM contribution for

$$(abc) \equiv (\nu_e WW),$$

involving the $WWZZ$ coupling. Finally, Fig.1f, which can only involve a fermionic triangle (leptons and quarks in SM, and charginos and neutralinos in MSSM), supplies the NAGC contribution to the couplings $f_5^{\gamma,Z}$ [16].

The set of these triangular contributions is described as

$$\begin{aligned} N_1^{Tri} &= N_2^{Tri} = \alpha^2 \left[\frac{2T_t^Z + T_t^{\prime Z}}{t} + \frac{2T_u^Z + T_u^{\prime Z}}{u} + N_1^{\prime\prime Z} P_L \right], \\ N_3^{Tri} &= N_9^{Tri} = 0, \\ N_4^{Tri} &= \alpha^2 \left[\frac{2T_t^Z}{t} - \frac{2T_u^Z}{u} \right], \\ N_5^{Tri} &= \alpha^2 \left[\left(\frac{m_Z^2 - t}{s} \right) \frac{2T_t^Z}{t} + \frac{1}{u} \left(\frac{(u - s - m_Z^2)}{s} 2T_u^Z - T_u^{\prime Z} \right) + N_5^{\prime\prime Z} P_L \right] + N_5^{AGC}, \\ N_6^{Tri} &= -N_8^{Tri} = \alpha^2 \left[-\frac{2}{s} \left(\frac{2T_t^Z}{t} + \frac{2T_u^Z}{u} \right) \right] + N_6^{AGC}, \\ N_7^{Tri} &= \alpha^2 \left[\frac{1}{t} \left(\frac{(t - m_Z^2 - s)}{s} 2T_t^Z - T_t^{\prime Z} \right) + \left(\frac{m_Z^2 - u}{s} \right) \frac{2T_u^Z}{u} + N_7^{\prime\prime Z} P_L \right] + N_7^{AGC}. \end{aligned} \quad (40)$$

The (L, R) decompositions for T and T' above, after including also the divergent Zee counter terms from (24), become

$$T^Z \equiv \frac{2s_W^2 - 1}{2s_W c_W} [T^{ZL} + \delta^{ZL}] P_L + \frac{s_W}{c_W} [T^{ZR} + \delta^{ZR}] P_R, \quad (41)$$

with

$$\delta^{ZL} = - \left(\frac{2\pi(2s_W^2 - 1)}{\alpha s_W c_W} \right) [\delta Z_{Le} + \frac{c_W^2}{1 - 2s_W^2} \delta \tilde{Z}_2], \quad (42)$$

$$\delta^{ZR} = - \left(\frac{4\pi s_W}{\alpha c_W} \right) \delta Z_{Re}, \quad (43)$$

and

$$T'^Z \equiv \frac{2s_W^2 - 1}{2s_W c_W} T'^{ZL} P_L + \frac{s_W}{c_W} T'^{ZR} P_R. \quad (44)$$

The SM Figs.1d,e triangle contributions to them are given by

$$T_t^{ZL \text{ SM}} = \frac{2s_W^2 - 1}{2s_W c_W} b_\gamma^L(t) + \frac{(2s_W^2 - 1)^3}{8s_W^3 c_W^3} b_Z^L(t) + \frac{1}{4s_W^3 c_W} b_W''^L(t) - \frac{c_W}{2s_W^3} b_W'^L(t), \quad (45)$$

$$T_t^{ZR \text{ SM}} = \frac{s_W}{c_W} b_\gamma^R(t) + \frac{s_W^3}{c_W^3} b_Z^R(t), \quad (46)$$

$$T_t'^{ZL \text{ SM}} = \frac{2s_W^2 - 1}{2s_W c_W} a_\gamma^L(t) + \frac{(2s_W^2 - 1)^3}{8s_W^3 c_W^3} a_Z^L(t) + \frac{1}{4s_W^3 c_W} a_W''^L(t) - \frac{c_W}{2s_W^3} a_W'^L(t), \quad (47)$$

$$T_t'^{ZR \text{ SM}} = \frac{s_W}{c_W} a_\gamma^R(t) + \frac{s_W^3}{c_W^3} a_Z^R(t), \quad (48)$$

while the MSSM contributions are

$$T_t^{ZL \text{ MSSM}} = - \frac{1}{4s_W^3 c_W^3} b_{2\tilde{\chi}}^L(t) + \frac{1}{2s_W^3 c_W} b_{2\tilde{\chi}}''^L(t) - \frac{1}{s_W^3 c_W} b_{1\tilde{\chi}}^L(t) + \frac{1}{2s_W^3 c_W^3} b_{1\tilde{\chi}}''^L(t), \quad (49)$$

$$T_t^{ZR \text{ MSSM}} = - \frac{1}{4s_W^3 c_W^3} b_{2\tilde{\chi}}^R(t) + \frac{1}{2s_W^3 c_W} b_{1\tilde{\chi}}''^R(t), \quad (50)$$

$$T_t'^{ZL \text{ MSSM}} = - \frac{1}{4s_W^3 c_W^3} a_{2\tilde{\chi}}^L(t) + \frac{1}{2s_W^3 c_W} a_{2\tilde{\chi}}''^L(t) - \frac{1}{s_W^3 c_W} a_{1\tilde{\chi}}^L(t) + \frac{1}{2s_W^3 c_W^3} a_{1\tilde{\chi}}''^L(t), \quad (51)$$

$$T_t'^{ZR \text{ MSSM}} = - \frac{1}{4s_W^3 c_W^3} a_{2\tilde{\chi}}^R(t) + \frac{1}{2s_W^3 c_W} a_{1\tilde{\chi}}''^R(t), \quad (52)$$

where $a_i^{L,R}$, $b_i^{L,R}$, $N_{1,5}''^Z$ are calculated from the diagrams in Figs.1d,1e and given in (D.3, D.4).

Finally, the NAGC contribution induced from Fig.1f in (40) is

$$\begin{aligned} N_5^{AGC} &= -N_7^{AGC} = \left[\frac{2(m_Z^2 - u)}{s} - 1 \right] N^{AGC}, \\ N_6^{AGC} &= -N_8^{AGC} = \frac{4}{s} N^{AGC}, \end{aligned} \quad (53)$$

with

$$N^{AGC} = \left(\frac{e^2}{m_Z^2}\right) \left[f_5^\gamma (P_R - P_L) - f_5^Z \left(\frac{1 - 2s_W^2}{2s_W c_W} P_L + \frac{s_W}{c_W} P_R \right) \right], \quad (54)$$

where $f_5^{\gamma,Z}$ are taken from [17], apart from the neutralino loop case with general mixings which was not considered in [17] and is given in (D.5).

As for the $\gamma\gamma$ production case, the dominant logarithmic terms in the asymptotic regime where s, t, u are much larger than all internal propagator masses, are given in Appendix E.

• $e^-e^+ \rightarrow Z\gamma$

Contributions in this case arise from diagrams of type Fig.1d already considered for the $e^-e^+ \rightarrow \gamma\gamma$ and $e^-e^+ \rightarrow ZZ$ process. In addition we also have the $(\nu_e WW)$ contribution from the diagram of Fig.1e with the 4-leg $WW\gamma Z$ vertex, and a Fig.1f NAGC contribution to the couplings $h_3^{\gamma,Z}$ [16, 17] containing a fermionic triangle consisting of leptons, quarks in SM, and charginos, neutralinos in MSSM. The whole set of these triangular contributions may be written as

$$\begin{aligned} N_1^{Tri} &= \alpha^2 \left[\left(1 - \frac{m_Z^2}{s}\right) \left(\frac{T_t^{\gamma Z}}{t} + \frac{T_u^{\gamma Z}}{u}\right) + \frac{T_t^{\prime\gamma Z}}{t} + \frac{T_u^{\prime\gamma Z}}{u} + N_1^{\prime\prime\gamma Z} \right] + N_1^{AGC \gamma Z}, \\ N_2^{Tri} &= \alpha^2 \left[\left(1 + \frac{m_Z^2}{s}\right) \left(\frac{T_t^{\gamma Z}}{t} + \frac{T_u^{\gamma Z}}{u}\right) + \frac{T_t^{\prime Z\gamma}}{t} + \frac{T_u^{\prime Z\gamma}}{u} + N_1^{\prime\prime\gamma Z} \right] + N_2^{AGC \gamma Z}, \\ N_3^{Tri} &= N_9^{Tri} = 0, \\ N_4^{Tri} &= \alpha^2 \left[\frac{T_t^{\gamma Z}}{t} - \frac{T_u^{\gamma Z}}{u} \right], \\ N_5^{Tri} &= \alpha^2 \left[\left(\frac{u-s}{s}\right) \frac{T_u^{\gamma Z}}{u} + \left(\frac{m_Z^2-t}{s}\right) \frac{T_t^{\gamma Z}}{t} - \frac{T_u^{\prime\gamma Z}}{u} + N_5^{\prime\prime\gamma Z} \right] + N_5^{AGC \gamma Z}, \\ N_6^{Tri} &= \alpha^2 \left[-\frac{2}{s} \left(\frac{T_t^{\gamma Z}}{t} + \frac{T_u^{\gamma Z}}{u}\right) \right] + N_6^{AGC \gamma Z}. \end{aligned} \quad (55)$$

Decomposing $T^{\gamma Z}, T^{\prime\gamma Z}, T^{\prime Z\gamma}$ in their L,R components as

$$T \equiv T^L P_L + T^R P_R, \quad (56)$$

in analogy with (28) and including also the divergent contributions from Sect.3.2, already defined in (29, 30, 42, 43), we get

$$\begin{aligned} T_t^{\gamma ZL} &= -[T_t^{ZL} + \delta^{ZL}] - \left(\frac{2s_W^2 - 1}{2s_W c_W}\right) [T_t^{\gamma L} + \delta^{\gamma L}], \\ T_t^{\gamma ZR} &= -[T_t^{ZR} + \delta^{ZR}] - \frac{s_W}{c_W} [T_t^{\gamma R} + \delta^{\gamma R}], \end{aligned} \quad (57)$$

and

$$\begin{aligned} T_t^{\prime\gamma ZL} &= -T_t^{ZL} & T_t^{\prime\gamma ZR} &= -T_t^{ZR} \\ T_t^{\prime Z\gamma L} &= -\left(\frac{2s_W^2 - 1}{2s_W c_W}\right) T_t^{\gamma L} & T_t^{\prime Z\gamma R} &= -\frac{s_W}{c_W} T_t^{\gamma R}, \end{aligned} \quad (58)$$

using the triangle functions already defined for the $\gamma\gamma$ and ZZ cases in (32-39, 45-52). The quantities $N_{1,5}^{\gamma\gamma Z}$ are derived from Fig.1e and given in (D.6)

Finally, the NAGC parts induced by the diagram in Fig.1f are

$$\begin{aligned}
N_1^{AGC \gamma Z} &= -N_2^{AGC \gamma Z} = \left(1 - \frac{m_Z^2}{s}\right) N^{AGC \gamma Z}, \\
N_5^{AGC \gamma Z} &= \frac{u}{s} N^{AGC \gamma Z}, \\
N_6^{AGC \gamma Z} &= -\frac{2}{s} N^{AGC \gamma Z}, \\
N^{AGC \gamma Z} &= \frac{e^2}{m_Z^2} \left[h_3^\gamma (P_R - P_L) - h_3^Z \left(\frac{1 - 2s_W^2}{2s_W c_W} P_L + \frac{s_W}{c_W} P_R \right) \right], \tag{59}
\end{aligned}$$

with the form factors $h_3^{\gamma, Z}$ obtained from [17].

The leading logarithmic terms in the asymptotic regime are again given in Appendix E.

3.4 Box contributions

The generic box diagrams contributing to the processes $e^+e^- \rightarrow V'V$ are shown in Fig.1g,h labeled as $(abcd)$, according to the particles in the four propagators. There are seven kinds ($k = 1, \dots, 7$) of such box contributions, which combined with the nature of particles (fermion f , vector V , scalar S) running inside the loop, create altogether 11 types of contributions labeled as

type 1: Fig.1g($Vfff$);	type 2: Fig.1g($fVVV$);
type 3: Fig.1h($VffV$);	type 4A, 4B, 4C, 4D: Fig.1g($Sfff$);
type 5: Fig.1g($fSSS$);	type 6A, 6B: Fig.1g($SffS$);
type 7: Fig.1g($fVSV$).	

Concerning the above list, we should note that the separation of the $k = 4$ contributions into four parts labeled 4A, 4B, 4C and 4D, and the analogous separation of the $k = 6$ ones into 6A and 6B, is induced by the appearance of different combinations of the kinetic and mass parts in the fermion propagators.

The generic contributions to each of these eleven types are denoted as $\bar{N}_j^{k, Box}(s, t, u)$ and expressed in terms of Passarino-Veltman functions [20]. Because of their complexity, we only write in Appendix F their leading logarithmic contributions, which serve also to define them. MATHEMATICA and FORTRAN codes determining $\bar{N}_j^{k, Box}(s, t, u)$ in terms of the Passarino-Veltman functions, are available upon request.

Multiplying the $\bar{N}_j^{k, Box}(s, t, u)$ functions by the appropriate coupling combinations, we obtain the contributions N_j^{Box} to be inserted in (19). These are given below in the SM and MSSM cases, for each of the three neutral gauge boson production processes considered.

- $e^-e^+ \rightarrow \gamma\gamma$

The SM contributions arise from the type 1 boxes: $(\gamma e e e)$ and $(Z e e e)$, the type 2:

$(\nu_e W^+ W^+ W^+)$, and the type 7: $(\nu_e W^+ G^+ W^+)$. The additional MSSM contributions come from the type 4 boxes: $(\tilde{\nu}_e \tilde{\chi}_i^+ \tilde{\chi}_j^+ \tilde{\chi}_k^+)$, and the type 5: $(\tilde{\chi}_i^0 \tilde{e} \tilde{e} \tilde{e})$. These are

$$\begin{aligned}
N_j^{\gamma\gamma SM Box} &= \alpha^2 \left\{ \bar{N}_j^{1,Box}(\gamma)[P_L + P_R] + \bar{N}_j^{1,Box}(Z) \left[\frac{(2s_W^2 - 1)^2}{4s_W^2 c_W^2} P_L + \frac{s_W^2}{c_W^2} P_R \right] \right. \\
&\quad \left. + \bar{N}_j^{2,Box}(W) \left[\frac{1}{2s_W^2} P_L \right] + \bar{N}_j^{7,Box}(G^+) \left[\frac{m_W^2}{2s_W^2} P_L \right] + \text{"sym"} \right\}, \quad (60) \\
N_j^{\gamma\gamma MSSM Box} &= \alpha^2 \left\{ -\frac{1}{s_W^2} \sum_i |Z_{1i}^+|^2 [\bar{N}_j^{4A} + M_{\tilde{\chi}_i}^2 (\bar{N}_j^{4B} + \bar{N}_j^{4C} + \bar{N}_j^{4D})] P_L \right. \\
&\quad \left. + \frac{1}{2s_W^2 c_W^2} \sum_i |Z_{1i}^N s_W + Z_{2i}^N c_W|^2 \bar{N}_j^5(\tilde{e}_L) P_L \right. \\
&\quad \left. + \frac{2}{c_W^2} \sum_i |Z_{1i}^N|^2 \bar{N}_j^5(\tilde{e}_R) P_R + \text{"sym"} \right\}, \quad (61)
\end{aligned}$$

where +”sym” implies symmetrizations of the form

$$\begin{aligned}
\bar{N}_1^{k,Box} + \bar{N}_2^{k,Box}, \quad \bar{N}_2^{k,Box} + \bar{N}_1^{k,Box}, \quad \bar{N}_3^{k,Box} - \bar{N}_3^{k,Box}, \quad \bar{N}_4^{k,Box} - \bar{N}_4^{k,Box}, \\
\bar{N}_5^{k,Box} + \bar{N}_7^{k,Box}, \quad \bar{N}_6^{k,Box} - \bar{N}_8^{k,Box}, \quad \bar{N}_7^{k,Box} + \bar{N}_5^{k,Box}, \\
\bar{N}_8^{k,Box} - \bar{N}_6^{k,Box}, \quad \bar{N}_9^{k,Box} - \bar{N}_9^{k,Box}, \quad (62)
\end{aligned}$$

in which $\tilde{\bar{N}}_j$ is constructed from \bar{N}_j by interchanging $t \Leftrightarrow u$ and $V \Leftrightarrow V'$. The notation for the chargino and neutralino mixing matrices appearing in (61) (and (64,66) below), is summarized in Appendix B.

- $e^- e^+ \rightarrow ZZ$

The SM contributions arise from type 1: $(\gamma e e e)$, $(Z e e e)$, $(W \nu_e \nu_e \nu_e)$; type 2: $(\nu_e W W W)$; type 7: $(e Z H_{SM} Z)$ and $(\nu_e W^+ G^+ W^+)$; and type 3: $(W \nu_e \nu_e W)$. These are

$$\begin{aligned}
N_j^{ZZ SM Box} &= \alpha^2 \left\{ \bar{N}_j^{1,Box}(\gamma) \left[\frac{(2s_W^2 - 1)^2}{4s_W^2 c_W^2} P_L + \frac{s_W^2}{c_W^2} P_R \right] + \bar{N}_j^{1,Box}(Z) \left[\frac{(2s_W^2 - 1)^4}{16s_W^4 c_W^4} P_L \right. \right. \\
&\quad \left. \left. + \frac{s_W^4}{c_W^4} P_R \right] + \bar{N}_j^{1,Box}(W) \left[\frac{1}{8s_W^4 c_W^2} P_L \right] + \bar{N}_j^{2,Box}(W) \left[\frac{c_W^2}{2s_W^4} P_L \right] + \bar{N}_j^{3,Box}(W) \left[\frac{1}{4s_W^4} P_L \right] \right. \\
&\quad \left. + \bar{N}_j^{7,Box}(G^+) \left[\frac{m_W^2}{2c_W^2} P_L \right] + \bar{N}_j^{7,Box}(H_{SM}) \left[\frac{m_W^2 [(2s_W^2 - 1)^2 P_L + 4s_W^4 P_R]}{4s_W^4 c_W^6} \right] + \text{"sym"} \right\} \quad (63)
\end{aligned}$$

The additional MSSM contributions arise from type 4: $(\tilde{\nu}_e \tilde{\chi}_i^+ \tilde{\chi}_j^+ \tilde{\chi}_k^+)$, $(\tilde{e} \tilde{\chi}_i^0 \tilde{\chi}_j^0 \tilde{\chi}_k^0)$; type 5: $(\tilde{\chi}_i^+ \tilde{\nu}_e \tilde{\nu}_e \tilde{\nu}_e)$, $(\tilde{\chi}_i^0 \tilde{e} \tilde{e} \tilde{e})$; and from⁴ type 3: $[(e Z H^0 Z) + (e Z h^0 Z) - (e Z H_{SM} Z)]$, and type 6:

⁴In order to get the ”additional MSSM contribution due to H^0 , h^0 ” which should added to the SM one without making a double counting of the Higgs sector, one has to subtract the H_{SM} contribution.

$(\tilde{\nu}_e \tilde{\chi}_i^+ \tilde{\chi}_j^+ \tilde{\nu}_e)$, $(\tilde{e} \tilde{\chi}_i^0 \tilde{\chi}_j^0 \tilde{e})$. They are given by

$$\begin{aligned}
N_j^{ZZ \text{ MSSM } Box} = & \alpha^2 \left\{ - \frac{1}{4s_W^4 c_W^2} \sum_{ilk} Z_{1i}^{+*} Z_{1k}^+ [\bar{N}_j^{4A} (Z_{1i}^+ Z_{1l}^{+*} + \delta_{il}(1 - 2s_W^2)) (Z_{1l}^+ Z_{1k}^{+*} \right. \\
& + \delta_{lk}(1 - 2s_W^2)) + M_{\tilde{\chi}_i} M_{\tilde{\chi}_k} \bar{N}_j^{4B} (Z_{1i}^- Z_{1l}^{-*} + \delta_{il}(1 - 2s_W^2)) (Z_{1l}^- Z_{1k}^{-*} + \delta_{lk}(1 - 2s_W^2)) \\
& + M_{\tilde{\chi}_i} M_{\tilde{\chi}_l} \bar{N}_j^{4C} (Z_{1i}^- Z_{1l}^{-*} + \delta_{il}(1 - 2s_W^2)) (Z_{1l}^+ Z_{1k}^{+*} + \delta_{lk}(1 - 2s_W^2)) \\
& + M_{\tilde{\chi}_l} M_{\tilde{\chi}_k} \bar{N}_j^{4D} (Z_{1i}^+ Z_{1l}^{+*} + \delta_{il}(1 - 2s_W^2)) (Z_{1l}^- Z_{1k}^{-*} + \delta_{lk}(1 - 2s_W^2)) \left. \right] P_L \\
& - \frac{1}{8s_W^4 c_W^4} \sum_{ilk} (Z_{1i}^{N*} s_W + Z_{2i}^{N*} c_W) (Z_{1k}^N s_W + Z_{2k}^N c_W) \\
& \cdot [\bar{N}_j^{4A} (\tilde{e}_L) (Z_{4i}^N Z_{4l}^{N*} - Z_{3i}^N Z_{3l}^{N*}) (Z_{4l}^N Z_{4k}^{N*} - Z_{3l}^N Z_{3k}^{N*}) \\
& + M_{\tilde{\chi}_i^0} M_{\tilde{\chi}_k^0} \bar{N}_j^{4B} (\tilde{e}_L) (Z_{4i}^{N*} Z_{4l}^N - Z_{3i}^{N*} Z_{3l}^N) (Z_{4l}^{N*} Z_{4k}^N - Z_{3l}^{N*} Z_{3k}^N) \\
& - M_{\tilde{\chi}_i^0} M_{\tilde{\chi}_l^0} \bar{N}_j^{4C} (\tilde{e}_L) (Z_{4i}^{N*} Z_{4l}^N - Z_{3i}^{N*} Z_{3l}^N) (Z_{4l}^N Z_{4k}^{N*} - Z_{3l}^N Z_{3k}^{N*}) \\
& - M_{\tilde{\chi}_l^0} M_{\tilde{\chi}_k^0} \bar{N}_j^{4D} (\tilde{e}_L) (Z_{4i}^N Z_{4l}^{N*} - Z_{3i}^N Z_{3l}^{N*}) (Z_{4l}^{N*} Z_{4k}^N - Z_{3l}^{N*} Z_{3k}^N) \left. \right] P_L \\
& - \frac{1}{2s_W^2 c_W^4} \sum_{ilk} Z_{1i}^N Z_{1k}^{N*} [\bar{N}_j^{4A} (\tilde{e}_R) (Z_{4i}^{N*} Z_{4l}^N - Z_{3i}^{N*} Z_{3l}^N) (Z_{4l}^{N*} Z_{4k}^N - Z_{3l}^{N*} Z_{3k}^N) \\
& + M_{\tilde{\chi}_i^0} M_{\tilde{\chi}_k^0} \bar{N}_j^{4B} (\tilde{e}_R) (Z_{4i}^N Z_{4l}^{N*} - Z_{3i}^N Z_{3l}^{N*}) (Z_{4l}^N Z_{4k}^{N*} - Z_{3l}^N Z_{3k}^{N*}) \\
& - M_{\tilde{\chi}_i^0} M_{\tilde{\chi}_l^0} \bar{N}_j^{4C} (\tilde{e}_R) (Z_{4i}^N Z_{4l}^{N*} - Z_{3i}^N Z_{3l}^{N*}) (Z_{4l}^{N*} Z_{4k}^N - Z_{3l}^{N*} Z_{3k}^N) \\
& - M_{\tilde{\chi}_l^0} M_{\tilde{\chi}_k^0} \bar{N}_j^{4D} (\tilde{e}_R) (Z_{4i}^{N*} Z_{4l}^N - Z_{3i}^{N*} Z_{3l}^N) (Z_{4l}^N Z_{4k}^{N*} - Z_{3l}^N Z_{3k}^{N*}) \left. \right] P_R \\
& + \frac{1}{4s_W^4 c_W^2} \sum_i |Z_{1i}^+|^2 \bar{N}_j^5 (\tilde{\nu}_L) P_L + \frac{(1 - 2s_W^2)^2}{8s_W^4 c_W^4} \sum_i |Z_{1i}^N s_W + Z_{2i}^N c_W|^2 \bar{N}_j^5 (\tilde{e}_L) P_L \\
& + \frac{(2s_W^2)}{c_W^4} \sum_i |Z_{1i}^N|^2 \bar{N}_j^5 (\tilde{e}_R) P_R + \frac{1}{4s_W^4 c_W^2} \sum_{il} Z_{1i}^{+*} Z_{1l}^+ (\bar{N}_j^{6A} (Z_{1i}^+ Z_{1l}^{+*} + \delta_{il}(1 - 2s_W^2)) \\
& - M_{\tilde{\chi}_i} M_{\tilde{\chi}_l} \bar{N}_j^{6B} (Z_{1i}^- Z_{1l}^{-*} + \delta_{il}(1 - 2s_W^2))) P_L \\
& + \frac{1 - 2s_W^2}{8s_W^4 c_W^4} \sum_{il} (Z_{1i}^{N*} s_W + Z_{2i}^{N*} c_W) (Z_{1l}^N s_W + Z_{2l}^N c_W) [\bar{N}_j^{6A} (\tilde{e}_L) (Z_{4i}^N Z_{4l}^{N*} - Z_{3i}^N Z_{3l}^{N*}) \\
& + M_{\tilde{\chi}_i^0} M_{\tilde{\chi}_l^0} \bar{N}_j^{6B} (\tilde{e}_L) (Z_{4i}^{N*} Z_{4l}^N - Z_{3i}^{N*} Z_{3l}^N)] P_L \\
& + \frac{1}{c_W^4} \sum_{il} Z_{1i}^N Z_{1l}^{N*} [\bar{N}_j^{6A} (\tilde{e}_R) (Z_{4i}^{N*} Z_{4l}^N - Z_{3i}^{N*} Z_{3l}^N) \\
& + M_{\tilde{\chi}_i^0} M_{\tilde{\chi}_l^0} \bar{N}_j^{6B} (\tilde{e}_R) (Z_{4i}^N Z_{4l}^{N*} - Z_{3i}^N Z_{3l}^{N*})] P_R \\
& + [\bar{N}_j^{7,Box} (H^0) \cos^2(\beta - \alpha) + \bar{N}_j^{7,Box} (h^0) \sin^2(\beta - \alpha) - \bar{N}_j^{7,Box} (H_{SM})] \\
& \cdot \left[\frac{m_W^2 ((2s_W^2 - 1)^2 P_L + 4s_W^4 P_R)}{4s_W^4 c_W^6} \right] + \text{"sym"} \left. \right\}. \tag{64}
\end{aligned}$$

- $e^- e^+ \rightarrow Z \gamma$

The SM contributions come from type 1: $(\gamma e e)$, $(Z e e)$; type 2: $(\nu_e W^+ W^+ W^+)$; type 7:

$(\nu_e W^+ G^+ W^+)$; and from type 3: $(\nu_e W W \nu_e)$. They give

$$\begin{aligned}
N_j^{\gamma Z \text{ SM Box}} = \alpha^2 \left\{ \left[\bar{N}_j^{1, \text{Box}}(\gamma) \left(\frac{(1 - 2s_W^2)}{2s_W c_W} P_L - \frac{s_W}{c_W} P_R \right) + \bar{N}_j^{1, \text{Box}}(Z) \left(\frac{(1 - 2s_W^2)^3}{8s_W^3 c_W^3} P_L \right. \right. \right. \\
\left. \left. - \frac{s_W^3}{c_W^3} P_R \right) + \bar{N}_j^{2, \text{Box}}(W) \frac{c_W}{2s_W^3} P_L - \bar{N}_j^{7, \text{Box}}(G^+) \frac{m_W^2}{2s_W c_W} P_L + \text{"sym"} \right] \\
\left. + \bar{N}_j^{3, \text{Box}}(W) \frac{1}{4s_W^3 c_W} P_L \text{ (no "sym")} \right\}. \quad (65)
\end{aligned}$$

The additional MSSM contributions are from type 4: $(\tilde{\nu}_e \tilde{\chi}_i^+ \tilde{\chi}_j^+ \tilde{\chi}_k^+)$; type 5: $(\tilde{\chi}_i^0 \tilde{e} \tilde{e} \tilde{e})$; and type 6: $(\tilde{\nu}_e \tilde{\chi}_i^+ \tilde{\chi}_j^+ \tilde{\nu}_e)$, $(\tilde{\chi}_i^0 \tilde{e} \tilde{e} \tilde{\chi}_j^0)$.

$$\begin{aligned}
N_j^{\gamma Z \text{ MSSM Box}} = \alpha^2 \left\{ - \frac{1}{2s_W^3 c_W} \sum_{ik} Z_{1i}^{+*} Z_{1k}^+ \{ \bar{N}_j^{4A}(Z_{1i}^+ Z_{1k}^{+*} + \delta_{ik}(1 - 2s_W^2)) \right. \\
+ M_{\tilde{\chi}_i} M_{\tilde{\chi}_k} (\bar{N}_j^{4B} + \bar{N}_j^{4D})(Z_{1i}^- Z_{1k}^{-*} + \delta_{ik}(1 - 2s_W^2)) + M_{\tilde{\chi}_i}^2 \bar{N}_j^{4C}(Z_{1i}^+ Z_{1k}^{+*} + \delta_{ik}(1 - 2s_W^2)) \\
+ [\bar{N}_j^{4A}(Z_{1i}^+ Z_{1k}^{+*} + \delta_{ik}(1 - 2s_W^2)) + M_{\tilde{\chi}_i} M_{\tilde{\chi}_k} (\bar{N}_j^{4B} + \bar{N}_j^{4C})(Z_{1i}^- Z_{1k}^{-*} + \delta_{ik}(1 - 2s_W^2)) \\
+ M_{\tilde{\chi}_k}^2 \bar{N}_j^{4D}(Z_{1i}^+ Z_{1k}^{+*} + \delta_{ik}(1 - 2s_W^2))]^{sym} \} P_L \\
+ \left[\frac{(1 - 2s_W^2)}{4s_W^3 c_W^3} \sum_i |Z_{1i}^N s_W + Z_{2i}^N c_W|^2 \bar{N}_j^5(\tilde{e}_L) P_L - \frac{2s_W}{c_W^3} \sum_i |Z_{1i}^N|^2 \bar{N}_j^5(\tilde{e}_R) P_R + \text{"sym"} \right] \\
+ \frac{1}{2s_W^3 c_W} \sum_i |Z_{1i}^+|^2 [\bar{N}_j^{6A} - |M_{\tilde{\chi}_i}|^2 \bar{N}_j^{6B}] P_L + \frac{1}{4s_W^3 c_W^3} \sum_{il} (Z_{1i}^{N*} s_W + Z_{2i}^{N*} c_W)(Z_{1l}^N s_W \\
+ Z_{2l}^N c_W) [(Z_{4i}^N Z_{4l}^{N*} - Z_{3i}^N Z_{3l}^{N*}) \bar{N}_j^{6A}(\tilde{e}_L) + M_{\tilde{\chi}_i^0} M_{\tilde{\chi}_l^0} \bar{N}_j^{6B}(\tilde{e}_L)(Z_{4i}^{N*} Z_{4l}^N - Z_{3i}^{N*} Z_{3l}^N)]^{sym} P_L \\
- \frac{1}{s_W c_W^3} \sum_{il} Z_{1i}^N Z_{1l}^{N*} [(Z_{4i}^{N*} Z_{4l}^N - Z_{3i}^{N*} Z_{3l}^N) \bar{N}_j^{6A}(\tilde{e}_R) \\
+ M_{\tilde{\chi}_i^0} M_{\tilde{\chi}_l^0} \bar{N}_j^{6B}(\tilde{e}_R)(Z_{4i}^N Z_{4l}^{N*} - Z_{3i}^N Z_{3l}^{N*})]^{sym} P_R \left. \right\}. \quad (66)
\end{aligned}$$

In all cases, the symmetrization "sym" is done according to the rules given in (62).

4 Asymptotic amplitudes at one loop

It is interesting to construct asymptotic expressions for the N_j invariant amplitudes for the processes $e^- e^+ \rightarrow \gamma\gamma$, $Z\gamma$, ZZ , which should in principle be valid when (s, t, u) are much larger than m_Z^2 and any of the masses of the particles in the loop. Such asymptotic expressions for the $N_j^{\text{ren+Born}}$, N_j^{Tri} and N_j^{Box} parts of these invariant amplitudes, are given in Appendices E and F.

These asymptotic expressions are very interesting since they provide a simple picture for the physical amplitudes, which turns out to approximate the exact 1-loop results at the percent level, as soon as we pass the one TeV energy range. We give them below for each

of the N_j amplitudes, always omitting N_3 and N_9 , which never receive any leading-log contribution.

- $N_j(e^-e^+ \rightarrow \gamma\gamma)$; ($j = 1, 2, 4$)

$$N_j \simeq N_j^{Born,L} [1 + c_L^{(\gamma)} + c_L^{(Z)} + c_L^{(W)} + c_L^{(MSSM)}] + d_{j,L}^{(W)} + N_j^{Born,R} [c_R^{(\gamma)} + c_R^{(Z)} + c_R^{(MSSM)}] . \quad (67)$$

The structure of this expression is very intuitive. It consists of the Born term (10), to which the universal leading-log correction factors generated by

$$c_L^{(\gamma)} = c_R^{(\gamma)} = \frac{\alpha}{4\pi} \left[3 \ln \frac{s}{M_\gamma^2} - \ln^2 \frac{s}{M_\gamma^2} \right] , \quad (68)$$

$$c_L^{(Z)} = \frac{\alpha(2s_W^2 - 1)^2}{16\pi s_W^2 c_W^2} \left[3 \ln \frac{s}{m_Z^2} - \ln^2 \frac{s}{m_Z^2} \right] , \quad c_R^{(Z)} = \frac{\alpha s_W^2}{4\pi c_W^2} \left[3 \ln \frac{s}{m_Z^2} - \ln^2 \frac{s}{m_Z^2} \right] , \quad (69)$$

$$c_L^{(W)} = \frac{\alpha}{8\pi s_W^2} \left[\left(3 \ln \frac{s}{m_W^2} - \ln^2 \frac{s}{m_W^2} \right) - 2 \ln^2 \frac{s}{m_W^2} \right] , \quad (70)$$

$$c_L^{(MSSM)} = - \frac{\alpha(1 + 2c_W^2)}{16\pi s_W^2 c_W^2} \ln \frac{s}{m_W^2} , \quad c_R^{(MSSM)} = - \frac{\alpha}{4\pi c_W^2} \ln \frac{s}{m_W^2} , \quad (71)$$

are applied. These corrections are generated by diagrams involving photon, Z , W and MSSM partner exchanges. In the photon correction (68), the quantity M_γ has been introduced, which separates the ultraviolet and infrared contributions, the latter being generally absorbed to the so-called electromagnetic radiative corrections. In addition to these corrections, the W exchange boxes also induce an angular dependent contribution

$$d_{j,L}^{(W)} = \frac{\alpha^2}{s_W^2} P_L \left\{ \eta_t^j \left[2 \ln \frac{s}{m_W^2} \ln \frac{1 - \cos \theta}{2} + \ln^2 \frac{1 - \cos \theta}{2} \right] + \eta_u^j \left[2 \ln \frac{s}{m_W^2} \ln \frac{1 + \cos \theta}{2} + \ln^2 \frac{1 + \cos \theta}{2} \right] \right\} , \quad (72)$$

where

$$\eta_t^{1,2} = \frac{1}{t} , \quad \eta_t^4 = \frac{1}{t} + \frac{2}{s} , \quad \eta_u^{1,2} = \frac{1}{u} , \quad \eta_u^4 = -\frac{1}{u} - \frac{2}{s} . \quad (73)$$

Taking $M_\gamma \simeq m_Z \simeq m_W$, one gets from (68-71) the universal SM combinations [11, 12]

$$c_L^{(\gamma)} + c_L^{(Z)} + c_L^{(W)} = \frac{\alpha(1 + 2c_W^2)}{16\pi s_W^2 c_W^2} \left[3 \ln \frac{s}{m_W^2} - \ln^2 \frac{s}{m_W^2} \right] - \frac{\alpha}{4\pi s_W^2} \ln^2 \frac{s}{m_W^2} , \\ c_R^{(\gamma)} + c_R^{(Z)} = \frac{\alpha}{4\pi c_W^2} \left[3 \ln \frac{s}{m_W^2} - \ln^2 \frac{s}{m_W^2} \right] , \quad (74)$$

and the MSSM ones [9]

$$c_L^{(\gamma)} + c_L^{(Z)} + c_L^{(W)} + c_L^{(MSSM)} = \frac{\alpha(1 + 2c_W^2)}{16\pi s_W^2 c_W^2} \left[2 \ln \frac{s}{m_W^2} - \ln^2 \frac{s}{m_W^2} \right] - \frac{\alpha}{4\pi s_W^2} \ln^2 \frac{s}{m_W^2} , \\ c_R^{(\gamma)} + c_R^{(Z)} + c_R^{(MSSM)} = \left[\frac{\alpha}{4\pi} \right] \left[\frac{1}{c_W^2} \right] \left[2 \ln \frac{s}{m_W^2} - \ln^2 \frac{s}{m_W^2} \right] , \quad (75)$$

which satisfy the rules established in [12, 13]. Indeed, we find again that the radiative corrections associated to the electron line create the logarithmic factors $[3 \ln(s/m_W^2) - \ln^2(s/m_W^2)]$ in SM, and $[2 \ln(s/m_W^2) - \ln^2(s/m_W^2)]$ in MSSM; while their coefficients are determined by⁵ $\alpha/(4\pi)[I_e(I_e+1)/s_W^2 + Y_e^2/(4c_W^2)]$, which equals to $\alpha(1+2c_W^2)/(16\pi s_W^2 c_W^2)$ for the Left case, and $\alpha/(4\pi c_W^2)$ for the Right case [12, 13]. The photon lines supply the additional term $-\alpha/(4\pi s_W^2) \ln^2(s/m_W^2)$ in (74,75) [12, 13].

The non universal angular dependent term $d_{j,L}^{(W)}$ in (72), is a specific SM gauge W box contribution whose coefficient is fixed by the γWW coupling [12, 13].

- $N_j(e^-e^+ \rightarrow Z\gamma)$; ($j = 1, 2, 4, 5, 6$)

The asymptotic expressions now are

$$N_j \simeq N_j^{Born,L} [c_L^{(\gamma)} + c_L^{(Z)} + c_L^{(W)} + c_L^{(MSSM)}] + d_{j,L}^{(W)} + N_j^{Born,R} [c_R^{(\gamma)} + c_R^{(Z)} + c_R^{(MSSM)}] , \quad (76)$$

with

$$\begin{aligned} c_L^{(\gamma)} &= c_R^{(\gamma)} = \frac{\alpha}{4\pi} \left[3 \ln \frac{s}{M_\gamma^2} - \ln^2 \frac{s}{M_\gamma^2} \right] , \\ c_L^{(Z)} &= \frac{\alpha(2s_W^2 - 1)^2}{16\pi s_W^2 c_W^2} \left[3 \ln \frac{s}{m_Z^2} - \ln^2 \frac{s}{m_Z^2} \right] , \quad c_R^{(Z)} = \frac{\alpha s_W^2}{4\pi c_W^2} \left[3 \ln \frac{s}{m_Z^2} - \ln^2 \frac{s}{m_Z^2} \right] , \\ c_L^{(W)} &= \frac{\alpha}{8\pi s_W^2} \left[\left(3 \ln \frac{s}{m_W^2} - \ln^2 \frac{s}{m_W^2} \right) + \frac{(3 - 4s_W^2)}{(2s_W^2 - 1)} \left(\ln^2 \frac{s}{m_W^2} \right) \right] , \\ c_L^{(MSSM)} &= -\frac{\alpha(1 + 2c_W^2)}{16\pi s_W^2 c_W^2} \ln \frac{s}{m_W^2} , \quad c_R^{(MSSM)} = -\frac{\alpha}{4\pi c_W^2} \ln^2 \frac{s}{m_W^2} , \end{aligned} \quad (77)$$

$$\begin{aligned} d_{j,L}^{(W)} &= \frac{\alpha^2}{4s_W^3 c_W} P_L \left\{ \eta_t^j \left[2 \ln \frac{s}{m_W^2} \ln \frac{1 - \cos \theta}{2} + \ln^2 \frac{1 - \cos \theta}{2} \right] \right. \\ &\left. + \eta_u^j \left[2 \ln \frac{s}{m_W^2} \ln \frac{1 + \cos \theta}{2} + \ln^2 \frac{1 + \cos \theta}{2} \right] \right\} , \end{aligned} \quad (78)$$

and

$$\begin{aligned} \eta_t^{1,2} &= -\frac{s}{2} \eta_t^6 = \frac{3 - 4s_W^2}{t} - \frac{1}{u} , \quad \eta_u^{1,2} = -\frac{s}{2} \eta_u^6 = \frac{3 - 4s_W^2}{u} - \frac{1}{t} , \\ \eta_t^4 &= \frac{3 - 4s_W^2}{t} + \frac{1}{u} + \frac{8c_W^2}{s} , \quad \eta_u^4 = -\frac{3 - 4s_W^2}{u} - \frac{1}{t} - \frac{8c_W^2}{s} , \\ \eta_t^5 &= \frac{1}{u} + \frac{4c_W^2}{s} , \quad \eta_u^5 = -\frac{3 - 4s_W^2}{u} - \frac{4c_W^2}{s} . \end{aligned} \quad (79)$$

The universal SM and MSSM contribution of the electron line are again found to be in agreement with (74,75) [12]. There exist an additional $c_L^{(W)}$ contribution though in (77),

⁵Here I_e refers to the total isospin of the electron e , while $Y_e = 2(Q_e - I_e^3)$. The same formulae should apply also to any quark or lepton, and to their supersymmetric partners.

caused by the $Z\gamma$ final state. The angular dependent box term $d_{j,L}^{(W)}$ fixed by the γWW and the ZWW couplings [12].

- $N_j(e^-e^+ \rightarrow ZZ)$; ($j = 1, 2, 4, 5, 6, 7, 8$)

In a similar way we have

$$N_j \simeq N_j^{Born,L} [c_L^{(\gamma)} + c_L^{(Z)} + c_L^{(W)} + c_L^{(MSSM)}] + d_{j,L}^{(W)} + N_j^{Born,R} [c_R^{(\gamma)} + c_R^{(Z)} + c_R^{(MSSM)}], \quad (80)$$

with

$$\begin{aligned} c_L^{(\gamma)} &= c_R^{(\gamma)} = \frac{\alpha}{4\pi} \left[3 \ln \frac{s}{M_\gamma^2} - \ln^2 \frac{s}{M_\gamma^2} \right], \\ c_L^{(Z)} &= \frac{\alpha(2s_W^2 - 1)^2}{16\pi s_W^2 c_W^2} \left[3 \ln \frac{s}{m_Z^2} - \ln^2 \frac{s}{m_Z^2} \right], \quad c_R^{(Z)} = \frac{\alpha s_W^2}{4\pi c_W^2} \left[3 \ln \frac{s}{m_Z^2} - \ln^2 \frac{s}{m_Z^2} \right], \\ c_L^{(W)} &= \frac{\alpha}{8\pi s_W^2} \left[\left(3 \ln \frac{s}{m_W^2} - \ln^2 \frac{s}{m_W^2} \right) + \frac{4c_W^2}{2s_W^2 - 1} \left(\ln^2 \frac{s}{m_W^2} \right) \right], \\ c_L^{(MSSM)} &= -\frac{\alpha(1 + 2c_W^2)}{16\pi s_W^2 c_W^2} \ln \frac{s}{m_W^2}, \quad c_R^{(MSSM)} = -\frac{\alpha}{4\pi c_W^2} \ln^2 \frac{s}{m_W^2}, \end{aligned} \quad (81)$$

$$\begin{aligned} d_{j,L}^{(W)} &= \frac{\alpha^2}{2s_W^4} P_L \left\{ \eta_t^j \left[2 \ln \frac{s}{m_W^2} \ln \frac{1 - \cos \theta}{2} + \ln^2 \frac{1 - \cos \theta}{2} \right] \right. \\ &\left. + \eta_u^j \left[2 \ln \frac{s}{m_W^2} \ln \frac{1 + \cos \theta}{2} + \ln^2 \frac{1 + \cos \theta}{2} \right] \right\}, \end{aligned} \quad (82)$$

with

$$\begin{aligned} \eta_t^{1,2} &= \frac{1 - 2s_W^2}{t} - \frac{1}{u}, \quad \eta_u^{1,2} = \frac{1 - 2s_W^2}{u} - \frac{1}{t}, \\ \eta_t^4 &= \frac{1 - 2s_W^2}{t} + \frac{1}{u} + \frac{4c_W^2}{s}, \quad \eta_u^4 = -\frac{1 - 2s_W^2}{u} - \frac{1}{t} - \frac{4c_W^2}{s}, \\ \eta_t^5 &= \frac{1}{u} + \frac{2c_W^2}{s}, \quad \eta_u^5 = -\frac{1 - 2s_W^2}{u} - \frac{2c_W^2}{s}, \\ \eta_t^6 &= -\eta_t^8 = -\frac{2}{s} \left[\frac{1 - 2s_W^2}{t} - \frac{1}{u} \right], \quad \eta_u^6 = -\eta_u^8 = -\frac{2}{s} \left[\frac{1 - 2s_W^2}{u} - \frac{1}{t} \right], \\ \eta_t^7 &= \frac{2s_W^2 - 1}{t} - \frac{2c_W^2}{s}, \quad \eta_u^7 = \frac{1}{t} + \frac{2c_W^2}{s}. \end{aligned} \quad (83)$$

As expected, the universal electron line SM and MSSM contributions to (81), are the same, as in the $\gamma\gamma$ case [12]. The only modifications are due to the ZZ final state universal contribution $c_L^{(W)}$, and the angular dependent term $d_{j,L}^{(W)}$ determined by the ZWW coupling.

Finally we should comment about the asymptotic behaviour of the longitudinal ZZ production amplitudes. Contrary to the Born level TT amplitudes which behave like a

constant at asymptotic energies, and the TL ones which vanish only like m_Z/\sqrt{s} , the LL amplitudes diminish like m_Z^2/s . This latter property can be explicitly seen in

$$F_{\lambda 00}^{Born} \simeq - (2\lambda) \frac{16m_Z^2 \cos \theta}{s \sin \theta} \left\{ \frac{(2s_W^2 - 1)^2}{4s_W^2 c_W^2} P_L + \frac{s_W^2}{c_W^2} P_R \right\}. \quad (84)$$

When one loop effects are included, the asymptotic behaviours of the TT and TL remain largely the same, modified only by logarithmic enhancements determined by (80, 81), and (to a lesser extent) (82). But for the LL amplitudes a strikingly different structure arises, since the rapidly vanishing $\sim m_Z^2/s$ Born behaviour is replaced by a logarithmically increasing one involving $\ln^2 |t|/M^2$ and $\ln^2 |u|/M^2$ terms. This structure is induced by Higgs sector Box diagrams, whose contribution asymptotically dominates the tree-level one.

The simplest way to obtain it, is to use the equivalence theorem and consider the processes $e^+e^- \rightarrow G^0 G^0$. Since in the $m_e = 0$ limit this later process has no Born term, its only contribution comes from the boxes ($eZHZ$) and (νWGW), where H stands for the standard Higgs boson in SM, while in MSSM it represents a mixture of the CP-even states H^0 and the h^0 . The resulting asymptotic helicity amplitudes then is

$$\begin{aligned} F_{\lambda 00} &\simeq (2\lambda) \frac{\alpha^2 \sin \theta}{4} \left\{ \left[\ln^2 \frac{|t|}{m_W^2} - \ln^2 \frac{|u|}{m_W^2} \right] \right\} \left\{ \left(\frac{1}{s_W^4} + \frac{(2s_W^2 - 1)^2}{2s_W^4 c_W^4} \right) P_L + \left(\frac{2}{c_W^4} \right) P_R \right\} \\ &\simeq (2\lambda) \frac{\alpha^2 \sin \theta}{2} \ln \left(\frac{s}{m_W^2} \right) \ln \left(\frac{1 - \cos \theta}{1 + \cos \theta} \right) \left\{ \left(\frac{1}{s_W^4} + \frac{(2s_W^2 - 1)^2}{2s_W^4 c_W^4} \right) P_L + \left(\frac{2}{c_W^4} \right) P_R \right\}, \quad (85) \end{aligned}$$

in both, SM and MSSM. Thus, at sufficiently high energy, the order α^2 contribution of (85), becomes larger than the (suppressed) Born LL contribution of (84). We note that the cross-over of these two terms is around 1TeV.

Note also that, asymptotically, there is no difference between the SM and the MSSM predictions for longitudinal ZZ production. This is due to the fact that the H^0 contribution is proportional to $\cos^2(\beta - \alpha)$ and the h^0 one proportional to $\sin^2(\beta - \alpha)$, producing a result identical to the SM one.

5 Numerical Illustrations

Results for $e^+e^- \rightarrow \gamma\gamma$

Due to the electron exchange diagrams in the t and u channels, the angular distribution is strongly peaked in the forward and backward directions. Because of detection difficulties along the beam directions, we only consider scattering angles larger than 30° and smaller than 150° . The Born contribution is then shown for unpolarized beams and energies at 0.5 TeV and 5 TeV in Figs.2a,b.

The 1-loop⁶ radiative correction effects in the angular distribution, are described in Figs.2c,d, presenting the ratios of the unpolarized differential cross sections to the Born

⁶The numerical computation of the Passarino-Veltman functions is done using the FF-package [21].

contribution $d\sigma/d\sigma_{\text{Born}}$, for SM and a representative set of MSSM SUGRA models suggested in [22, 23]. As seen in these figures, the effect of the radiative corrections is always negative and increases with the energy and scattering angle. In the SM case it is of about -7% at 0.5TeV, and -27% at 5TeV. The differences among the various MSSM cases and the SM one, are within $\pm 1\%$.

The total cross section is calculated by integrating for scattering angles in the region $30^\circ < \theta < 150^\circ$. The Born contributions to it for all $e^-e^+ \rightarrow \gamma\gamma, \gamma Z, ZZ$ processes, and various polarization of the final Z states, are shown in Figs.3. Since the dominant Born amplitudes are energy-independent at high energies, the integrated cross sections decrease like $1/s$, as shown in Figs.3.

The radiative corrections to the integrated cross sections are described in Figs.4a, by the ratios $\sigma/\sigma_{\text{Born}}$ of the total cross section to the Born one, for SM and the aforementioned set of MSSM models. The energy behaviour of these ratios agrees with the asymptotic leading log expressions (74) and (75), for SM and MSSM respectively. According to them, the main difference between SM and MSSM at high energy, stems from the respective factors $(3 \ln s - \ln^2 s)$ and $(2 \ln s - \ln^2 s)$, and is independent of any other MSSM parameter. A measurement of the coefficient of the linear log term, could thus provide a signature discriminating between SM and MSSM. The magnitude of the effect is determined by the remark that if one puts an additional constant to the asymptotic cross section expression, and fits its value so that it agrees with the exact 1-loop result at 5TeV, then the departure at 0.2TeV appears to be at the permille level.

We also note that the above agreement between the exact 1-loop and the asymptotic predictions for the $e^-e^+ \rightarrow \gamma\gamma$ amplitudes, turns out to be rather insensitive to the masses of the virtual particles running along the loops. This applies also to all cases involving production of transverse gauge bosons; see below. On the contrary, as we will also see below, a large sensitivity to mass effects appears in the LT $e^-e^+ \rightarrow Z\gamma$ amplitudes, as well in the LT and LL $e^-e^+ \rightarrow ZZ$ ones.

The Left-Right polarization asymmetry A_{LR} defined in (8), with all final gauge polarizations summed over, is shown in Fig.4b. Since there is no Born contribution in $e^+e^- \rightarrow \gamma\gamma$, A_{LR} is totally due to the electroweak loop-corrections. Comparing Figs.4a,b, one can see that about the same type of effects appear in both, the cross sections and the A_{LR} asymmetries; (magnitude and sign of the SM and MSSM effects). Since A_{LR} should be not affected by normalization uncertainties though, its measurement may be experimentally more interesting.

As a final comment we note that in $e^-e^+ \rightarrow \gamma\gamma$, there is no Higgs or NAGC contributions. So this process is suited for studying the pure gauge and the gauge-lepton coupling structures of the electroweak corrections as well as their supersymmetric (gaugino and gaugino-slepton) counterparts.

Results for $e^+e^- \rightarrow Z\gamma$

The unpolarized angular distribution in the Born approximation, and its radiative corrections described by the ratios of the differential cross sections $d\sigma/d\sigma_{\text{Born}}$ at 0.5TeV and 5TeV, are shown in Figs.5a-d. Thus, the radiative correction effects are now of about

−8% at 0.5TeV, and −40% at 5TeV in SM; while the sensitivity to the various MSSM models is larger than in the $e^-e^+ \rightarrow \gamma\gamma$ process, (several percent at 0.5TeV, and few percent at 5TeV). This increase of sensitivity is mainly due to the LT amplitudes, and will disappear at asymptotic energies; see below. In any case, it is therefore interesting to study separately the behaviour of the cross sections for TT and LT final $Z\gamma$ states.

The Born cross sections $\sigma_{Born}(e^+e^- \rightarrow (Z\gamma)_{TT, LT})$, (for producing TT or LT $Z\gamma$ final states), are shown in Figs.3a. As seen there, the TT cross section behaves like $1/s$ and quickly dominates the LT one behaving as m_Z^2/s^2 . As a result, the not-shown unpolarized Born cross section $\sigma_{Born}(e^+e^- \rightarrow (Z\gamma)_{unp})$, is almost identical to $\sigma_{Born}(e^+e^- \rightarrow (Z\gamma)_{TT})$ for most of the energy region of the figure.

The radiative correction effects on the unpolarized, TT and LT integrated cross sections are described by the ratios in Figs.6a,b,c. Correspondingly, the radiative corrections to the Left-Right asymmetry are constructed in Fig.6d, by subtracting the $A_{LR}(Born) = 0.2181$ contribution, from the 1-loop result.

As one can see from Figs.6a,b,d, the radiative corrections to the unpolarized and TT cross sections and to the A_{LR} asymmetry, have a similar structure, which is also rather close to that of the $\gamma\gamma$ case, for both the SM and MSSM aspects. We have also checked that the high energy behaviour of the TT cross section⁷ agrees, with the asymptotic logarithmic expressions of (76-79), and that its characteristics are similar to those of the $\gamma\gamma$ case.

The radiative correction to the LT cross section presented in Figs.6c, requires a special discussion though; since the relevant helicity amplitudes are suppressed, behaving like \mathcal{M}/\sqrt{s} . Probably because of this, they are also very sensitive to the (real and virtual) masses involved in the various diagrams. In SM, the scale \mathcal{M} is determined essentially by $m_{W,Z}$ or m_t (for the NAGC contribution); while in MSSM, the various new masses generate a strong model dependence. Illustrations are given for the same sample of models of [22] used in the previous figures. One can then see in Fig.6c various energy dependence structures, induced by chargino, neutralino or slepton thresholds. These appear in an energy range where σ_{LT} should still be measurable. At higher energies, σ_{LT} becomes very small and marginally observable except with very high luminosity colliders.

There exist NAGC contributions to $e^+e^- \rightarrow \gamma Z$ arising from the diagram in Fig.1f involving a fermionic loop; but no Higgs contributions. The magnitude of NAGC for SM and a representative set of MSSM models [22] is shown in Fig.7a-c, where one plots the difference between the ratios to the Born cross sections, with and without NAGC, for unpolarized, as well as TT and LT final gauge boson states. In Fig.7d, the difference between the Left-Right asymmetry with and without NAGC, is also shown.

As mentioned in Section 3, the magnitude of the NAGC effects, (created by fermionic triangular loops), decreases with energy faster than $1/s$, [17]. Moreover, at high energies, there is no interference between the NAGC and Born amplitudes because the Born TT amplitudes involve opposite gauge helicities, while the NAGC TT amplitudes concern equal gauge helicities only; in addition the Born LT amplitudes drop down so quickly,

⁷This is also true for the unpolarized cross section to which the TT part is by far the dominant one.

that their NAGC interference is also forced to vanish quickly. Thus, the SM and MSSM NAGC effects for the models in Figs.7 are at the permille level, and should be only marginally observable, except with very high luminosity colliders.

It is conceivable, that forms of fermionic NP exist (beyond SM or MSSM), that only contribute through the NAGC diagram of Fig.1f. We have looked at the sensitivity of such contributions to the h_3^γ and h_3^Z couplings at first order, in a model independent way [16]. Assuming a given experimental accuracy on the unpolarized integrated cross section and the Left-Right asymmetry, we obtain observability limits for the total NAGC contribution. Such effects are illustrated in Fig.8a, assuming 1% accuracy, and taking the energies 0.5TeV and 1TeV.

Note that the σ_{unp} and A_{LR} constraints are almost orthogonal, allowing a good limitation on both NAGC couplings. This arises because σ_{np} mainly depends on h_3^γ , whereas A_{LR} is more sensitive to h_3^Z ; which is just because the photon couples vectorially, while the Zee coupling is essentially purely axial. As seen from Fig.8a, the implied sensitivity is likely to increase with energy. Thus, on the basis of Fig.8a, we conclude that only NP forms inducing *e.g.* percent level NAGC effects, could be observable through $e^-e^+ \rightarrow Z\gamma$ measurements.

Finally we come back to a point mentioned in the Introduction concerning the search for NP through NAGC measurements. Since the NAGC effects are intrinsically small, it is essential to have a good evaluation of the complete SM or MSSM radiative corrections, before looking for possible NP contributions. For example, at 1TeV these radiative correction effects are of the order of 10% on σ or A_{LR} , so that neglecting (or approximating) them, would invalidate the bounds one would put on the basis of NAGC.

Results for $e^+e^- \rightarrow ZZ$

The unpolarized angular distributions at 0.5TeV and 5TeV are shown in Fig.9a,b for the Born contribution, and in Fig.9c,d for the ratio $(d\sigma/d\cos\theta)/(d\sigma/d\cos\theta)_{\text{Born}}$. The radiative correction effects are now larger than in the $\gamma\gamma$ and $Z\gamma$ production cases. In SM they reach -15% at 0.5TeV, and -58% at 5TeV. The sensitivity to MSSM models is also increased, up to an additional -15% , especially at large angles.

The integrated Born cross sections (using the same angular cut at 30°), are given in Figs.3b for TT, TL and LL final states. As in the $\gamma\gamma$ and $Z\gamma$ cases, $\sigma_{\text{Born}}^{TT} \simeq 1/s$ at high energies, which is much larger than the TL or LL cross sections, and therefore almost identical to the unpolarized one. In analogy to the $Z\gamma$ case, the TL cross section is suppressed like m_Z^2/s^2 ; while $\sigma_{\text{Born}}^{LL} \simeq 1/s^3$, compare (84).

The energy dependence of the radiative corrections to the unpolarized and TT cross sections is presented in Figs.10a,b; it is similar to that observed for the other processes, and agrees with the logarithmic analysis at high energy contained in (80).

The same effects are also found in the Left-Right polarization asymmetry A_{LR} , (for unpolarized final ZZ states). The A_{LR} Born value is 0.4164, and the radiative correction to this value is shown in Fig.11a.

The radiative correction to σ_{LT} is presented in Fig.10c where, one observes a strong model dependence, similar to the one seen in Fig.6c for the $Z_L\gamma$ case.

The case of σ_{LL} is even more interesting, because of the change of behaviour around 1TeV appearing in Fig.10d. For $\sqrt{s} \lesssim 1\text{TeV}$, one observes a suppression like \mathcal{M}^4/s^3 , already mentioned in connection with the Born LL contribution. Above 1TeV though, a logarithmic increase arises, caused by the Higgs sector and discussed at the end of Section 4; compare (85).

Finally, in Figs.11b,c,d, we show the Higgs mass dependence of the radiative corrections in the SM case, for TT, TL and LL productions. We plot the ratios to the Born contribution, of the differences between the $m_H = 0.3 \text{ TeV}$ or $m_H = 1 \text{ TeV}$ cross sections, from the $m_H = 0.113 \text{ TeV}$ case.

The role of the NAGC

In the $e^+e^- \rightarrow ZZ$ process, the SM or MSSM NAGC contributions $f_5^{\gamma,Z}$ only exist for the TL amplitudes [16]. In the above illustrations, the unpolarized or TL cross sections, as well as the A_{LR} asymmetry, are containing these contributions. The situation is different from the $e^+e^- \rightarrow Z\gamma$ case because the roles of $\gamma - NAGC$ and of $Z - NAGC$ are interchanged due to the different chirality structure of the Born terms which interfere with the NAGC amplitudes. Consequently σ_{unp} is mainly sensitive to f_5^Z whereas A_{LR} is mainly sensitive to f_5^γ . The net NAGC effects are shown in Fig.12a-c, and as in the $Z\gamma$ case, they are at most at the permille level.

As for the $Z\gamma$ case, we have also made a model independent analysis of the sensitivity to unknown $f_5^{\gamma,Z}$ couplings, at first order in σ_{unp} and A_{LR} . The result is shown in Fig.8b for 0.5 and 1 TeV, assuming again 1% accuracy on these observables. The orders of magnitude and the prospects for observability are comparable to the $Z\gamma$ case. Thus, SM and MSSM contributions will be marginally observable and only stronger NP contributions may be constrained.

6 Physics issues and Conclusions

In this paper we have made a complete analysis of the processes $e^+e^- \rightarrow \gamma\gamma, \gamma Z, ZZ$, including electroweak corrections at the one loop level in the context of SM and MSSM.

These processes are particularly interesting in various aspects. From an experimental point of view, the final states are easy to detect. From the theoretical point of view, these processes have a simple structure providing clean tests of the properties of the electroweak interactions. At tree level there is no s-channel term (contrary to the WW case); the Born terms are only due to electron exchanges in the t and u channels. There are no QCD or Yukawa contributions; the identification of the electroweak corrections should then be very clean.

We have computed them completely, both within SM and within MSSM. We have given these results, in analytical form, apart from the exact 1-loop Box contributions to the 11 types of independent contributions, for which we provide MATHEMATICA and FORTRAN codes upon request. In all cases, we have shown how the corrections are constructed in each sector; gauge neutral, gauge charged, Higgs, and the supersymmetric

counterparts. Special emphasis has been put to the study of how these contributions behave with the energy, and how they match with the high energy logarithmic expressions expected from general rules.

We have then computed numerically the effects on many possible observables at variable energies; *i.e.* integrated cross sections, Left-Right asymmetries and angular distributions, for unpolarized and polarized initial and final states. We next summarize the results and the physics issues.

The electroweak radiative corrections are large and grow with the energy. They are of a few percent in an energy range of at few hundreds of GeV, reaching already 10% at 1 TeV. They then continue to grow according to the logarithmic rules. Such effects should be observable at the high precision future colliders [1, 2], whose accuracy should reach the percent level or even better.

In $e^+e^- \rightarrow \gamma\gamma$, the natural observables (angular distribution at large angles, integrated cross section, A_{LR} asymmetry for unpolarized $\gamma\gamma$ final states) reflect the gauge (gaugino) structure of the electroweak interactions in a clean way. Below 1 TeV, the various considered MSSM benchmark models of [22], differ from SM within the $\pm 1\%$ level. Above 1 TeV, the model dependence (for models involving relatively light supersymmetric particles) vanishes, and the effects match the asymptotic rules giving in MSSM a growing contribution like $2 \ln s - \ln^2 s$ (times the Born amplitude), instead of the $3 \ln s - \ln^2 s$ factor expected in SM. So at asymptotic energies, we could in principle discriminate between SM and MSSM; although we would have no means to choose among MSSM models involving relatively light supersymmetric particles. The A_{LR} asymmetry shows the same effects as the unpolarized cross section, a feature which may be experimentally interesting.

The same properties can be observed in the unpolarized or Transverse-Transverse $e^+e^- \rightarrow Z\gamma$, ZZ cross sections and A_{LR} asymmetries. The model dependence is somewhat larger at low energies, but it also vanishes in agreement with the logarithmic rules at high energies. In these processes the "mass suppressed" TL cross sections are strongly decreasing with the energy and model dependent. Up to the 1 TeV range though, these TL cross sections should still be measurable, giving interesting tests of the MSSM models.

In $e^+e^- \rightarrow ZZ$, the LL cross section has peculiar features associated to the Higgs sector. It is strongly decreasing with the energy up to 1 TeV, but above 1 TeV a flattening of the energy dependence appears which depends on the value of the Higgs mass. However this happens at a level which is only marginally observable with the expected LC luminosities.

The $e^+e^- \rightarrow Z\gamma$, ZZ processes are sensitive to the so-called NAGC, $h_3^{\gamma,Z}$ and $f_5^{\gamma,Z}$. Below 1 TeV, the SM and MSSM contributions to these couplings should be marginally observable. But the above processes could give interesting limits on possible additional NP NAGC contributions, which (to the extent they are described by local effective Lagrangians) would lead to contributions growing with the energy.

In conclusion these three processes present a large panel of interesting properties. They are extremely simple at Born level, but extremely rich in information at the one loop level. The $\gamma\gamma$, $Z\gamma$, ZZ final states are complementary for the study of the gauge (gaugino)

sector, the MSSM models, the Higgs sector and the search for Neutral Anomalous Gauge Couplings. They should be considered as a part of the research program at the future high energy colliders, demanding for the highest luminosities. In the very high energy range (several TeV), higher order effects (two loop effects and/or resummation) should also be computed, in order to make really accurate theoretical predictions,. The several TeV domain indeed appears to be the region where the electroweak interactions start becoming strong.

Appendix A: Kinematical details.

According to (1, 2, 3), the invariant amplitude of the process

$$e^-(\lambda, l) + e^+(\lambda', l') \rightarrow V(e, p) + V'(e', p') \quad , \quad (\text{A.1})$$

may be written as

$$F_{\lambda, \mu, \mu'} = \sum_{j=1,9} \bar{v}(\lambda', l') I_j N_j(s, t, u, \lambda) u(\lambda, l) \quad . \quad (\text{A.2})$$

When the electron mass is neglected, so that $\lambda' = -\lambda$ in both the SM and MSSM models, and the 9 invariant forms is (A.2) are

$$\begin{aligned} I_1 &= (e \cdot l)(\gamma \cdot e') & , & \quad I_2 = (e' \cdot l)(\gamma \cdot e) & \quad , & \quad I_3 = (e \cdot l)(e' \cdot l)(\gamma \cdot p), \\ I_4 &= (e \cdot e')(\gamma \cdot p) & \quad , & \quad I_5 = (e \cdot p')(\gamma \cdot e') & \quad , & \quad I_6 = (e \cdot p')(e' \cdot l)(\gamma \cdot p) \quad , \\ I_7 &= (e' \cdot p)(\gamma \cdot e) & \quad , & \quad I_8 = (e' \cdot p)(e \cdot l)(\gamma \cdot p) & \quad , & \quad I_9 = (e \cdot p')(e' \cdot p)(\gamma \cdot p) \quad . \end{aligned} \quad (\text{A.3})$$

The related scalar amplitudes $N_j(s, t, u, \lambda)$ may be split according to the electron helicity as in (3,4).

The transverse and longitudinal amplitudes implied by (A.2), are:

- TT amplitudes, $\mu = \pm 1$ and $\mu' = \pm 1$

$$\begin{aligned} F_{\lambda, \mu, \mu'} &= \frac{s \sin \theta}{4} \left\{ \mu(1 - 2\lambda\mu' \cos \theta)N_1 - \mu'(1 + 2\lambda\mu \cos \theta)N_2 \right. \\ &\quad \left. - \frac{\beta s}{4} \sin^2 \theta (2\lambda\mu\mu')N_3 + \beta(2\lambda)(1 + \mu\mu')N_4 \right\} \quad , \end{aligned} \quad (\text{A.4})$$

- TL amplitudes, $\mu = \pm 1, \mu' = 0$

$$\begin{aligned} F_{\lambda, \mu, 0} &= \frac{s\sqrt{2s}}{8M'} \left\{ - (2\lambda\mu)\beta'_0 \sin^2 \theta N_1 + (\beta + \beta'_0 \cos \theta)(1 + 2\lambda\mu \cos \theta)N_2 \right. \\ &\quad \left. + \frac{\beta s}{4}(\beta + \beta'_0 \cos \theta)(2\lambda\mu) \sin^2 \theta N_3 + 2\beta(1 + 2\lambda\mu \cos \theta)N_7 + \frac{s \beta^2 \sin^2 \theta}{2} 2\lambda\mu N_8 \right\} \quad (\text{A.5}) \end{aligned}$$

- LT amplitudes, $\mu = 0, \mu' = \pm 1$

$$\begin{aligned} F_{\lambda, 0, \mu'} &= \frac{s\sqrt{2s}}{8M'} \left\{ \beta_0(2\lambda\mu') \sin^2 \theta N_2 - (\beta - \beta_0 \cos \theta)(1 - 2\lambda\mu' \cos \theta)N_1 \right. \\ &\quad \left. + \frac{\beta s}{4}(\beta - \beta_0 \cos \theta)(2\lambda\mu') \sin^2 \theta N_3 - 2\beta(1 - 2\lambda\mu' \cos \theta)N_5 \right. \\ &\quad \left. + \frac{s \beta^2 \sin^2 \theta}{2}(2\lambda\mu')N_6 \right\} \quad , \end{aligned} \quad (\text{A.6})$$

- LL amplitudes, $\mu = 0, \mu' = 0$

$$\begin{aligned}
F_{\lambda,0,0} = & \frac{s^2 \sin \theta(2\lambda)}{32MM'} \left\{ 4\beta'_0(\beta - \beta_0 \cos \theta)N_1 - 4\beta_0(\beta + \beta'_0 \cos \theta)N_2 \right. \\
& - \beta s(\beta - \beta_0 \cos \theta)(\beta + \beta'_0 \cos \theta)N_3 - 4\beta(\beta_0\beta'_0 + \beta^2)N_4 \\
& + 8\beta(\beta'_0 N_5 - \beta_0 N_7) - 2s\beta^2(\beta + \beta'_0 \cos \theta)N_6 \\
& \left. - 2s\beta^2(\beta - \beta_0 \cos \theta)N_8 - 4s\beta^3 N_9 \right\} , \tag{A.7}
\end{aligned}$$

where θ is the c.m. scattering angle and

$$\beta \equiv \frac{2|\vec{p}|}{\sqrt{s}} \quad , \quad \beta_0 \equiv \frac{2p_0}{\sqrt{s}} \quad , \quad \beta'_0 \equiv \frac{2p'_0}{\sqrt{s}} \quad ,$$

with $|\vec{p}|$ being the magnitude of the c.m. momenta of the final gauge bosons and p_0, p'_0 their energies.

In the specific case of the process $e^-e^+ \rightarrow \gamma\gamma$, only 4 TT amplitudes appear involving the (N_1, N_2, N_3, N_4) functions. In this case

$$s + t + u = 0 \quad , \quad \beta = \beta_0 = \beta'_0 = 1 \quad .$$

In the case of $e^-e^+ \rightarrow Z\gamma$, where the gauge boson polarization and momenta are defined by $Z(e(\mu), \vec{p})$ and $\gamma(e'(\mu'), \vec{p}')$, there exist only 6 TT and LT amplitudes receiving contributions from (N_1, \dots, N_6) . In this case

$$s + t + u = m_Z^2 \quad , \quad \beta = \beta'_0 = 1 - \frac{m_Z^2}{s} \quad , \quad \beta_0 = 1 + \frac{m_Z^2}{s} \quad .$$

Finally, for $e^-e^+ \rightarrow ZZ$ the complete set of N_1, \dots, N_9 contributes to the 9 TT, TL, LT and LL amplitudes with

$$s + t + u = 2m_Z^2 \quad , \quad \beta^2 = 1 - \frac{4m_Z^2}{s} \quad , \quad \beta_0 = \beta'_0 = 1 \quad .$$

Appendix B: The chargino and neutralino mixing matrices.

The chargino mixing.

The Left flavor space chargino fields of positive and negative electric charge⁸

$$\tilde{\psi}_L^+ = \begin{pmatrix} \tilde{W}^+ \\ \tilde{H}_2^+ \end{pmatrix}_L \quad , \quad \tilde{\psi}_L^- = \begin{pmatrix} \tilde{W}^- \\ \tilde{H}_1^- \end{pmatrix}_L \tag{B.1}$$

⁸See *e.g.* Eqs.(A.26-A.35) in [28].

are related to the mass-eigenstate chargino fields by

$$\tilde{\psi}_{\alpha L}^+ = \sum_{j=1}^2 V_{j\alpha} \eta_{ej} \tilde{\chi}_{jL}^+ \quad , \quad \tilde{\psi}_{\alpha L}^- = \sum_{j=1}^2 U_{j\alpha} \tilde{\chi}_{jL}^- \quad , \quad (\text{B.2})$$

where $\alpha = 1, 2$ counts the charginos in the flavor space, while $j = 1, 2$ in space of the mass eigenstates. Assuming that the MSSM breaking parameters M_1, M_2, μ are real and choosing the arbitrary phases so that $M_2 > 0$, the chargino physical masses may be written as

$$M_{\tilde{\chi}_1, \tilde{\chi}_2} = \frac{1}{\sqrt{2}} [M_2^2 + \mu^2 + 2m_W^2 \mp \tilde{D}]^{1/2} \quad , \quad (\text{B.3})$$

where

$$\tilde{D} \equiv [(M_2^2 + \mu^2 + 2m_W^2)^2 - 4(M_2\mu - m_W^2 \sin(2\beta))^2]^{1/2} \quad , \quad (\text{B.4})$$

while the mixing matrices defined in (B.2) for the negative and positive Left-charginos are

$$U = \begin{pmatrix} \cos \phi_L & \tilde{\mathcal{B}}_L \sin \phi_L \\ -\tilde{\mathcal{B}}_L \sin \phi_L & \cos \phi_L \end{pmatrix} \quad , \quad V = \begin{pmatrix} \cos \phi_R & \tilde{\mathcal{B}}_R \sin \phi_R \\ -\tilde{\mathcal{B}}_R \sin \phi_R & \cos \phi_R \end{pmatrix} \quad (\text{B.5})$$

where ϕ_L, ϕ_R are defined as

$$\begin{aligned} \cos \phi_L &= -\frac{1}{\sqrt{2\tilde{D}}} [\tilde{D} - M_2^2 + \mu^2 + 2m_W^2 \cos 2\beta]^{1/2} \quad , \\ \cos \phi_R &= -\frac{1}{\sqrt{2\tilde{D}}} [\tilde{D} - M_2^2 + \mu^2 - 2m_W^2 \cos 2\beta]^{1/2} \quad , \end{aligned} \quad (\text{B.6})$$

so that they always lie in the second quarter

$$\frac{\pi}{2} \leq \phi_L < \pi \quad , \quad \frac{\pi}{2} \leq \phi_R < \pi \quad . \quad (\text{B.7})$$

Because of this definition $\sin \phi_{L,R}$ are always positive demanding that the appearance of the sign coefficients

$$\begin{aligned} \tilde{\mathcal{B}}_L &= \text{Sign}(\mu \sin \beta + M_2 \cos \beta) \quad , \\ \tilde{\mathcal{B}}_R &= \text{Sign}(\mu \cos \beta + M_2 \sin \beta) \quad , \end{aligned} \quad (\text{B.8})$$

appear in (B.5). In addition the sign-coefficients

$$\begin{aligned} \eta_{e1} &= \text{Sign}(M_2[\tilde{D} - M_2^2 + \mu^2 - 2m_W^2] - 2m_W^2 \mu \sin 2\beta) \quad , \\ \eta_{e2} &= \text{Sign}(\mu[\tilde{D} - M_2^2 + \mu^2 + 2m_W^2] + 2m_W^2 M_2 \sin 2\beta) \quad , \end{aligned} \quad (\text{B.9})$$

also enter (B.2), determining the way the left and right charginos combine in the Dirac field.

For comparison with the notation of [24] we note that the Z^\pm matrices defined there are given by

$$Z_{\alpha j}^+ = V_{j\alpha} \eta_{ej} \quad , \quad Z_{\alpha j}^- = U_{j\alpha} \quad , \quad (\text{B.10})$$

for real M_1 , M_2 and μ parameters.

Using (B.10, B.5), the chargino contribution to (C.24) is then determined from

$$|Z_{1j}^+|^2 = |V_{j1}|^2 \quad . \quad (\text{B.11})$$

The neutralino mixing.

We follow the notation of [25] and continue restricting to real M_1 , M_2 and μ parameters. In the space of the Left neutralino fields

$$\psi_L^0 \equiv \begin{pmatrix} \tilde{B}_L \\ \tilde{W}_L^{(3)} \\ \tilde{H}_{1L}^0 \\ \tilde{H}_{2L}^0 \end{pmatrix} \quad , \quad (\text{B.12})$$

the mass-matrix is of course symmetric and given by

$$Y = \begin{pmatrix} M_1 & 0 & -m_Z s_W \cos \beta & m_Z s_W \sin \beta \\ 0 & M_2 & m_Z c_W \cos \beta & -m_Z c_W \sin \beta \\ -m_Z s_W \cos \beta & m_Z c_W \cos \beta & 0 & -\mu \\ m_Z s_W \sin \beta & -m_Z c_W \sin \beta & -\mu & 0 \end{pmatrix} \quad . \quad (\text{B.13})$$

This is diagonalized through the real orthogonal transformation U^0 giving

$$U^{0\top} Y U^0 = \begin{pmatrix} \tilde{M}_{\tilde{\chi}_1^0} & 0 & 0 & 0 \\ 0 & \tilde{M}_{\tilde{\chi}_2^0} & 0 & 0 \\ 0 & 0 & \tilde{M}_{\tilde{\chi}_3^0} & \\ 0 & 0 & 0 & \tilde{M}_{\tilde{\chi}_4^0} \end{pmatrix} \quad , \quad (\text{B.14})$$

where the real eigenvalues $\tilde{M}_{\tilde{\chi}_j}$ can be of either sign and have been ordered so that

$$|\tilde{M}_{\tilde{\chi}_1^0}| \leq |\tilde{M}_{\tilde{\chi}_2^0}| \leq |\tilde{M}_{\tilde{\chi}_3^0}| \leq |\tilde{M}_{\tilde{\chi}_4^0}| \quad . \quad (\text{B.15})$$

The quantities $\tilde{M}_{\tilde{\chi}_j^0}$ are the "signed" neutralino masses which are directly determined by solving the characteristic equation implied by (B.14) using *e.g.* the formalism in [26] or Eqs.(10-18) in [25]. Their absolute values determine the physical neutralino masses $M_{\tilde{\chi}_j^0}$, while the related signs η_j are determined by

$$\tilde{M}_{\tilde{\chi}_j^0} = \eta_j M_{\tilde{\chi}_j^0} \quad \text{with} \quad \eta_j = \pm 1 \quad . \quad (\text{B.16})$$

Following ([25], the definition ($\tilde{\eta}_j = 1$ or i) is also introduced, so that $\eta_j = \tilde{\eta}_j^2$. The relation between the flavor and mass-eigenstate neutralino fields is then given by

$$\psi_{\alpha L}^0 = \sum_{j=1}^4 U_{\alpha j}^0 \tilde{\eta}_j \tilde{\chi}_{jL}^0 \quad (\text{B.17})$$

where the index α (as well as β in the next paragraph) counts the neutralino flavor components, while the index j refers to the mass-eigenstate ones. Of course both indices run from 1 to 4. The above U^0 neutralino matrix is related to the Z^N one defined in [24] by absorbing it in the $\tilde{\eta}_j$ phases as

$$Z_{\alpha j}^N = U_{\alpha j}^0 \tilde{\eta}_j \quad . \quad (\text{B.18})$$

As shown in [25], all neutralino related physical observables in the case of real (M_1 , M_2 and μ), can then be expressed in terms of the signs η_j , and the four density matrices P_j , ($j = 1, \dots, 4$) describing the flavor composition of each of the four neutralinos. These density matrices act in the flavor space and are given by

$$P_{j\alpha\beta}^0 = U_{\alpha j}^0 U_{\beta j}^0 \quad . \quad (\text{B.19})$$

As expected for any density matrix describing pure states, they have the mathematical properties of projection operators and may be immediately calculated from [25, 27]

$$\begin{aligned} P_1^0 &= \frac{(\tilde{M}_{\tilde{\chi}_4^0} - Y)(\tilde{M}_{\tilde{\chi}_3^0} - Y)(\tilde{M}_{\tilde{\chi}_2^0} - Y)}{(\tilde{M}_{\tilde{\chi}_4^0} - \tilde{M}_{\tilde{\chi}_1^0})(\tilde{M}_{\tilde{\chi}_3^0} - \tilde{M}_{\tilde{\chi}_1^0})(\tilde{M}_{\tilde{\chi}_2^0} - \tilde{M}_{\tilde{\chi}_1^0})} \quad , \\ P_2^0 &= \frac{(\tilde{M}_{\tilde{\chi}_4^0} - Y)(\tilde{M}_{\tilde{\chi}_3^0} - Y)(Y - \tilde{M}_{\tilde{\chi}_1^0})}{(\tilde{M}_{\tilde{\chi}_4^0} - \tilde{M}_{\tilde{\chi}_2^0})(\tilde{M}_{\tilde{\chi}_3^0} - \tilde{M}_{\tilde{\chi}_2^0})(\tilde{M}_{\tilde{\chi}_2^0} - \tilde{M}_{\tilde{\chi}_1^0})} \quad , \\ P_3^0 &= \frac{(\tilde{M}_{\tilde{\chi}_4^0} - Y)(Y - \tilde{M}_{\tilde{\chi}_2^0})(Y - \tilde{M}_{\tilde{\chi}_1^0})}{(\tilde{M}_{\tilde{\chi}_4^0} - \tilde{M}_{\tilde{\chi}_3^0})(\tilde{M}_{\tilde{\chi}_3^0} - \tilde{M}_{\tilde{\chi}_2^0})(\tilde{M}_{\tilde{\chi}_3^0} - \tilde{M}_{\tilde{\chi}_1^0})} \quad , \\ P_4^0 &= \frac{(Y - \tilde{M}_{\tilde{\chi}_3^0})(Y - \tilde{M}_{\tilde{\chi}_2^0})(Y - \tilde{M}_{\tilde{\chi}_1^0})}{(\tilde{M}_{\tilde{\chi}_4^0} - \tilde{M}_{\tilde{\chi}_3^0})(\tilde{M}_{\tilde{\chi}_4^0} - \tilde{M}_{\tilde{\chi}_2^0})(\tilde{M}_{\tilde{\chi}_4^0} - \tilde{M}_{\tilde{\chi}_1^0})} \quad , \end{aligned} \quad (\text{B.20})$$

where Y is given in (B.13).

In terms of by-linear forms of the Z^N mixing matrix defined in (B.18) [24], the above neutralino density matrices and signs satisfy

$$Z_{\alpha j}^N Z_{\beta j}^{N*} = Z_{\alpha j}^{N*} Z_{\beta j}^N = P_{j\alpha\beta}^0 = P_{j\beta\alpha}^0 \quad , \quad (\text{B.21})$$

$$Z_{\alpha j}^N Z_{\beta j}^N = Z_{\alpha j}^{N*} Z_{\beta j}^{N*} = P_{j\alpha\beta}^0 \eta_j = P_{j\beta\alpha}^0 \eta_j \quad , \quad (\text{B.22})$$

which fully describe all neutralino loop contributions.

The chargino and neutralino couplings.

In terms of the chargino and neutralino mixings defined above, we list explicitly below the couplings needed for describing the charginos and neutralino contributions to the Z

and W self-energies. They are given by the interaction Lagrangian

$$\begin{aligned}
\mathbb{L} = & -\frac{e}{2s_W c_W} Z_\mu \left\{ \sum_{i,j=1}^2 \left[O_{ij}^{ZL} \tilde{\chi}_{iL}^+ \gamma^\mu \tilde{\chi}_{jL}^+ + O_{ij}^{ZR} \tilde{\chi}_{iR}^+ \gamma^\mu \tilde{\chi}_{jR}^+ \right] \right. \\
& - \sum_{i,j=1}^4 O_{ij}^{0ZL} \tilde{\chi}_{iL}^0 \gamma^\mu \tilde{\chi}_{jL}^0 \left. \right\} \\
& + gW_\mu^+ \sum_{i=1}^2 \sum_{j=1}^4 \left\{ \tilde{\chi}_i^+ \gamma^\mu \left[O_{ij}^L \frac{(1-\gamma^5)}{2} + O_{ij}^R \frac{(1+\gamma^5)}{2} \right] \tilde{\chi}_j^0 \right. \\
& \left. + gW_\mu^- \sum_{i=1}^2 \sum_{j=1}^4 \left\{ \tilde{\chi}_j^0 \gamma^\mu \left[O_{ij}^{L*} \frac{(1-\gamma^5)}{2} + O_{ij}^{R*} \frac{(1+\gamma^5)}{2} \right] \tilde{\chi}_i^+ \right\} \right. . \quad (\text{B.23})
\end{aligned}$$

The Z -chargino couplings in (B.23) are given by (compare (B.10))

$$\begin{aligned}
O_{ij}^{ZL} &= Z_{1i}^{+*} Z_{1j}^+ + \delta_{ij}(1 - 2s_W^2) = \eta_{ci} \eta_{cj} V_{i1} V_{j1} + \delta_{ij}(1 - 2s_W^2) , \\
O_{ij}^{ZR} &= Z_{1i}^- Z_{1j}^{-*} + \delta_{ij}(1 - 2s_W^2) = U_{i1} U_{j1} + \delta_{ij}(1 - 2s_W^2) , \quad (\text{B.24})
\end{aligned}$$

where (B.5), B.6) are needed. For the neutralino couplings

$$\begin{aligned}
O_{ij}^{0ZL} = O_{ji}^{0ZL*} = -O_{ji}^{0ZR} = -O_{ij}^{0ZR*} &= Z_{4i}^{N*} Z_{4j}^N - Z_{3i}^{N*} Z_{3j}^N \\
&= \tilde{\eta}_i^* \tilde{\eta}_j (U_{4i}^0 U_{4j}^0 - U_{3i}^0 U_{3j}^0) , \quad (\text{B.25})
\end{aligned}$$

the needed bilinear terms are

$$\begin{aligned}
O_{ij}^{0ZL} O_{ji}^{0ZL} = O_{ij}^{0ZR} O_{ji}^{0ZR} &= P_{i33}^0 P_{j33}^0 + P_{i44}^0 P_{j44}^0 - 2P_{i34}^0 P_{j34}^0 , \\
O_{ij}^{0ZL} O_{ji}^{0ZR} = O_{ij}^{0ZR} O_{ji}^{0ZL} &= -\eta_i \eta_j [P_{i33}^0 P_{j33}^0 + P_{i44}^0 P_{j44}^0 - 2P_{i34}^0 P_{j34}^0] , \quad (\text{B.26})
\end{aligned}$$

fully defined in terms of the neutralino density matrices in (B.20).

Finally, the W -couplings in (B.23) are given using (B.5, B.10, B.17, B.18)

$$\begin{aligned}
O_{ij}^L &= Z_{1i}^+ Z_{2j}^N - \frac{1}{\sqrt{2}} Z_{2i}^+ Z_{4j}^N = \eta_{ci} \tilde{\eta}_j (V_{i1} U_{2j}^0 - \frac{1}{\sqrt{2}} V_{i2} U_{4j}^0) , \\
O_{ij}^R &= Z_{1i}^- Z_{2j}^{N*} + \frac{1}{\sqrt{2}} Z_{2i}^- Z_{3j}^{N*} = \tilde{\eta}_j^* (U_{i1} U_{2j}^0 + \frac{1}{\sqrt{2}} U_{i2} U_{3j}^0) , \quad (\text{B.27})
\end{aligned}$$

where the first index counts the chargino and the second the neutralino. The corresponding bilinears needed for the W -self-energies are

$$\begin{aligned}
O_{ij}^L O_{ij}^{L*} + O_{ij}^R O_{ij}^{R*} &= [(V_{i1})^2 + (U_{i1})^2] P_{j22}^0 + \frac{1}{2} [(V_{i2})^2 P_{j44}^0 + (U_{i2})^2 P_{j33}^0] \\
&\quad - \sqrt{2} V_{i1} V_{i2} P_{j24}^0 + \sqrt{2} U_{i1} U_{i2} P_{j23}^0 , \\
O_{ij}^L O_{ij}^{R*} + O_{ij}^{L*} O_{ij}^R &= 2\eta_{ci} \eta_j \left[V_{i1} U_{i1} P_{j22}^0 + \frac{1}{\sqrt{2}} V_{i1} U_{i2} P_{j23}^0 \right. \\
&\quad \left. - \frac{1}{\sqrt{2}} V_{i2} U_{i1} P_{j24}^0 - \frac{1}{2} V_{i2} U_{i2} P_{j34}^0 \right] . \quad (\text{B.28})
\end{aligned}$$

The use of (B.18) allows to express the neutralino contribution to (C.24) in terms of the neutralino density matrix elements defined in (B.20) through

$$\begin{aligned} |Z_{1j}^N s_W + Z_{2j}^N c_W|^2 &= P_{j11}^0 s_W^2 + P_{j22}^0 c_W^2 + 2s_W c_W P_{j12}^0 \\ |Z_{1j}^N|^2 &= P_{j11}^0 \quad . \end{aligned} \quad (\text{B.29})$$

Finally we should emphasize that for calculating the virtual chargino and neutralino contributions, it is essential that all masses and couplings are calculated together at the same accuracy, from the "electroweak scale" values of M_2 , M_1 , μ , $\tan\beta$; otherwise the chargino-neutralino contribution to *e.g.* the renormalized gauge self energies will not be finite, inducing spurious scale dependencies to the numerical results.

Appendix C: Gauge self-energies, Electron self-energies and renormalization constants.

C1) Gauge self-energies.

The needed gauge renormalization constants are expressed (using the renormalization conditions, [19]) in terms of gauge self-energies denoted by⁹ $\Sigma_{VV'}$ are given in Appendix B, for SM and the generic minimal MSSM case.

Using the unrenormalized gauge self-energies and (18), the gauge wave-function renormalization constants satisfy (compare (17))

$$\begin{aligned} \delta Z_W &= -\Re\left(\Sigma'_{\gamma\gamma}(0) - \frac{2c_W}{s_W m_Z^2} \Sigma_{\gamma Z}(0) + \frac{1}{s_W^2 m_Z^2} \left[\Sigma_{WW}(m_W^2) - c_W^2 \Sigma_{ZZ}(m_Z^2) \right]\right) , \\ \delta Z_B &= -\Re\left(\Sigma'_{\gamma\gamma}(0) + \frac{2s_W}{c_W m_Z^2} \Sigma_{\gamma Z}(0) - \frac{1}{c_W^2 m_Z^2} \left[\Sigma_{WW}(m_W^2) - c_W^2 \Sigma_{ZZ}(m_Z^2) \right]\right) , \end{aligned} \quad (\text{C.1})$$

while the additional renormalization needed for the $SU(2)$ gauge coupling is

$$\delta \tilde{Z}_2 = \frac{1}{m_Z^2 s_W c_W} \Sigma_{\gamma Z}(0) \quad . \quad (\text{C.2})$$

Using (C.1), we then write the derivative of the renormalized Z-self-energy and the γZ -mixing at the Z -shell contributions entering (11, 13) as

$$\begin{aligned} \hat{\Sigma}'_{ZZ}(m_Z^2) &= \Sigma'_{ZZ}(m_Z^2) + c_W^2 \delta Z_W + s_W^2 \delta Z_B \quad , \\ \hat{\Sigma}_{\gamma Z}(m_Z^2) &= \Sigma_{\gamma Z}(m_Z^2) + m_Z^2 s_W c_W (\delta Z_W - \delta Z_B - \delta \tilde{Z}_2) \quad . \end{aligned} \quad (\text{C.3})$$

⁹To define their phase we give their relation to the S-matrix element as $S_{fi} = -ig_{\mu\nu} \Sigma_{VV'}$. The various couplings are defined as in [24]. See also *e.g.* [3, 28].

We now give the expressions for the various contributions to the transverse unrenormalized gauge self-energies in the MSSM (without CP-violation) and at the end of this part we give the recipe for restricting to the SM case. The relevant MSSM couplings for the chargino and neutralino loops are summarized in Appendix A. In each case, we first give the contributions from the gauge bosons, from the two Higgs doublets, from the standard quarks and leptons with isospin I_3^f , charge Q_f and Z-couplings

$$v_f = \frac{I_3^f - 2Q_f s_W^2}{2s_W c_W} \quad , \quad a_f = \frac{I_3^f}{2s_W c_W} \quad , \quad (\text{C.4})$$

subsequently the contribution from a sfermion \tilde{f} whose mixing angles we denote as

$$c_{\tilde{\theta}_f} = \cos(\tilde{\theta}_f) \quad , \quad s_{\tilde{\theta}_f} = \sin(\tilde{\theta}_f) \quad ,$$

following the same notation as in [3], and finally the contribution from the chargino and/or neutralino loop.

All soft MSSM breaking parameters and μ are taken as real, and the phases of the appropriate fields are selected so that $M_2 > 0$.

Contributions to $\Sigma_{ZZ}(k^2)$.

The respective W plus Higgs, fermion and sfermion contributions to the Z -self-energy are

$$\begin{aligned} \Sigma_{ZZ}(k; \text{gauge} + 2\text{H}) &= \frac{\alpha}{4\pi s_W^2 c_W^2} \left\{ \sin^2(\beta - \alpha) [m_Z^2 B_0^{Zh^0} - B_{22}^{Zh^0} - B_{22}^{A^0 H^0}] \right. \\ &+ \cos^2(\beta - \alpha) [m_Z^2 B_0^{ZH^0} - B_{22}^{ZH^0} - B_{22}^{A^0 h^0}] - \cos^2(2\theta_W) B_{22}^{H^+ H^+} + \frac{1}{4} [A^{h^0} + A^{H^0} \\ &+ A^{A^0} + A^Z] + \frac{\cos^2(2\theta_W)}{2} A^{H^+} - [8c_W^4 + \cos^2(2\theta_W)] B_{22}^{WW} \\ &\left. - [4c_W^4 k^2 + 2m_W^2 \cos(2\theta_W)] B_0^{WW} + \frac{1}{2} [12c_W^4 - 4c_W^2 + 1] A^W - \frac{2}{3} c_W^4 k^2 \right\} \quad , \quad (\text{C.5}) \end{aligned}$$

$$\begin{aligned} \Sigma_{ZZ}(k; f) &= -\frac{\alpha}{\pi} \sum_f N_c^f \left\{ (v_f^2 + a_f^2) [-2B_{22}^{ff} + A^f + (m_f^2 - \frac{k^2}{2}) B_0^{ff}] \right. \\ &\left. - (v_f^2 - a_f^2) m_f^2 B_0^{ff} \right\} \quad , \quad (\text{C.6}) \end{aligned}$$

$$\begin{aligned} \Sigma_{ZZ}(k; \tilde{f}) &= -\frac{\alpha}{4\pi s_W^2 c_W^2} \sum_f N_c^f \left\{ 4[I_3^f c_{\tilde{\theta}_f}^2 - Q_f s_W^2]^2 B_{22}^{\tilde{f}_1 \tilde{f}_1} + s_{\tilde{\theta}_f}^2 c_{\tilde{\theta}_f}^2 [B_{22}^{\tilde{f}_1 \tilde{f}_2} + B_{22}^{\tilde{f}_2 \tilde{f}_1}] \right. \\ &+ 4[I_3^f s_{\tilde{\theta}_f}^2 - Q_f s_W^2]^2 B_{22}^{\tilde{f}_2 \tilde{f}_2} - 2[(I_3^f - Q_f s_W^2)^2 c_{\tilde{\theta}_f}^2 + Q_f^2 s_W^4 s_{\tilde{\theta}_f}^2] A^{\tilde{f}_1} \\ &\left. - 2[(I_3^f - Q_f s_W^2)^2 s_{\tilde{\theta}_f}^2 + Q_f^2 s_W^4 c_{\tilde{\theta}_f}^2] A^{\tilde{f}_2} \right\} \quad . \quad (\text{C.7}) \end{aligned}$$

In (C.6, C.7) N_c^f is 3 or 1, depending on whether f is a quark or a lepton respectively. For the neutralino and chargino contributions we get

$$\begin{aligned} \Sigma_{ZZ}(k; \tilde{\chi}_j^0) &= -\frac{\alpha}{8\pi s_W^2 c_W^2} \sum_{i,j=1}^4 \left(P_{i33}^0 P_{j33}^0 + P_{i44}^0 P_{j44}^0 - 2P_{i34}^0 P_{j34}^0 \right) \cdot \left[-2B_{22}^{\tilde{\chi}_i^0 \tilde{\chi}_j^0} \right. \\ &\quad \left. + A^{\tilde{\chi}_j^0} + M_{\tilde{\chi}_i^0} (M_{\tilde{\chi}_i^0} + \eta_i \eta_j M_{\tilde{\chi}_j^0}) B_0^{\tilde{\chi}_i^0 \tilde{\chi}_j^0} + k^2 B_1^{\tilde{\chi}_i^0 \tilde{\chi}_j^0} \right] , \end{aligned} \quad (\text{C.8})$$

$$\begin{aligned} \Sigma_{ZZ}(k; \tilde{\chi}_j^\pm) &= -\frac{\alpha}{8\pi s_W^2 c_W^2} \sum_{i,j=1}^2 \left\{ \left(O_{ij}^{ZL} O_{ji}^{ZL} + O_{ij}^{ZR} O_{ji}^{ZR} \right) \left[-2B_{22}^{\tilde{\chi}_i^\pm \tilde{\chi}_j^\pm} + A^{\tilde{\chi}_j^\pm} \right. \right. \\ &\quad \left. \left. + M_{\tilde{\chi}_j^\pm}^2 B_0^{\tilde{\chi}_i^\pm \tilde{\chi}_j^\pm} + k^2 B_1^{\tilde{\chi}_i^\pm \tilde{\chi}_j^\pm} \right] - \left(O_{ij}^{ZL} O_{ji}^{ZR} + O_{ij}^{ZR} O_{ji}^{ZL} \right) M_{\tilde{\chi}_i^\pm} M_{\tilde{\chi}_j^\pm} B_0^{\tilde{\chi}_i^\pm \tilde{\chi}_j^\pm} \right\} . \end{aligned} \quad (\text{C.9})$$

Contributions to $\Sigma_{\gamma\gamma}(k^2)$.

The respective W plus Higgs, fermion, sfermion and chargino contributions to the photon self-energy are

$$\begin{aligned} \Sigma_{\gamma\gamma}(k; \text{gauge} + 2\text{H}) &= -\frac{\alpha}{2\pi} \left\{ 6B_{22}^{WW} + 2B_{22}^{H^+H^+} - A^{H^+} - 3A^W \right. \\ &\quad \left. + 2k^2 B_0^{WW} + \frac{k^2}{3} \right\} , \end{aligned} \quad (\text{C.10})$$

$$\Sigma_{\gamma\gamma}(k; f) = -\frac{\alpha}{\pi} \sum_f N_c^f Q_f^2 \left\{ -2B_{22}^{ff} + A^f - \frac{k^2}{2} B_0^{ff} \right\} , \quad (\text{C.11})$$

$$\Sigma_{\gamma\gamma}(k; \tilde{f}) = -\frac{\alpha}{2\pi} \sum_f N_c^f Q_f^2 \left\{ -A^{\tilde{f}_1} - A^{\tilde{f}_2} + 2B_{22}^{\tilde{f}_1 \tilde{f}_1} + 2B_{22}^{\tilde{f}_2 \tilde{f}_2} \right\} , \quad (\text{C.12})$$

$$\Sigma_{\gamma\gamma}(k; \tilde{\chi}_j^\pm) = -\frac{\alpha}{\pi} \sum_{j=1}^2 \left\{ -2B_{22}^{\tilde{\chi}_j^\pm \tilde{\chi}_j^\pm} + A^{\tilde{\chi}_j^\pm} - \frac{k^2}{2} B_0^{\tilde{\chi}_j^\pm \tilde{\chi}_j^\pm} \right\} . \quad (\text{C.13})$$

Contributions to $\Sigma_{\gamma Z}(k^2)$.

The respective W plus Higgs, fermion, sfermion and chargino contributions to the photon- Z mixing are

$$\begin{aligned} \Sigma_{\gamma Z}(k; \text{gauge} + 2\text{H}) &= -\frac{\alpha}{4\pi} \left\{ \frac{\cos(2\theta_W)}{s_W c_W} \left[-A^W - A^{H^+} + 2B_{22}^{H^+H^+} + 2B_{22}^{WW} \right] \right. \\ &\quad \left. + \frac{c_W}{s_W} \left[8B_{22}^{WW} - 4A^W + (2m_Z^2 + 4k^2) B_0^{WW} + \frac{2k^2}{3} \right] + 2m_Z^2 s_W c_W B_0^{WW} \right\} , \end{aligned} \quad (\text{C.14})$$

$$\Sigma_{\gamma Z}(k; f) = -\frac{\alpha}{\pi} \sum_f N_c^f Q_f v_f \left[A^f - 2B_{22}^{ff} - \frac{k^2}{2} B_0^{ff} \right] , \quad (\text{C.15})$$

$$\Sigma_{\gamma Z}(k; \tilde{f}) = -\frac{\alpha}{2\pi s_W c_W} \sum_f N_c^f Q_f \left\{ (I_3^f c_{\theta_f}^2 - Q_f s_W^2) (2B_{22}^{\tilde{f}_1 \tilde{f}_1} - A^{\tilde{f}_1}) \right.$$

$$+(I_3^f s_{\theta_f}^2 - Q_f s_W^2)(2B_{22}^{\tilde{f}_2\tilde{f}_2} - A^{\tilde{f}_2}) \} , \quad (\text{C.16})$$

$$\Sigma_{\gamma Z}(k; \tilde{\chi}_j) = -\frac{\alpha}{4\pi s_W c_W} \sum_{j=1}^2 (O_{jj}^{ZL} + O_{jj}^{ZR}) [A^{\tilde{\chi}_j^+} - 2B_{22}^{\tilde{\chi}_j^+ \tilde{\chi}_j^+} - \frac{k^2}{2} B_0^{\tilde{\chi}_j^+ \tilde{\chi}_j^+}] . \quad (\text{C.17})$$

Contributions to $\Sigma_{WW}(k^2)$.

The respective gauge plus Higgs, fermion and sfermion contributions to the W self-energy are

$$\begin{aligned} \Sigma_{WW}(k; \text{gauge} + 2\text{H}) &= \frac{\alpha}{4\pi s_W^2} \left\{ \frac{1}{4} [A^{H^0} + A^{h^0} + (1 + 8c_W^2)A^Z + A^{A^0} + 10A^W + 2A^{H^+}] \right. \\ &+ \cos^2(\beta - \alpha) [m_W^2 B_0^{H^0 W} - B_{22}^{H^0 W} - B_{22}^{h^0 H^+}] + \sin^2(\beta - \alpha) [m_W^2 B_0^{h^0 W} - B_{22}^{h^0 W} - B_{22}^{H^0 H^+}] \\ &- B_{22}^{A^0 H^+} - (1 + 8c_W^2) B_{22}^{ZW} - 8s_W^2 B_{22}^{\gamma W} + (m_Z^2 - 3m_W^2 - 4c_W^2 k^2) B_0^{ZW} \\ &\left. - 4s_W^2 k^2 B_0^{\gamma W} - \frac{2k^2}{3} \right\} , \quad (\text{C.18}) \end{aligned}$$

$$\Sigma_{WW}(k; f) = \frac{\alpha}{4\pi s_W^2} \sum_{f_{\text{doublet}}} N_c^f \left\{ 2B_{22}^{du} - \frac{A^u + A^d}{2} + \frac{(k^2 - m_d^2 - m_u^2)}{2} B_0^{du} \right\} , \quad (\text{C.19})$$

$$\begin{aligned} \Sigma_{WW}(k; \tilde{f}) &= -\frac{\alpha}{2\pi s_W^2} \sum_{f_{\text{doublet}}} N_c^f \left\{ c_{\tilde{\theta}_u}^2 c_{\tilde{\theta}_d}^2 B_{22}^{\tilde{d}_1 \tilde{u}_1} + c_{\tilde{\theta}_u}^2 s_{\tilde{\theta}_d}^2 B_{22}^{\tilde{d}_2 \tilde{u}_1} + s_{\tilde{\theta}_u}^2 c_{\tilde{\theta}_d}^2 B_{22}^{\tilde{d}_1 \tilde{u}_2} \right. \\ &\left. + s_{\tilde{\theta}_u}^2 s_{\tilde{\theta}_d}^2 B_{22}^{\tilde{d}_2 \tilde{u}_2} - \frac{1}{4} [c_{\tilde{\theta}_u}^2 A^{\tilde{u}_1} + s_{\tilde{\theta}_u}^2 A^{\tilde{u}_2} + c_{\tilde{\theta}_d}^2 A^{\tilde{d}_1} + s_{\tilde{\theta}_d}^2 A^{\tilde{d}_2}] \right\} , \quad (\text{C.20}) \end{aligned}$$

where the summation in (C.19, C.20) is over the fermion doublets $f_{\text{doublet}} = (u, d)$ with color factor N_c^f . Finally the chargino-neutralino loop gives

$$\begin{aligned} \Sigma_{WW}(k; \tilde{\chi}_i^+, \tilde{\chi}_j^0) &= -\frac{\alpha}{2\pi s_W^2} \sum_{i,j} \left\{ \left(O_{ij}^L O_{ij}^{L*} + O_{ij}^R O_{ij}^{R*} \right) \left[-2B_{22}^{\tilde{\chi}_i^+ \tilde{\chi}_j^0} + \frac{1}{2} (A^{\tilde{\chi}_i^+} + A^{\tilde{\chi}_j^0}) \right. \right. \\ &\left. \left. - \frac{1}{2} (k^2 - M_{\tilde{\chi}_i^+}^2 - M_{\tilde{\chi}_j^0}^2) B_0^{\tilde{\chi}_i^+ \tilde{\chi}_j^0} \right] - \left(O_{ij}^L O_{ij}^{R*} + O_{ij}^{L*} O_{ij}^R \right) M_{\tilde{\chi}_i^+} M_{\tilde{\chi}_j^0} B_0^{\tilde{\chi}_i^+ \tilde{\chi}_j^0} \right\} . \quad (\text{C.21}) \end{aligned}$$

The above expressions refer to the MSSM case. In the SM case, one should suppress the sfermion, chargino, neutralino, H^+ , A^0 and H^0 contributions. The h^0 contribution is then identified with the H_{SM} one, provided we put $\alpha = \beta - \pi/2$.

C2) Electron self-energies

The unrenormalized electron self-energy¹⁰ defined by

$$\Sigma_e(q) = \not{q} \frac{(1 - \gamma^5)}{2} \Sigma_{Le}(q^2) + \not{q} \frac{(1 + \gamma^5)}{2} \Sigma_{Re}(q^2) , \quad (\text{C.22})$$

¹⁰Its phase is related to the corresponding S-matrix element by $S_{ee} = i\Sigma_e$.

receives contributions from SM (photon, Z and W loops)

$$\begin{aligned}\Sigma_{Le}^{\text{SM}}(q^2) &= -\frac{\alpha}{2\pi} \left[B_1^{(e\gamma)}(q^2) + \frac{(2s_W^2 - 1)^2}{4s_W^2 c_W^2} B_1^{(eZ)}(q^2) + \frac{1}{2s_W^2} B_1^{(\nu W)}(q^2) + \frac{1 + 2c_W^2}{8s_W^2 c_W^2} \right] , \\ \Sigma_{Re}^{\text{SM}}(q^2) &= -\frac{\alpha}{2\pi} \left[B_1^{(e\gamma)}(q^2) + \frac{s_W^2}{c_W^2} B_1^{(eZ)}(q^2) + \frac{1}{2c_W^2} \right] ,\end{aligned}\tag{C.23}$$

and from the MSSM chargino and neutralino loops

$$\begin{aligned}\Sigma_{Le}^{\tilde{\chi}^\pm, \tilde{\chi}^0}(q^2) &= -\frac{\alpha}{4\pi s_W^2} \left[\frac{1}{2c_W^2} \sum_{j=1}^4 |Z_{1j}^N s_W + Z_{2j}^N c_W|^2 B_1^{(\tilde{\chi}_j^0 \tilde{e}_L)}(q^2) \right. \\ &\quad \left. + \sum_{j=1}^2 |Z_{1j}^+|^2 B_1^{(\tilde{\chi}_j \tilde{\nu}_L)}(q^2) \right] , \\ \Sigma_{Re}^{\tilde{\chi}^0}(q^2) &= -\frac{\alpha}{2\pi c_W^2} \sum_{j=1}^4 |Z_{1j}^N|^2 B_1^{(\tilde{\chi}_j^0 \tilde{e}_R)}(q^2) .\end{aligned}\tag{C.24}$$

The sum of (C.23) and (C.24) gives of course the total contribution to the electron self energy at the 1-loop level.

The electron renormalization constants are given by

$$\delta Z_{Le} \equiv Z_{Le} - 1 = -\Sigma_{Le}(0) \quad , \quad \delta Z_{Re} \equiv Z_{Re} - 1 = -\Sigma_{Re}(0) \quad ,\tag{C.25}$$

and the renormalized electron self-energies are as:

$$\begin{aligned}\hat{\Sigma}_{Le}(q^2) &= \Sigma_{Le}(q^2) + \delta Z_{Le} \quad , \\ \hat{\Sigma}_{Re}(q^2) &= \Sigma_{Re}(q^2) + \delta Z_{Re} \quad .\end{aligned}\tag{C.26}$$

All these contributions from the electron and gauge self energies have been included the renormalized Born contributions of Sect.3.2.

We may also remark that the renormalized electron self-energy contributions are induced by the t - and u -channel electron exchanges in Fig.1c and the related counter-terms. Since the residue of the renormalized electron propagator implied by (C.25) is unity, the contribution from a diagrams like in Fig.1a is cancelled by that induced from the electron self-energy counter term.

The terms involving the renormalized gauge boson self energies in Section 3.2 are generated by the non-unit residue of the renormalized Z -propagator and the non-vanishing γZ -mixing at the Z -mass shell. These contributions arise from diagrams like Fig.1b and the related gauge self-energy counter terms. Finally, the remaining renormalization contributions involving δZ_{Le} , δZ_{Re} and $\delta \tilde{Z}_2$ arise from the counter terms to the Vee vertices.

Asymptotic expression of the internal electron self-energies

For $x \equiv t, u$ much larger than all masses M in the loop, electron renormalized self-energies

behave like

$$\Sigma_{Le}(x) \rightarrow -\frac{\alpha}{4\pi} \left[\left(\frac{1+2c_W^2}{4s_W^2 c_W^2} \right)_{\text{SM}} + \left(\frac{1+2c_W^2}{4s_W^2 c_W^2} \right)_{\text{MSSM}} \right] \ln \frac{|x|}{M^2} , \quad (\text{C.27})$$

$$\Sigma_{Re}(x) \rightarrow -\frac{\alpha}{4\pi} \left[\left(\frac{1}{c_W^2} \right)_{\text{SM}} + \left(\frac{1}{c_W^2} \right)_{\text{MSSM}} \right] \ln \frac{|x|}{M^2} . \quad (\text{C.28})$$

These expressions will be useful for calculating the asymptotic expressions for the amplitudes $e^-e^+ \rightarrow VV'$.

Appendix D: Details of triangle contributions.

We express here, in terms of Passarino-Veltman functions, the triangle contributions to the quantities defined in Sect.3.3. The expressions are labeled by referring to the particles (abc) running inside the loops in Fig.1d,e,f. Through an arrow (\rightarrow) we also indicate the leading logarithmic terms arising in the asymptotic regime, together with the divergent part $\Delta = \frac{1}{\epsilon} - \gamma + \ln(4\pi)$.

- $e^-e^+ \rightarrow \gamma\gamma$

The contributions from Fig.1d, where the three particles running along the loop are indicated as upper indices, are:

$$b_{(\gamma \text{ or } Z)}^L(t) = b_{(\gamma \text{ or } Z)}^R(t) = -2[t(C_{12} + C_{23} + C_{11} + C_0) + 2C_{24} - 4]^{(\gamma ee \text{ or } Zee)} \rightarrow -(\Delta + \ln \frac{|t|}{m_Z^2}) ,$$

$$b_W^L(t) = [-t(C_{12} + 2C_{23} + 2C_{11}) - 12C_{24} + 8]^{(\nu_e WW)} \rightarrow -3\Delta + \ln^2 \frac{|t|}{m_W^2} ,$$

$$b_{2\tilde{\chi}}^L(t) = \sum_i |Z_{1i}^+|^2 [t(C_{12} + C_{13}) + 2C_{24} - \frac{1}{2} - M_{\tilde{\chi}_i}^2 C_0]^{(\tilde{\nu}_e \tilde{\chi}_i^+ \tilde{\chi}_i^+)} \rightarrow \frac{1}{2}(\Delta - \ln \frac{|t|}{M^2}) ,$$

$$b_{1\tilde{\chi}}^L(t) = \sum_i |Z_{1i}^N s_W + Z_{2i}^N c_W|^2 [C_{24}]^{(\tilde{\chi}_i^0 \tilde{e}_L \tilde{e}_L)} \rightarrow \frac{1}{4}(\Delta - \ln \frac{|t|}{M^2}) ,$$

$$b_{1\tilde{\chi}}^R(t) = \sum_i |Z_{1i}^N|^2 [C_{24}]^{(\tilde{\chi}_i^0 \tilde{e}_R \tilde{e}_R)} \rightarrow \frac{1}{4}(\Delta - \ln \frac{|t|}{M^2}) ,$$

$$a_{(\gamma \text{ or } Z)}^L(t) = a_{(\gamma \text{ or } Z)}^R(t) = 4t[C_0 + C_{11} + C_{12} + C_{23}]^{(\gamma ee \text{ or } Zee)} \rightarrow 4 \ln \frac{|t|}{m_Z^2} ,$$

$$a_W^L(t) = 2t[C_{11} - C_{12} - 2C_{23}]^{(\nu_e WW)} \rightarrow -\ln^2 \frac{|t|}{m_W^2} ,$$

$$a_{2\tilde{\chi}}^L(t) = -2t \sum_i |Z_{1i}^+|^2 [C_{12} + C_{23}]^{(\tilde{\nu}_e \tilde{\chi}_i^+ \tilde{\chi}_i^+)} \rightarrow 0 ,$$

$$\begin{aligned}
a_{1\tilde{\chi}}^L(t) &= t \sum_i |Z_{1i}^N s_W + Z_{2i}^N c_W|^2 [C_{12} + C_{23}]^{(\tilde{\chi}_i^0 \tilde{e}_L \tilde{e}_L)} \rightarrow 0 \quad , \\
a_{1\tilde{\chi}}^R(t) &= t \sum_i |Z_{1i}^N|^2 [C_{12} + C_{23}]^{(\tilde{\chi}_i^0 \tilde{e}_R \tilde{e}_R)} \rightarrow 0 \quad .
\end{aligned} \tag{D.1}$$

The only other triangular contribution, arising from Fig.1e and involving the $(\nu_e WW)$ string and the 4-leg $WW\gamma\gamma$ coupling, is

$$N_1''^\gamma = -\frac{1}{s_W^2} [C_0 + C_{11} - C_{12}]^{(\nu_e WW)} \rightarrow -\frac{2}{s_W^2 s} \ln \frac{s}{m_W^2} \quad . \tag{D.2}$$

• $e^- e^+ \rightarrow ZZ$

The diagram of Fig.1d now gives

$$\begin{aligned}
b_{(\gamma \text{ or } Z)}^L(t) &= b_{(\gamma \text{ or } Z)}^R(t) = -2[t(C_{12} + C_{23} + C_{11} + C_0) + 2C_{24} - 4 \\
&+ m_Z^2(C_{22} - C_{23} - C_{11} - C_0)]^{(\gamma ee \text{ or } Zee)} \rightarrow -(\Delta + \ln \frac{|t|}{m_Z^2}) \quad , \\
b_W''^L(t) &= -2[t(C_{12} + C_{23} + C_{11} + C_0) + m_Z^2(C_{22} - C_{23} - C_{11} - C_0) \\
&+ 2C_{24} - 4]^{(W\nu_e\nu_e)} \rightarrow -(\Delta + \ln \frac{|t|}{m_W^2}) \quad , \\
b_W^L(t) &= [-t(C_{12} + 2C_{23} + 2C_{11}) + 2m_Z^2(C_{11} + C_{23} - C_{22}) - 12C_{24} + 8]^{(\nu_e WW)} \\
&\rightarrow -3\Delta + \ln^2 \frac{|t|}{m_W^2} \quad , \\
b_{2\tilde{\chi}}^L(t) &= \sum_{ij} (Z_{1i}^{N*} s_W + Z_{2i}^{N*} c_W)(Z_{4i}^N Z_{4j}^{N*} - Z_{3i}^N Z_{3j}^{N*})(Z_{1j}^N s_W + Z_{2j}^N c_W)[t(C_{12} + C_{23}) \\
&+ m_Z^2(C_{22} - C_{23}) + 2C_{24} - \frac{1}{2} + M_{\tilde{\chi}_i^0} M_{\tilde{\chi}_j^0} (Z_{4i}^{N*} Z_{4j}^N - Z_{3i}^{N*} Z_{3j}^N) C_0]^{(\tilde{e}_L \tilde{\chi}_i^0 \tilde{\chi}_j^0)} \rightarrow 0 \quad , \\
b_{2\tilde{\chi}}''^L(t) &= \sum_{ij} Z_{1i}^{+*} Z_{1j}^+ \{ [Z_{1i}^+ Z_{1j}^{+*} + \delta_{ij}(1 - 2s_W^2)] [t(C_{12} + C_{23}) + m_Z^2(C_{22} - C_{23}) + \\
&+ 2C_{24} - \frac{1}{2}] - [Z_{1i}^{-*} Z_{1j}^- + \delta_{ij}(1 - 2s_W^2)] M_{\tilde{\chi}_i^+} M_{\tilde{\chi}_j^+} C_0 \}^{(\tilde{\nu}_e \tilde{\chi}_i^+ \tilde{\chi}_j^+)} \rightarrow c_W^2 (\Delta - \ln \frac{|t|}{M^2}) \quad , \\
b_{1\tilde{\chi}}^L(t) &= \sum_i |Z_{1i}^+|^2 [C_{24}]^{(\tilde{\chi}_i^+ \tilde{\nu}_e \tilde{\nu}_e)} \rightarrow \frac{1}{4} (\Delta - \ln \frac{|t|}{M^2}) \quad , \\
b_{1\tilde{\chi}}''^L(t) &= (1 - 2s_W^2) \sum_i |Z_{1i}^N s_W + Z_{2i}^N c_W|^2 [C_{24}]^{(\tilde{\chi}_i^0 \tilde{e}_L \tilde{e}_L)} \rightarrow \frac{(1 - 2s_W^2)}{4} (\Delta - \ln \frac{|t|}{M^2}) \quad , \\
b_{1\tilde{\chi}}''^R(t) &= -8s_W^4 \sum_i |Z_{1i}^N|^2 [C_{24}]^{(\tilde{\chi}_i^0 \tilde{e}_R \tilde{e}_R)} \rightarrow -2s_W^4 (\Delta - \ln \frac{|t|}{M^2}) \quad , \\
b_{2\tilde{\chi}}^R(t) &= -4s_W^2 \sum_{ij} Z_{1i}^N Z_{1j}^{N*} [Z_{4i}^{N*} Z_{4j}^N - Z_{3i}^{N*} Z_{3j}^N] [t(C_{12} + C_{23}) + m_Z^2(C_{22} - C_{23}) \\
&+ 2C_{24} - \frac{1}{2} + M_{\tilde{\chi}_i^0} M_{\tilde{\chi}_j^0} [Z_{4i}^N Z_{4j}^{N*} - Z_{3i}^N Z_{3j}^{N*}] C_0]^{(\tilde{e}_R \tilde{\chi}_i^0 \tilde{\chi}_j^0)} \rightarrow 0 \quad ,
\end{aligned}$$

$$\begin{aligned}
a_W^{\prime L}(t) &= 2t[C_{11} - C_{12} - 2C_{23}]^{\nu_e WW} \rightarrow -\ln^2 \frac{|t|}{m_W^2}, \\
a_W^{\prime\prime L}(t) &= 4t[C_0 + C_{11} + C_{12} + C_{23}]^{(W\nu_e\nu_e)} \rightarrow 4\ln \frac{|t|}{m_W^2}, \\
a_{2\tilde{\chi}}^{\prime L}(t) &= -2t \sum_{ij} (Z_{1i}^{N*} s_W + Z_{2i}^{N*} c_W)(Z_{4i}^N Z_{4j}^{N*} - Z_{3i}^N Z_{3j}^{N*})(Z_{1j}^N s_W + Z_{2j}^N c_W) \\
&\cdot [C_{12} + C_{23}]^{(\tilde{e}_L \tilde{\chi}_i^0 \tilde{\chi}_j^0)} \rightarrow 0, \\
a_{2\tilde{\chi}}^{\prime\prime L}(t) &= -2t \sum_{ij} Z_{1i}^+ Z_{1j}^{+*} [Z_{1i}^+ Z_{1j}^{+*} + \delta_{ij}(1 - 2s_W^2)] [C_{12} + C_{23}]^{(\tilde{\nu}_e \tilde{\chi}_i^+ \tilde{\chi}_j^+)} \rightarrow 0, \\
a_{1\tilde{\chi}}^{\prime L}(t) &= t \sum_i |Z_{1i}^+|^2 [C_{12} + C_{23}]^{(\tilde{\chi}_i^+ \tilde{\nu}_e \tilde{\nu}_e)} \rightarrow 0, \\
a_{1\tilde{\chi}}^{\prime\prime L}(t) &= t \sum_i (1 - 2s_W^2) |Z_{1i}^N s_W + Z_{2i}^N c_W|^2 [C_{12} + C_{23}]^{(\tilde{\chi}_i^0 \tilde{e}_L \tilde{e}_L)} \rightarrow 0, \\
a_{2\tilde{\chi}}^{\prime R}(t) &= 8s_W^2 t \sum_{ij} (Z_{1i}^{N*} Z_{1j}^N)(Z_{4i}^{N*} Z_{4j}^N - Z_{3i}^{N*} Z_{3j}^N) [C_{12} + C_{23}]^{(\tilde{e}_R \tilde{\chi}_i^0 \tilde{\chi}_j^0)} \rightarrow 0, \\
a_{1\tilde{\chi}}^{\prime\prime R}(t) &= -8s_W^4 t \sum_i |Z_{1i}^N|^2 [C_{12} + C_{23}]^{(\tilde{\chi}_i^0 \tilde{e}_R \tilde{e}_R)} \rightarrow 0, \tag{D.3}
\end{aligned}$$

while Fig.1e and the 4-leg $WWZZ$ coupling give

$$\begin{aligned}
N_1^{\prime\prime Z} &= -\frac{c_W^2}{s_W^4} [C_0 + C_{11} - C_{12}]^{\nu_e WW} \rightarrow -\frac{2c_W^2}{s_W^4 s} \ln \frac{s}{m_W^2}, \\
N_5^{\prime\prime Z} &= -\frac{c_W^2}{s_W^4} [C_{12}]^{\nu_e WW} \rightarrow \frac{c_W^2}{s_W^4 s} \ln \frac{s}{m_W^2}. \tag{D.4}
\end{aligned}$$

The NAGC contribution corresponding to Fig.1f and discussed in Sect.3.3, has been calculated in [17]; except for the neutralino contribution to the ZZZ -NAGC coupling, for which only restricted Z -neutralino couplings were considered allowing only one or at most two different neutralinos to be running along the triangular loop. Following the same formalism, we give bellow the neutralino contribution to the ZZZ -NAGC couplings for the most general CP-conserving Z -neutralino couplings of (B.25). This is

$$\begin{aligned}
f_5^Z &= \frac{e^2}{16\pi^2 s_W^3 c_W^3} \frac{m_Z^2}{(s - m_Z^2)(s - 4m_Z^2)} \cdot \sum_{jk} \left[\text{Re} \left(O_{j_3 j_1}^{0ZL} O_{j_1 j_2}^{0ZL} O_{j_2 j_3}^{0ZL} \right) \right. \\
&\cdot \left\{ -\frac{(s - m_Z^2)(s + 2m_Z^2)}{3s} [B_0(m_Z^2; j_1, j_2)(M_{\tilde{\chi}_{j_1}^0}^2 + M_{\tilde{\chi}_{j_2}^0}^2 - 2M_{\tilde{\chi}_{j_3}^0}^2) \right. \\
&+ B_0(s; j_1, j_3)(M_{\tilde{\chi}_{j_1}^0}^2 + M_{\tilde{\chi}_{j_3}^0}^2 - 2M_{\tilde{\chi}_{j_2}^0}^2) + B_0(m_Z^2; j_2, j_3)(M_{\tilde{\chi}_{j_2}^0}^2 + M_{\tilde{\chi}_{j_3}^0}^2 - 2M_{\tilde{\chi}_{j_1}^0}^2)] \\
&+ \frac{C_{ZZ}(s; j_1 j_2 j_3)}{2s(s - 4m_Z^2)} \left[2M_{\tilde{\chi}_{j_1}^0}^2 s^3 + s^2 [4(M_{\tilde{\chi}_{j_2}^0}^4 + m_Z^4 - M_{\tilde{\chi}_{j_2}^0}^2 m_Z^2) + 2M_{\tilde{\chi}_{j_1}^0}^2 M_{\tilde{\chi}_{j_3}^0}^2] \right. \\
&\left. \left. - 3(M_{\tilde{\chi}_{j_1}^0}^2 + M_{\tilde{\chi}_{j_3}^0}^2)(M_{\tilde{\chi}_{j_2}^0}^2 + m_Z^2) \right] + 4m_Z^2 s [M_{\tilde{\chi}_{j_1}^0}^4 + M_{\tilde{\chi}_{j_3}^0}^4 - M_{\tilde{\chi}_{j_1}^0}^2 M_{\tilde{\chi}_{j_3}^0}^2] \right.
\end{aligned}$$

$$\begin{aligned}
& - (M_{\tilde{\chi}_{j_2}^0}^2 - m_Z^2)^2] - 4m_Z^4(M_{\tilde{\chi}_{j_1}^0}^2 - M_{\tilde{\chi}_{j_3}^0}^2)^2] - \frac{(s - m_Z^2)}{3} \Big\} \\
& - \frac{1}{2} \left[M_{\tilde{\chi}_{j_1}^0} M_{\tilde{\chi}_{j_2}^0} \operatorname{Re} \left(O_{j_3 j_1}^{0ZL} O_{j_2 j_3}^{0ZL} O_{j_2 j_1}^{0ZL} \right) + M_{\tilde{\chi}_{j_2}^0} M_{\tilde{\chi}_{j_3}^0} \operatorname{Re} \left(O_{j_1 j_2}^{0ZL} O_{j_3 j_1}^{0ZL} O_{j_3 j_2}^{0ZL} \right) \right] \\
& \cdot \left\{ 2[B_0(m_Z^2; j_1 j_2) - B_0(s; j_1 j_2)] + (M_{\tilde{\chi}_{j_1}^0}^2 + M_{\tilde{\chi}_{j_3}^0}^2 - 2M_{\tilde{\chi}_{j_2}^0}^2 + 2m_Z^2 - s) C_{ZZ}(s; j_1 j_2 j_3) \right\} \\
& - \frac{1}{2} M_{\tilde{\chi}_{j_3}^0} M_{\tilde{\chi}_{j_1}^0} \operatorname{Re} \left(O_{j_2 j_3}^{0ZL} O_{j_1 j_2}^{0ZL} O_{j_1 j_3}^{0ZL} \right) \left\{ 2[B_0(m_Z^2; j_1 j_2) - B_0(s; j_1 j_2)] \right. \\
& \left. + (M_{\tilde{\chi}_{j_1}^0}^2 + M_{\tilde{\chi}_{j_3}^0}^2 - 2M_{\tilde{\chi}_{j_2}^0}^2 - 2m_Z^2) C_{ZZ}(s; j_1 j_2 j_3) \right\} \Big] . \tag{D.5}
\end{aligned}$$

- $e^- e^+ \rightarrow Z\gamma$

The quantities corresponding to Fig.1d are the same as those defined for the $\gamma\gamma$ and ZZ final states. We only need to add the specific contributions from Fig.1e, with $(abc) = (\nu_e WW)$ and the 4-leg $WW\gamma Z$ coupling

$$\begin{aligned}
N_1^{\prime\prime\gamma Z} &= - \frac{c_W}{s_W^3} [C_0 + C_{11} - C_{12}]^{(\nu_e WW)} \rightarrow - \frac{2c_W}{s_W^3 s} \ln \frac{s}{m_W^2} , \\
N_5^{\prime\prime\gamma Z} &= - \frac{c_W}{s_W^3} [C_{12}]^{(\nu_e WW)} \rightarrow \frac{c_W}{s_W^3 s} \ln \frac{s}{m_W^2} . \tag{D.6}
\end{aligned}$$

Appendix E: Asymptotic renormalized Born and triangle contributions.

We list here the single and double logarithmic leading contribution for $N_j^{\text{ren}+Born}$ and N_j^{Tri} entering (19), when (s, t, u) are much larger than the internal propagator masses. The Born terms $N_j^{\text{Born},L}$ and $N_j^{\text{Born},R}$ appearing below have already been defined in Sec.3.1.

Asymptotic contributions to $N_j^{\text{ren}+Born}$ for $(e^- e^+ \rightarrow \gamma\gamma, ZZ, Z\gamma)$.

$$\begin{aligned}
N_j^{\text{ren}+Born} &\rightarrow \frac{\alpha}{4\pi} N_j^{\text{Born},L} \left[\ln \frac{s}{M_\gamma^2} + \frac{(2s_W^2 - 1)^2}{4s_W^2 c_W^2} \ln \frac{s}{m_Z^2} + \frac{1}{2s_W^2} \ln \frac{s}{m_W^2} \right. \\
&+ \left. \left(\frac{1}{4s_W^2 c_W^2} + \frac{1}{2s_W^2} \right) \ln \frac{s}{M_{MSSM}^2} \right] P_L \\
&+ \frac{\alpha}{4\pi} N_j^{\text{Born},R} \left[\ln \frac{s}{M_\gamma^2} + \frac{s_W^2}{c_W^2} \ln \frac{s}{m_Z^2} + \frac{1}{c_W^2} \ln \frac{s}{M_{MSSM}^2} \right] P_R . \tag{E.1}
\end{aligned}$$

Asymptotic contributions to N_j^{Tri} .

- $e^-e^+ \rightarrow \gamma\gamma$

The leading-log contributions to the triangle amplitudes are:

$$\begin{aligned}
N_1^{Tri} = N_2^{Tri} &\rightarrow \alpha^2 \left\{ \left(\frac{1}{t} + \frac{1}{u} \right) \left(2 \left[\ln \frac{s}{M_\gamma^2} \right] (P_L + P_R) \right. \right. \\
&+ \frac{(2s_W^2 - 1)^2}{2s_W^2 c_W^2} \left[\ln \frac{s}{m_Z^2} \right] P_L + 2 \frac{s_W^2}{c_W^2} \left[\ln \frac{s}{m_Z^2} \right] P_R \\
&+ \left(\frac{1}{s_W^2} \left[\frac{1}{2t} \ln^2 \frac{|t|}{m_W^2} + \frac{1}{2u} \ln^2 \frac{|u|}{m_W^2} \right] - \frac{2}{s_W^2 s} \left[\ln \frac{s}{m_W^2} \right] \right) P_L \\
&\left. + \left(\frac{(1 + 2c_W^2)}{2s_W^2 c_W^2} \left[\ln \frac{s}{M_{MSSM}^2} \right] P_L + \frac{2}{c_W^2} \left[\ln \frac{s}{M_{MSSM}^2} \right] P_R \right) \left(\frac{1}{t} + \frac{1}{u} \right) \right\} , \quad (E.2)
\end{aligned}$$

$$\begin{aligned}
N_4^{Tri} &\rightarrow \alpha^2 \left\{ \left(\frac{1}{t} - \frac{1}{u} \right) \left(- 2 \left[\ln \frac{s}{M_\gamma^2} \right] (P_L + P_R) \right. \right. \\
&- \frac{(2s_W^2 - 1)^2}{2s_W^2 c_W^2} \left[\ln \frac{s}{m_Z^2} \right] P_L - 2 \frac{s_W^2}{c_W^2} \left[\ln \frac{s}{m_Z^2} \right] P_R \\
&+ \frac{1}{s_W^2} \left[\frac{1}{t} \ln^2 \frac{|t|}{m_W^2} - \frac{1}{u} \ln^2 \frac{|u|}{m_W^2} \right] P_L \\
&\left. + \left(\frac{(1 + 2c_W^2)}{2s_W^2 c_W^2} \left[\ln \frac{s}{M_{MSSM}^2} \right] P_L + \frac{2}{c_W^2} \left[\ln \frac{s}{M_{MSSM}^2} \right] P_R \right) \left(\frac{1}{t} - \frac{1}{u} \right) \right\} , \quad (E.3)
\end{aligned}$$

where the four lines in each equation are induced by the photon (with ultraviolet mass M_γ), Z , W and the $MSSM$ sectors, respectively.

- $e^-e^+ \rightarrow Z\gamma$

The triangle amplitudes receiving leading-log contributions are:

$$\begin{aligned}
N_1^{Tri} &\rightarrow \alpha^2 \left\{ \left(\frac{1}{t} + \frac{1}{u} \right) \left(- \frac{(2s_W^2 - 1)}{s_W c_W} \left[\ln \frac{s}{M_\gamma^2} \right] P_L - 2 \frac{s_W}{c_W} \left[\ln \frac{s}{M_\gamma^2} \right] P_R \right. \right. \\
&- \frac{(2s_W^2 - 1)^3}{4s_W^3 c_W^3} \left[\ln \frac{s}{m_Z^2} \right] P_L - 2 \frac{s_W^3}{c_W^3} \left[\ln \frac{s}{m_Z^2} \right] P_R - \frac{3}{4s_W^3 c_W} \left[\ln \frac{s}{m_W^2} \right] P_L \\
&- \left[\frac{2s_W^2 - 1}{4s_W^3 c_W} \left(\frac{1}{t} \ln^2 \frac{|t|}{m_W^2} + \frac{1}{u} \ln^2 \frac{|u|}{m_W^2} \right) + \frac{2c_W}{s_W^3 s} \ln \frac{s}{m_W^2} \right] P_L \\
&\left. + \left(\frac{(1 - 2s_W^2)(1 + 2c_W^2)}{4s_W^3 c_W^3} \left[\ln \frac{s}{M_{MSSM}^2} \right] P_L - \frac{2s_W}{c_W^3} \left[\ln \frac{s}{M_{MSSM}^2} \right] P_R \right) \left(\frac{1}{t} + \frac{1}{u} \right) \right\} , (E.4)
\end{aligned}$$

$$\begin{aligned}
N_2^{Tri} &\rightarrow \alpha^2 \left\{ \left(\frac{1}{t} + \frac{1}{u} \right) \left(- \frac{(2s_W^2 - 1)}{s_W c_W} \left[\ln \frac{s}{M_\gamma^2} \right] P_L - 2 \frac{s_W}{c_W} \left[\ln \frac{s}{M_\gamma^2} \right] P_R \right. \right. \\
&- \frac{(2s_W^2 - 1)^3}{4s_W^3 c_W^3} \left[\ln \frac{s}{m_Z^2} \right] P_L - 2 \frac{s_W^3}{c_W^3} \left[\ln \frac{s}{m_Z^2} \right] P_R + \frac{1}{4s_W^3 c_W} \left[\ln \frac{s}{m_W^2} \right] P_L \\
&+ \left[\left(\frac{c_W}{2s_W^3} \right) \left(\frac{1}{t} \ln^2 \frac{|t|}{m_W^2} + \frac{1}{u} \ln^2 \frac{|u|}{m_W^2} \right) - \frac{2c_W}{s_W^3 s} \ln \frac{s}{m_W^2} \right] P_L \\
&\left. \right\}
\end{aligned}$$

$$+ \left(\frac{(1 - 2s_W^2)(1 + 2c_W^2)}{4s_W^3 c_W^3} \left[\ln \frac{s}{M_{MSSM}^2} \right] P_L - \frac{2s_W}{c_W^3} \left[\ln \frac{s}{M_{MSSM}^2} \right] P_R \right) \left(\frac{1}{t} + \frac{1}{u} \right) \left. \vphantom{\frac{(1 - 2s_W^2)(1 + 2c_W^2)}{4s_W^3 c_W^3}} \right\} , \quad (\text{E.5})$$

$$\begin{aligned} N_4^{Tri} \rightarrow & \alpha^2 \left\{ \left(\frac{1}{t} - \frac{1}{u} \right) \left(\frac{(2s_W^2 - 1)}{s_W c_W} \left[\ln \frac{s}{M_\gamma^2} \right] P_L + 2 \frac{s_W}{c_W} \left[\ln \frac{s}{M_\gamma^2} \right] P_R \right. \right. \\ & + \frac{(2s_W^2 - 1)^3}{4s_W^3 c_W^3} \left[\ln \frac{s}{m_Z^2} \right] P_L + 2 \frac{s_W^3}{c_W^3} \left[\ln \frac{s}{m_Z^2} \right] P_R + \frac{1}{4s_W^3 c_W} \left[\ln \frac{s}{m_W^2} \right] P_L \left. \vphantom{\frac{(2s_W^2 - 1)^3}{4s_W^3 c_W^3}} \right) \\ & + \frac{(1 - 4c_W^2)}{4s_W^3 c_W} \left(-\frac{1}{t} \ln^2 \frac{|t|}{m_W^2} + \frac{1}{u} \ln^2 \frac{|u|}{m_W^2} \right) P_L \\ & + \left. \left(\frac{(1 - 2s_W^2)(1 + 2c_W^2)}{4s_W^3 c_W^3} \left[\ln \frac{s}{M_{MSSM}^2} \right] P_L - \frac{2s_W}{c_W^3} \left[\ln \frac{s}{M_{MSSM}^2} \right] P_R \right) \left(\frac{1}{t} - \frac{1}{u} \right) \right\} , \quad (\text{E.6}) \end{aligned}$$

$$\begin{aligned} N_5^{Tri} \rightarrow & \alpha^2 \left\{ \frac{1}{u} \left\{ \frac{(2s_W^2 - 1)}{s_W c_W} \left[\ln \frac{s}{M_\gamma^2} \right] P_L + 2 \frac{s_W}{c_W} \left[\ln \frac{s}{M_\gamma^2} \right] P_R \right. \right. \\ & + \frac{(2s_W^2 - 1)^3}{4s_W^3 c_W^3} \left[\ln \frac{s}{m_Z^2} \right] P_L + 2 \frac{s_W^3}{c_W^3} \left[\ln \frac{s}{m_Z^2} \right] P_R \\ & + \left. \left(\frac{c_W}{2s_W^3} \ln^2 \frac{|u|}{m_W^2} + \frac{1}{s_W^3 c_W} \ln \frac{s}{m_W^2} \right) P_L \right\} + \frac{c_W}{s_W^3 s} \left[\ln \frac{s}{m_W^2} \right] P_L \\ & + \frac{(u - s)}{us} \left(\frac{(4c_W^2 - 1)}{4s_W^3 c_W} \ln^2 \frac{|u|}{m_W^2} + \frac{1}{4s_W^3 c_W} \ln \frac{s}{m_W^2} \right) P_L \\ & - \frac{1}{s} \left(\frac{(4c_W^2 - 1)}{4s_W^3 c_W} \ln^2 \frac{|t|}{m_W^2} + \frac{1}{4s_W^3 c_W} \ln \frac{s}{m_W^2} \right) P_L \\ & - \left. \frac{1}{u} \left(\frac{(1 - 2s_W^2)(1 + 2c_W^2)}{4s_W^3 c_W^3} \left[\ln \frac{s}{M_{MSSM}^2} \right] P_L - \frac{2s_W}{c_W^3} \left[\ln \frac{s}{M_{MSSM}^2} \right] P_R \right) \right\} , \quad (\text{E.7}) \end{aligned}$$

$$\begin{aligned} N_6^{Tri} \rightarrow & -\frac{2\alpha^2}{s} \left\{ \left(\frac{1}{t} + \frac{1}{u} \right) \left(\frac{(2s_W^2 - 1)}{s_W c_W} \left[\ln \frac{s}{M_\gamma^2} \right] P_L + 2 \frac{s_W}{c_W} \left[\ln \frac{s}{M_\gamma^2} \right] P_R \right. \right. \\ & + \frac{(2s_W^2 - 1)^3}{4s_W^3 c_W^3} \left[\ln \frac{s}{m_Z^2} \right] P_L + 2 \frac{s_W^3}{c_W^3} \left[\ln \frac{s}{m_Z^2} \right] P_R + \frac{1}{4s_W^3 c_W} \left[\ln \frac{s}{m_W^2} \right] P_L \left. \vphantom{\frac{(2s_W^2 - 1)^3}{4s_W^3 c_W^3}} \right) \\ & - \frac{(1 - 4c_W^2)}{4s_W^3 c_W} \left[\frac{1}{t} \ln^2 \frac{|t|}{m_W^2} + \frac{1}{u} \ln^2 \frac{|u|}{m_W^2} \right] P_L \\ & + \left. \left(\frac{(1 - 2s_W^2)(1 + 2c_W^2)}{4s_W^3 c_W^3} \left[\ln \frac{s}{M_{MSSM}^2} \right] P_L - \frac{2s_W}{c_W^3} \left[\ln \frac{s}{M_{MSSM}^2} \right] P_R \right) \left(\frac{1}{t} + \frac{1}{u} \right) \right\} . \quad (\text{E.8}) \end{aligned}$$

- $e^-e^+ \rightarrow ZZ$

The triangle amplitudes receiving leading-log contributions are:

$$N_1^{Tri} = N_2^{Tri} \rightarrow \alpha^2 \left\{ \left(\frac{1}{t} + \frac{1}{u} \right) \left(\frac{(2s_W^2 - 1)^2}{2s_W^2 c_W^2} \left[\ln \frac{s}{M_\gamma^2} \right] P_L + 2 \frac{s_W^2}{c_W^2} \left[\ln \frac{s}{M_\gamma^2} \right] P_R \right. \right.$$

$$\begin{aligned}
& + \frac{(2s_W^2 - 1)^4}{8s_W^4 c_W^4} \left[\ln \frac{s}{m_Z^2} \right] P_L + 2 \frac{s_W^4}{c_W^4} \left[\ln \frac{s}{m_Z^2} \right] P_R + \frac{2s_W^2 - 1}{4s_W^4 c_W^2} \left[\ln \frac{s}{m_W^2} \right] P_L \\
& - \frac{(2s_W^2 - 1)}{2s_W^4} \left[\frac{1}{2t} \ln^2 \frac{|t|}{m_W^2} + \frac{1}{2u} \ln^2 \frac{|u|}{m_W^2} \right] P_L - \frac{2c_W^2}{s_W^4 s} \left[\ln \frac{s}{m_W^2} \right] P_L \\
& + \left(\frac{(2s_W^2 - 1)^2 (1 + 2c_W^2)}{8s_W^4 c_W^4} \left[\ln \frac{s}{M_{MSSM}^2} \right] P_L + \frac{2s_W^2}{c_W^4} \left[\ln \frac{s}{M_{MSSM}^2} \right] P_R \right) \left(\frac{1}{t} + \frac{1}{u} \right) \Big\} , \quad (E.9)
\end{aligned}$$

$$\begin{aligned}
N_4^{Tri} & \rightarrow \alpha^2 \left\{ \left(\frac{1}{t} - \frac{1}{u} \right) \left(- \frac{(2s_W^2 - 1)^2}{2s_W^2 c_W^2} \left[\ln \frac{s}{M_\gamma^2} \right] P_L - 2 \frac{s_W^2}{c_W^2} \left[\ln \frac{s}{M_\gamma^2} \right] P_R \right. \right. \\
& - \frac{(2s_W^2 - 1)^4}{8s_W^4 c_W^4} \left[\ln \frac{s}{m_Z^2} \right] P_L - 2 \frac{s_W^4}{c_W^4} \left[\ln \frac{s}{m_Z^2} \right] P_R - \frac{(2s_W^2 - 1)}{4s_W^4 c_W^2} \left[\ln \frac{s}{m_W^2} \right] P_L \\
& - \frac{(2s_W^2 - 1)}{2s_W^4} \left[\frac{1}{t} \ln^2 \frac{|t|}{m_W^2} - \frac{1}{u} \ln^2 \frac{|u|}{m_W^2} \right] P_L \\
& \left. + \left(\frac{(2s_W^2 - 1)^2 (1 + 2c_W^2)}{8s_W^4 c_W^4} \left[\ln \frac{s}{M_{MSSM}^2} \right] P_L + \frac{2s_W^2}{c_W^4} \left[\ln \frac{s}{M_{MSSM}^2} \right] P_R \right) \left(\frac{1}{t} - \frac{1}{u} \right) \right\} , \quad (E.10)
\end{aligned}$$

$$\begin{aligned}
N_5^{Tri} & \rightarrow \alpha^2 \left\{ - \frac{1}{u} \left(\frac{(2s_W^2 - 1)^2}{2s_W^2 c_W^2} \left[\ln \frac{s}{M_\gamma^2} \right] P_L + \frac{2s_W^2}{c_W^2} \left[\ln \frac{s}{M_\gamma^2} \right] P_R \right. \right. \\
& + \frac{(2s_W^2 - 1)^4}{8s_W^4 c_W^4} \left[\ln \frac{s}{m_Z^2} \right] P_L + \frac{2s_W^4}{c_W^4} \left[\ln \frac{s}{m_Z^2} \right] P_R \\
& + \left(\frac{(u - s)}{us} \left[- \frac{(2s_W^2 - 1)}{2s_W^4} \ln^2 \frac{|u|}{m_W^2} - \frac{(2s_W^2 - 1)}{4s_W^4 c_W^2} \ln \frac{s}{m_W^2} \right] P_L \right. \\
& + \frac{(2s_W^2 - 1)}{2s_W^4 s} \left[\ln^2 \frac{|t|}{m_W^2} \right] P_L - \frac{(2s_W^2 - 1)}{4s_W^4 u} \ln^2 \frac{|u|}{m_W^2} P_L + \frac{c_W^2}{s_W^4 s} \left[\ln \frac{s}{m_W^2} \right] P_L \\
& \left. \left. - \frac{1}{u} \left(\frac{(2s_W^2 - 1)^2 (1 + 2c_W^2)}{8s_W^4 c_W^4} \left[\ln \frac{s}{M_{MSSM}^2} \right] P_L + \frac{2s_W^2}{c_W^4} \left[\ln \frac{s}{M_{MSSM}^2} \right] P_R \right) \right\} , \quad (E.11)
\end{aligned}$$

$$\begin{aligned}
N_6^{Tri} = -N_8^{Tri} & \rightarrow \left(- \frac{2\alpha^2}{s} \right) \left\{ \left(\frac{1}{t} + \frac{1}{u} \right) \left(- \frac{(2s_W^2 - 1)^2}{2s_W^2 c_W^2} \left[\ln \frac{s}{M_\gamma^2} \right] P_L - \frac{2s_W^2}{c_W^2} \left[\ln \frac{s}{M_\gamma^2} \right] P_R \right. \right. \\
& - \frac{(2s_W^2 - 1)^4}{8s_W^4 c_W^4} \left[\ln \frac{s}{m_Z^2} \right] P_L - 2 \frac{s_W^4}{c_W^4} \left[\ln \frac{s}{m_Z^2} \right] P_R - \frac{(2s_W^2 - 1)}{4s_W^4 c_W^2} \left[\ln \frac{s}{m_W^2} \right] P_L \\
& - \frac{(2s_W^2 - 1)}{2s_W^4} \left[\frac{1}{t} \ln^2 \frac{|t|}{m_W^2} + \frac{1}{u} \ln^2 \frac{|u|}{m_W^2} \right] P_L \\
& \left. + \left(\frac{(2s_W^2 - 1)^2 (1 + 2c_W^2)}{8s_W^4 c_W^4} \left[\ln \frac{s}{M_{MSSM}^2} \right] P_L + \frac{2s_W^2}{c_W^4} \left[\ln \frac{s}{M_{MSSM}^2} \right] P_R \right) \left(\frac{1}{t} + \frac{1}{u} \right) \right\} , \quad (E.12)
\end{aligned}$$

$$N_7^{Tri} \rightarrow \alpha^2 \left\{ - \frac{1}{t} \left(\frac{(2s_W^2 - 1)^2}{2s_W^2 c_W^2} \left[\ln \frac{s}{M_\gamma^2} \right] P_L + \frac{2s_W^2}{c_W^2} \left[\ln \frac{s}{M_\gamma^2} \right] P_R \right. \right.$$

$$\begin{aligned}
& + \frac{(2s_W^2 - 1)^4}{8s_W^4 c_W^4} \left[\ln \frac{s}{m_Z^2} \right] P_L + \frac{2s_W^4}{c_W^4} \left[\ln \frac{s}{m_Z^2} \right] P_R \\
& + \left(\frac{t-s}{ts} \left[- \frac{(2s_W^2 - 1)}{2s_W^4} \ln^2 \frac{|t|}{m_W^2} \right] - \frac{(2s_W^2 - 1)}{4s_W^4 c_W^2 t} \ln \frac{s}{m_W^2} \right) P_L \\
& + \frac{(2s_W^2 - 1)}{2s_W^4 s} \left[\ln^2 \frac{|u|}{m_W^2} \right] P_L - \frac{(2s_W^2 - 1)}{4s_W^4 t} \ln^2 \frac{|t|}{m_W^2} P_L + \frac{c_W^2}{s_W^4 s} \left[\ln \frac{s}{m_W^2} \right] P_L \\
& - \frac{1}{t} \left(\frac{(2s_W^2 - 1)^2 (1 + 2c_W^2)}{8s_W^4 c_W^4} \left[\ln \frac{s}{M_{MSSM}^2} \right] P_L + \frac{2s_W^2}{c_W^4} \left[\ln \frac{s}{M_{MSSM}^2} \right] P_R \right) \} . \quad (E.13)
\end{aligned}$$

Concerning the NAGC couplings discussed in Section 3.3, and calculated in [17] and (D.5), we note that in the asymptotic regime they are always found to vanish; *i.e.* $f_5^{\gamma, Z} \rightarrow 0$, $h_3^{\gamma, Z} \rightarrow 0$.

Appendix F: Asymptotic contributions from box diagrams

Leading $\ln s$ and $\ln^2 s$ order contributions only arise from SM boxes of the types $k = 1, 2, 3$ defined in Sec.3.4. The purely MSSM boxes, which are of types ($k = 4, 5, 6$), provide only subleading logarithmic contributions like $\ln(s/t)$. The SM or MSSM contributions from the type $k = 7$ box, vanish asymptotically like M^2/s .

The box amplitudes receiving leading-log contributions are:

- $e^- e^+ \rightarrow \gamma\gamma$

$$\begin{aligned}
N_j^{Box} &= \alpha^2 \left\{ \bar{N}_j^{1,Box}(M_\gamma) [P_L + P_R] + \bar{N}_j^{1,Box}(m_Z) \left[\frac{(2s_W^2 - 1)^2}{4s_W^2 c_W^2} P_L + \frac{s_W^2}{c_W^2} P_R \right] \right. \\
&\quad \left. + \bar{N}_j^{2,Box}(m_W) \frac{1}{2s_W^2} P_L + \text{"sym"} \right\} , \quad (F.1)
\end{aligned}$$

- $e^- e^+ \rightarrow Z\gamma$

$$\begin{aligned}
N_j^{Box} &= \alpha^2 \left\{ \left(\bar{N}_j^{1,Box}(M_\gamma) \left[\frac{(1 - 2s_W^2)}{2s_W c_W} P_L - \frac{s_W}{c_W} P_R \right] + \bar{N}_j^{1,Box}(m_Z) \left[\frac{(1 - 2s_W^2)^3}{8s_W^3 c_W^3} P_L - \frac{s_W^3}{c_W^3} P_R \right] \right. \right. \\
&\quad \left. \left. + \bar{N}_j^{2,Box}(m_W) \frac{c_W}{2s_W^3} P_L + \text{"sym"} \right) + \bar{N}_j^{3,Box}(m_W) \frac{1}{4s_W^3 c_W} P_L \text{ (no "sym")} \right\} , \quad (F.2)
\end{aligned}$$

- $e^- e^+ \rightarrow ZZ$

$$N_j^{Box} = \alpha^2 \left\{ \bar{N}_j^{1,Box}(M_\gamma) \left[\frac{(2s_W^2 - 1)^2}{4s_W^2 c_W^2} P_L + \frac{s_W^2}{c_W^2} P_R \right] + \bar{N}_j^{1,Box}(m_Z) \left[\frac{(2s_W^2 - 1)^4}{16s_W^4 c_W^4} P_L + \frac{s_W^4}{c_W^4} P_R \right] \right\}$$

$$+\bar{N}_j^{1,Box}(m_W) \frac{1}{8s_W^4 c_W^2} P_L + \bar{N}_j^{2,Box}(m_W) \frac{c_W^2}{2s_W^4} P_L + \bar{N}_j^{3,Box}(m_W) \frac{1}{4s_W^4} P_L + \text{"sym"} \} . \quad (\text{F.3})$$

The meaning of +”sym” in the above equations has been given in Section.3.4, while discussing (62).

Tables of asymptotic values for $\bar{N}_j^{k, Box}$

The complete Box contributions to \bar{N}_j^{Box} have been analytically calculated and used in the numerical calculations presented in this paper. Since, these expressions are enormous though, we refrain from giving them in the text and only list their asymptotic leading-log contribution. Below we write for each such form, in a first step (\rightarrow) the full logarithmic expressions obtained from the asymptotic expansion of the Passarino-Veltman D_{ij} functions; and in a second step (\Rightarrow) the leading ($\ln \frac{s}{M^2}$, $\ln^2 \frac{|s|}{M^2}$, $\ln^2 \frac{|t|}{M^2}$, $\ln^2 \frac{|u|}{M^2}$) terms [29].

• **Box type $k = 1$; $(abcd) = (Vfff)$**

$$\begin{aligned} \bar{N}_1^{1, Box} &= \bar{N}_2^{1, Box} \rightarrow \frac{1}{tu^2} \left[-(s^2 + tu) \ln^2 \frac{|t|}{s} + u^2 \ln^2 \frac{s}{M^2} + 2tu \ln \frac{s}{M^2} \right. \\ &\quad \left. - (2t^2 + 4s^2 + 6st) \ln \frac{|t|}{M^2} \right] \Rightarrow \frac{1}{t} \left[\ln^2 \frac{s}{M^2} - 4 \ln \frac{s}{M^2} \right] , \\ \bar{N}_3^{1, Box} &\rightarrow -\frac{4}{tu^3} \left[t(s-u) \ln^2 \frac{|t|}{s} + (3s^2 + 4st + t^2) \ln \frac{s}{|t|} \right] \Rightarrow 0 , \\ \bar{N}_4^{1, Box} &\rightarrow \frac{1}{tu^2} \left[(tu - s^2) \ln^2 \frac{|t|}{s} + u^2 \ln^2 \frac{s}{m_Z^2} + 2tu \ln \frac{s}{|t|} \right] \Rightarrow \frac{1}{t} \ln^2 \frac{s}{M^2} , \\ \bar{N}_5^{1, Box} &\rightarrow -\frac{1}{su^2} \left[(s^2 + tu) \ln^2 \frac{|t|}{s} + u^2 \ln^2 \frac{s}{M^2} - (4t^2 + 6s^2 + 10st) \ln \frac{s}{|t|} \right] \\ &\quad \Rightarrow -\frac{1}{s} \ln^2 \frac{s}{M^2} , \\ \bar{N}_6^{1, Box} &\rightarrow \frac{2}{stu^3} \left[-(s^3 + t^3 + 2st^2) \ln^2 \frac{|t|}{s} - u^3 \ln^2 \frac{s}{M^2} \right. \\ &\quad \left. - (12st^2 + 4t^3 + 8s^2t) \ln \frac{s}{|t|} \right] \Rightarrow -\frac{2}{st} \ln^2 \frac{s}{M^2} , \\ \bar{N}_7^{1, Box} &\rightarrow \frac{1}{stu} \left[(st - s^2 + t^2) \ln^2 \frac{|t|}{s} + (s^2 - t^2) \ln^2 \frac{s}{M^2} - 4tuln \frac{s}{M^2} - 4u^2 \ln \frac{|t|}{M^2} \right] \\ &\quad \Rightarrow \frac{(t-s)}{st} \ln^2 \frac{s}{M^2} + \frac{4}{t} \ln \frac{s}{M^2} , \\ \bar{N}_8^{1, Box} &\rightarrow \frac{2}{stu^2} \left[-(t^2 + s^2 + 3st) \ln^2 \frac{|t|}{s} + u^2 \ln^2 \frac{s}{M^2} - (4t^2 + 6s^2 + 10st) \ln \frac{s}{|t|} \right] \\ &\quad \Rightarrow \frac{2}{st} \ln^2 \frac{s}{M^2} , \\ \bar{N}_9^{1, Box} &\rightarrow 0 . \end{aligned} \quad (\text{F.4})$$

- **Box type** $k = 2$; $(abcd) = (fVVV)$

$$\begin{aligned}
\bar{N}_1^{2, Box} &= \bar{N}_2^{2, Box} \rightarrow \frac{1}{stu^2} \left[-s^2(s+2t) \ln^2 \frac{|t|}{s} + su^2 \left(\ln^2 \frac{s}{M^2} + \ln^2 \frac{|t|}{M^2} \right) \right. \\
&\quad \left. - 2s(s^2 + 3st + 2t^2) \ln \frac{|t|}{M^2} + 2t(t^2 + 3st + 2s^2) \ln \frac{s}{M^2} \right] \\
&\implies \frac{1}{t} \left(\ln^2 \frac{s}{M^2} + \ln^2 \frac{|t|}{M^2} \right) + 2 \frac{(t-s)}{st} \ln \frac{s}{M^2} , \\
\bar{N}_3^{2, Box} &= \rightarrow - \frac{4}{tu^3} \left[t(s+2t) \ln^2 \frac{|t|}{s} + (3s^2 + 8st + 5t^2) \ln \frac{|t|}{s} \right] \\
&\implies 0 , \\
\bar{N}_4^{2, Box} &\rightarrow \frac{1}{2stu^2} \left[(s^3 + 4s^2t + 6st^2 + 4t^3) \ln^2 \frac{|t|}{s} \right. \\
&\quad \left. + u^2(2s+t) \ln^2 \frac{s}{M^2} + 8u^2t \ln^2 \frac{|t|}{M^2} + 4ut^2 \ln \frac{s}{M^2} + 4us(s+2t) \ln \frac{|t|}{M^2} \right] \\
&\implies \frac{(2s+t)}{2st} \ln^2 \frac{s}{M^2} + \frac{4}{s} \ln^2 \frac{|t|}{M^2} + \frac{2u}{st} \ln \frac{s}{M^2} , \\
\bar{N}_5^{2, Box} &\rightarrow \frac{1}{su^2} \left[-s(s+2t) \ln^2 \frac{|t|}{s} + 4u^2 \ln^2 \frac{|t|}{M^2} + u(s-t) \ln \frac{s}{M^2} + u(4s+6t) \ln \frac{|t|}{M^2} \right] \\
&\implies \frac{4}{s} \ln^2 \frac{|t|}{M^2} - \frac{5}{s} \ln \frac{s}{M^2} , \\
\bar{N}_6^{2, Box} &\rightarrow \frac{2}{stu^3} \left[(-3ts^2 - s^3 - 4st^2 - 4t^3) \ln^2 \frac{|t|}{s} \right. \\
&\quad \left. - u^3 \ln^2 \frac{s}{M^2} + (6t^3 + 6st^2 - 2s^3 - 2ts^2) \ln \frac{|t|}{M^2} \right. \\
&\quad \left. - (4ts^2 + 12st^2 + 8t^3) \ln \frac{s}{M^2} \right] \\
&\implies \frac{2}{st} \left(-\ln^2 \frac{s}{M^2} + 2 \ln \frac{s}{M^2} \right) , \\
\bar{N}_7^{2, Box} &\rightarrow \frac{1}{stu} \left[-s(s+2t) \ln^2 \frac{|t|}{s} - us \ln^2 \frac{s}{M^2} \right. \\
&\quad \left. + (s^2 + 5st + 4t^2) \ln^2 \frac{|t|}{M^2} - 3tu \ln \frac{s}{M^2} - (2s^2 + t(8s+6t)) \ln \frac{|t|}{M^2} \right] \\
&\implies - \frac{1}{t} \ln^2 \frac{s}{M^2} + \frac{4u+3s}{st} \ln^2 \frac{|t|}{M^2} - \frac{3u+s}{st} \ln \frac{s}{M^2} , \\
\bar{N}_8^{2, Box} &\rightarrow \frac{2}{stu^2} \left[-(s+2t)^2 \ln^2 \frac{|t|}{s} + u^2 \ln^2 \frac{s}{M^2} + 2u(3s+4t) \ln \frac{s}{M^2} - 2u(2s+3t) \ln \frac{|t|}{M^2} \right] \\
&\implies - \frac{2}{st} \left(-\ln^2 \frac{s}{M^2} + 2 \ln \frac{s}{M^2} \right) , \\
\bar{N}_9^{2, Box} &\rightarrow 0 .
\end{aligned} \tag{F.5}$$

Box type $k = 3$; $(abcd) = (VffV)$

$$\begin{aligned}
\bar{N}_1^{3, Box} &\rightarrow \frac{1}{tu} \left[-s \ln^2 \frac{|t|}{u} - t \ln^2 \frac{|t|}{M^2} - u \ln^2 \frac{|u|}{M^2} + 5t \ln \frac{|u|}{M^2} + 5u \ln \frac{|t|}{M^2} \right] \\
&\implies -\frac{1}{t} \ln^2 \frac{|u|}{M^2} - \frac{1}{u} \ln^2 \frac{|t|}{M^2} - \frac{5s}{ut} \ln \frac{s}{M^2} , \\
\bar{N}_2^{3, Box} &\rightarrow \frac{1}{tu} \left[-s \ln^2 \frac{|t|}{u} + s \left(\ln^2 \frac{|u|}{M^2} + \ln^2 \frac{|t|}{M^2} \right) + t \ln \frac{|u|}{M^2} + u \ln \frac{|t|}{M^2} \right] \\
&\implies \frac{s}{tu} \left[\ln^2 \frac{u}{M^2} + \ln^2 \frac{t}{M^2} - \ln \frac{s}{M^2} \right] , \\
\bar{N}_3^{3, Box} &\rightarrow \frac{12}{tu} \ln \frac{u}{t} \implies 0 , \\
\bar{N}_4^{3, Box} &\rightarrow \frac{1}{tu} \left[(u-t) \ln^2 \left| \frac{t}{u} \right| + t \ln^2 \frac{|t|}{M^2} - u \ln^2 \frac{|u|}{M^2} + u \ln \frac{|t|}{M^2} - t \ln \frac{|u|}{M^2} \right] \\
&\implies \frac{1}{u} \ln^2 \frac{|t|}{M^2} - \frac{1}{t} \ln^2 \frac{|u|}{M^2} + \frac{u-t}{ut} \ln \frac{s}{M^2} , \\
\bar{N}_5^{3, Box} &\rightarrow \frac{1}{tus^3} \left[(t^4 + u^3t + 3t^3u + 3t^2u^2) \ln^2 \left| \frac{t}{u} \right| \right. \\
&\quad \left. + s^2tu \ln^2 \frac{|u|}{M^2} + s^2t(s-u) \ln^2 \frac{|t|}{M^2} + 5s^2tu \ln \frac{|t|}{M^2} + 5s^2t^2 \ln \frac{|u|}{M^2} \right] \\
&\implies \frac{1}{s} \ln^2 \frac{|u|}{M^2} + \frac{s-u}{us} \ln^2 \frac{|t|}{M^2} - \frac{5}{u} \ln \frac{s}{M^2} , \\
\bar{N}_6^{3, Box} &\rightarrow \frac{2}{s^2tu} \left[s^2 \ln^2 \left| \frac{t}{u} \right| + us \ln^2 \frac{|u|}{M^2} + st \ln^2 \frac{|t|}{M^2} + (6t^2 + 7tu + u^2) \ln \frac{|t|}{M^2} \right. \\
&\quad \left. + 5ts \ln \frac{|u|}{M^2} \right] \implies \frac{2}{st} \ln^2 \frac{|u|}{M^2} + \frac{2}{su} \ln^2 \frac{|t|}{M^2} + \frac{2}{tu} \ln \frac{s}{M^2} , \\
\bar{N}_7^{3, Box} &\rightarrow -\frac{1}{uts^2} \left[(u^4 + t^3u + 3u^3t + 3u^2t^2) \ln^2 \left| \frac{t}{u} \right| + su^2 \ln^2 \frac{|t|}{M^2} \right. \\
&\quad \left. - su(u+2s) \ln^2 \frac{|u|}{m_W^2} - 5stu \ln \frac{|u|}{M^2} + u(u^2 - 3tu - 4t^2) \ln \frac{|t|}{M^2} \right] \\
&\implies -\frac{u}{st} \ln^2 \frac{|t|}{M^2} + \frac{u+2s}{st} \ln^2 \frac{|u|}{M^2} - \frac{1}{t} \ln \frac{s}{M^2} , \\
\bar{N}_8^{3, Box} &\rightarrow \frac{2}{s^2tu} \left[-s^2 \ln^2 \left| \frac{t}{u} \right| - us \ln^2 \frac{|u|}{M^2} - ts \ln^2 \frac{|t|}{M^2} \right. \\
&\quad \left. - 6us \ln \left| \frac{t}{u} \right| + ts \ln \frac{|u|}{M^2} + us \ln \frac{|t|}{M^2} \right] \\
&\implies -\frac{2}{st} \ln^2 \frac{|u|}{M^2} - \frac{2}{su} \ln^2 \frac{|t|}{M^2} - \frac{2}{tu} \ln \frac{s}{M^2} , \\
\bar{N}_9^{3, Box} &\rightarrow 0 .
\end{aligned} \tag{F.6}$$

Box type $k = 4$; $(abcd) = (Sfff)$.

In sect.3.4 we have separated this box contribution into 4 parts coming from different

combinations of the kinetic and massive parts of the three fermion propagators. The $k = 4B, 4C, 4D$ parts asymptotically vanish like M^2/s .

$$\begin{aligned}
\bar{N}_1^{4A, Box} &= \bar{N}_2^{4A, Box} = \bar{N}_4^{4A, Box} \rightarrow -\frac{1}{2u^2} \left[t \ln^2 \frac{|t|}{s} - 2u \ln \frac{s}{|t|} \right] \implies 0 , \\
\bar{N}_3^{4A, Box} &\rightarrow \frac{2}{tu^3} \left[t^2 \ln^2 \frac{|t|}{s} - (3t^2 + 4st + s^2) \ln \frac{|t|}{s} \right] \implies 0 , \\
\bar{N}_5^{4A, Box} &\rightarrow -\frac{1}{2su^2} \left[t^2 \ln^2 \frac{|t|}{s} - 2(2t^2 + 3st + s^2) \ln \frac{|t|}{s} \right] \implies 0 , \\
\bar{N}_6^{4A, Box} &\rightarrow -\frac{1}{stu^3} \left[t^2 (s-t) \ln^2 \frac{|t|}{s} - 4ut^2 \ln \frac{|t|}{s} \right] \implies 0 , \\
\bar{N}_7^{4A, Box} &\rightarrow -\frac{1}{2su} \left[t \ln^2 \frac{|t|}{s} + 4u \ln \frac{|t|}{s} \right] \implies 0 , \\
\bar{N}_8^{4A, Box} &\rightarrow \frac{1}{stu^2} \left[t^2 \ln^2 \frac{|t|}{s} - 2(2t^2 + s^2 + 3st) \ln \frac{|t|}{s} \right] \implies 0 , \\
\bar{N}_9^{4A, Box} &\rightarrow 0 .
\end{aligned} \tag{F.7}$$

Box type $k = 5$; $(abcd) = (fSSS)$

$$\begin{aligned}
\bar{N}_1^{5, Box} &= \bar{N}_2^{5, Box} = \bar{N}_4^{5, Box} \rightarrow -\frac{1}{2u^2} \left[-s \ln^2 \frac{|t|}{s} + 2u \ln \frac{|t|}{s} \right] \implies 0 , \\
\bar{N}_3^{5, Box} &\rightarrow -\frac{2}{tu^3} \left[ts \ln^2 \frac{|t|}{s} + (t^2 - s^2) \ln \frac{|t|}{s} \right] \implies 0 , \\
\bar{N}_5^{5, Box} &\rightarrow \frac{1}{2u^2} \left[t \ln^2 \frac{|t|}{s} + 2u \ln \frac{|t|}{s} \right] \implies 0 , \\
\bar{N}_6^{5, Box} &\rightarrow -\frac{1}{tu^3} \left[t(t-s) \ln^2 \frac{|t|}{s} + 4ut \ln \frac{|t|}{s} \right] \implies 0 , \\
\bar{N}_7^{5, Box} &\rightarrow \frac{1}{2u} \ln^2 \frac{|t|}{s} \implies 0 , \\
\bar{N}_8^{5, Box} &\rightarrow -\frac{1}{tu^2} \left[t \ln^2 \frac{|t|}{s} + 2u \ln \frac{|t|}{s} \right] \implies 0 , \\
\bar{N}_9^{5, Box} &\rightarrow 0 .
\end{aligned} \tag{F.8}$$

Box type $k = 6$; $(abcd) = (SffS)$

In Section 3.4 we have separated the contribution of this box into two parts: $6A$ coming from the kinetic part of the fermion propagators and $6B$ coming from their massive part. The $k = 6B$ part asymptotically vanish like M^2/s .

$$\begin{aligned}
\bar{N}_1^{6A, Box} &= \bar{N}_2^{6A, Box} = \bar{N}_4^{6A, Box} \rightarrow 0 , \\
\bar{N}_3^{6A, Box} &\rightarrow -\frac{2}{tu} \ln \left| \frac{t}{u} \right| \implies 0 , \\
\bar{N}_5^{6A, Box} &\rightarrow \frac{1}{s} \ln \left| \frac{t}{u} \right| \implies 0 ,
\end{aligned} \tag{F.9}$$

$$\begin{aligned}
\bar{N}_6^{6A, Box} &\rightarrow -\frac{2}{stu} \left[t \ln \left| \frac{t}{u} \right| \right] \quad \Rightarrow 0 \ , \\
\bar{N}_7^{6A, Box} &\rightarrow -\frac{1}{s} \ln \left| \frac{t}{u} \right| \quad \Rightarrow 0 \ , \\
\bar{N}_8^{6A, Box} &\rightarrow -\frac{2}{stu} \left[u \ln \left| \frac{t}{u} \right| \right] \quad \Rightarrow 0 \ , \\
\bar{N}_9^{6A, Box} &\rightarrow 0 \ .
\end{aligned}
\tag{F.10}$$

References

- [1] Opportunities and Requirements for Experimentation at a Very High Energy e^+e^- Collider, SLAC-329(1928); Proc. Workshops on Japan Linear Collider, KEK Reports, 90-2, 91-10 and 92-16; P.M. Zerwas, DESY 93-112, Aug. 1993; Proc. of the Workshop on e^+e^- Collisions at 500 GeV: The Physics Potential, DESY 92-123A,B,(1992), C(1993), D(1994), E(1997) ed. P. Zerwas; E. Accomando *et.al.* Phys. Rep. **C299**,1 (1998).
- [2] ” The CLIC study of a multi-TeV e^+e^- linear collider”, CERN-PS-99-005-LP (1999).
- [3] G.J. Gounaris, P.I. Porfyriadis and F.M. Renard, hep-ph/9909243, Eur. Phys. J. **C13**,79 (2000); G.J. Gounaris, J. Layssac, P.I. Porfyriadis and F.M. Renard, hep-ph/9904450, Eur. Phys. J. **C10**,499 (1999); G.J. Gounaris, P.I. Porfyriadis and F.M. Renard, hep-ph/9902230, Eur. Phys. J. **C9**,673 (1999).
- [4] V. V. Sudakov, Sov. Phys. JETP 3, 65 (1956); Landau-Lifshits: Relativistic Quantum Field theory IV tome (MIR, Moscow) 1972.
- [5] M. Kuroda, G. Moultaqa and D. Schildknecht, Nucl. Phys. **B350**,25 (1991); G.Degrassi and A Sirlin, Phys. Rev. **D46**,3104 (1992); W. Beenakker et al, Nucl. Phys. **B410**, 245 (1993), Phys. Lett. **B317**, 622 (1993); A. Denner, S. Dittmaier and R. Schuster, Nucl. Phys. **B452**, 80 (1995); A. Denner, S. Dittmaier and T. Hahn, Phys. Rev. **D56**, 117 (1997); P. Ciafaloni and D. Comelli, Phys. Lett. **B446**, 278 (1999).
- [6] M. Beccaria, P. Ciafaloni, D. Comelli, F. Renard, C. Verzegnassi, Phys.Rev. **D 61**, 073005 (2000); Phys.Rev. **D 61**, 011301 (2000) %
- [7] A. Denner, S. Pozzorini, Eur. Phys. J. **C18**,461 (2001); Eur. Phys. J. **C21**,63 (2001), hep-ph/0010201.
- [8] M. Beccaria, F.M. Renard and C. Verzegnassi, Phys. Rev. **D63**, 095010 (2001); Phys.Rev.**D63**, 053013 (2001).
- [9] M. Beccaria, M. Melles, F.M. Renard and C. Verzegnassi, Phys.Rev.**D65**, 093007 (2002).
- [10] M. Ciafaloni, P. Ciafaloni and D. Comelli, Nucl. Phys. **B589**, 4810 (2000); V. S. Fadin, L. N. Lipatov, A. D. Martin and M. Melles, Phys. Rev. **D61**, 094002 (2000); J. H. Kühn, A. A. Penin and V. A. Smirnov, Eur. Phys. J **C17**, 97 (2000); M. Melles, hep-ph/0104232; J. H. Kühn, S. Moch, A. A. Penin and V. A. Smirnov, Nucl. Phys. **B616**, 286 (2001). M. Melles, PSI-PR-01-11, Aug 2001, hep-ph/0108221. M. Melles Phys. Rev. **D63**, 034003 (2001); Phys. Rev. **D64**, 014011 (2001), Phys. Rev. **D64**, 054003 (2001). M. Melles, Phys. Lett. **B495**, 81 (2000); W. Beenakker, A. Werthenbach, Phys. Lett. **B489**, 148 (2000); hep-ph/0112030; M. Hori, H. Kawamura and J. Kodaira, Phys. Lett. **B491**, 275 (2000).

- [11] M. Beccaria, F.M. Renard and C. Verzegnassi, Phys.Rev.**D64**, 073008 (2001).
- [12] M. Beccaria, F.M. Renard and C. Verzegnassi, hep-ph/0203254.
- [13] J. Layssac and F.M. Renard, Phys.Rev.**D 64**,053018 (2001).
- [14] I.F. Ginzburg, G.L. Kotkin, V.G. Serbo and V.I. Telnov, Nucl. Instr. and Meth. **205**, 47 (1983); I.F. Ginzburg, G.L. Kotkin, V.G. Serbo, S.L. Panfil and V.I. Telnov, Nucl. Instr. and Meth. **219**,5 (1984); J.H. Kühn, E.Mirkes and J. Steegborn, Zeit.f.Phys.bf C57,615(1993). V. Telnov, hep-ex/0003024, hep-ex/0001029, hep-ex/9802003, hep-ex/9805002, hep-ex/9908005; I.F. Ginzburg, hep-ph/9907549; R. Brinkman hep-ex/9707017. V. Telnov, talk at the International Workshop on High Energy Photon Colliders, <http://www.desy.de/gg2000>, June 14-17, 2000, DESY Hamburg, Germany, to appear in Nucl.Instr. & Meth. A.; D.S. Gorbunov, V.A. Illyn, V.I. Telnov, hep-ph/0012175.
- [15] M. Bohm, T. Sack, Z. f. Phys. **C33**,157 (1986); M. Bohm, T. Sack, Z. f. Phys. **C35**,119 (1987); A. Denner, T. Sack, Nucl. Phys. **B306**,221 (1988).
- [16] K. Hagiwara, R.D. Peccei and D. Zeppenfeld, Nucl. Phys. **B282**,253 (1987); G.J. Gounaris, J. Layssac and F.M. Renard, Phys. Rev. **D61**,073013 (2000).
- [17] G.J. Gounaris, J. Layssac and F.M. Renard, Phys. Rev. **D62**,073013 (2000); Phys. Rev. **D62**,073012 (2000); D. Choudhury, S. Dutta, S. Rakshit and S. Rindani, Int. J. Mod. Phys. **A16**,4891 (2001), hep-ph/0011205.
- [18] ALEPH, DELPHI, L3, OPAL, LEP Electroweak Working Group and SLD Heavy Flavor and Electroweak Groups (D. Abbaneo et al.), hep-ex/0112021; P. Bambade et al, "Study of Trilinear Gauge Boson Couplings ZZZ , $ZZ\gamma$ and $Z\gamma\gamma$ ", DELPHI 2001-097 CONF 525, contributed to EPS HEP 2001 Conference in Budapest; L3 (M. Acciarri et al.), Phys. Lett. **B497**,23 (2001), hep-ex/0010004; J. Alcaraz Phys. Rev. **D65**,075020 (2002), hep-ph/0111283.
- [19] See *e.g.* W. Hollik, in "Precision Tests of the Standard Electroweak Model", edited by P. Langacker (1993) p.37; MPI-Ph-93-021, BI-TP-93-16.
- [20] G. Passarino and M. Veltman, Nucl. Phys. **B160**,151 (1979).
- [21] G.J. van Oldenborgh and J.A.M. Vermaseren, Z. f. Phys. **C46**,1990 (425); G.J. van Oldenborgh "FF: A package to evaluate one loop Feynman diagrams" Comput. Phys. Commun. **66**,, (1)1991.
- [22] M. Battaglia, A. De Roeck, J. Ellis, F. Giannotti, K.T. Matchev, K.A. Olive, L. Pape and G. Wilson, hep-ph/01006204; S. P. Martin, <http://zippy.physics.niu.edu/modellines.html>; S. P. Martin, S. Moretti, J. Qian and G. W. Wilson, Snowmass P3-46.

- [23] "The Snowmass Points and Slopes", B.C. Allanach *et.al.* , hep-ph/0202233.
- [24] J. Rosiek, Phys. Rev. **D41**,3464 (1990), hep-ph/9511250 (E).
- [25] G.J. Gounaris C. Le Mouél and P.I. Porfyriadis, hep-ph/0107249, to appear in Phys. Rev. D.
- [26] M.M. El Kheishen, A.A. Shafik and A.A. Aboshousha, Phys. Rev. **D45**,4345 (1992); V. Barger, M.S. Berger and P. Ohman, Phys. Rev. **D49**,4908 (1994).
- [27] C. Jarlskog, Phys. Rev. **D36**,2128 (1987); C. Jarlskog, Z. f. Phys. **C29**,491 (1985); C. Jarlskog, Stockhol Report USIP 87-14.
- [28] G.J. Gounaris, P.I. Porfyriadis and F.M. Renard, hep-ph/0010006, Eur. Phys. J. **C19**,57 (2001).
- [29] M. Roth and A. Denner, Nucl. Phys. **B479**,495 (1996)

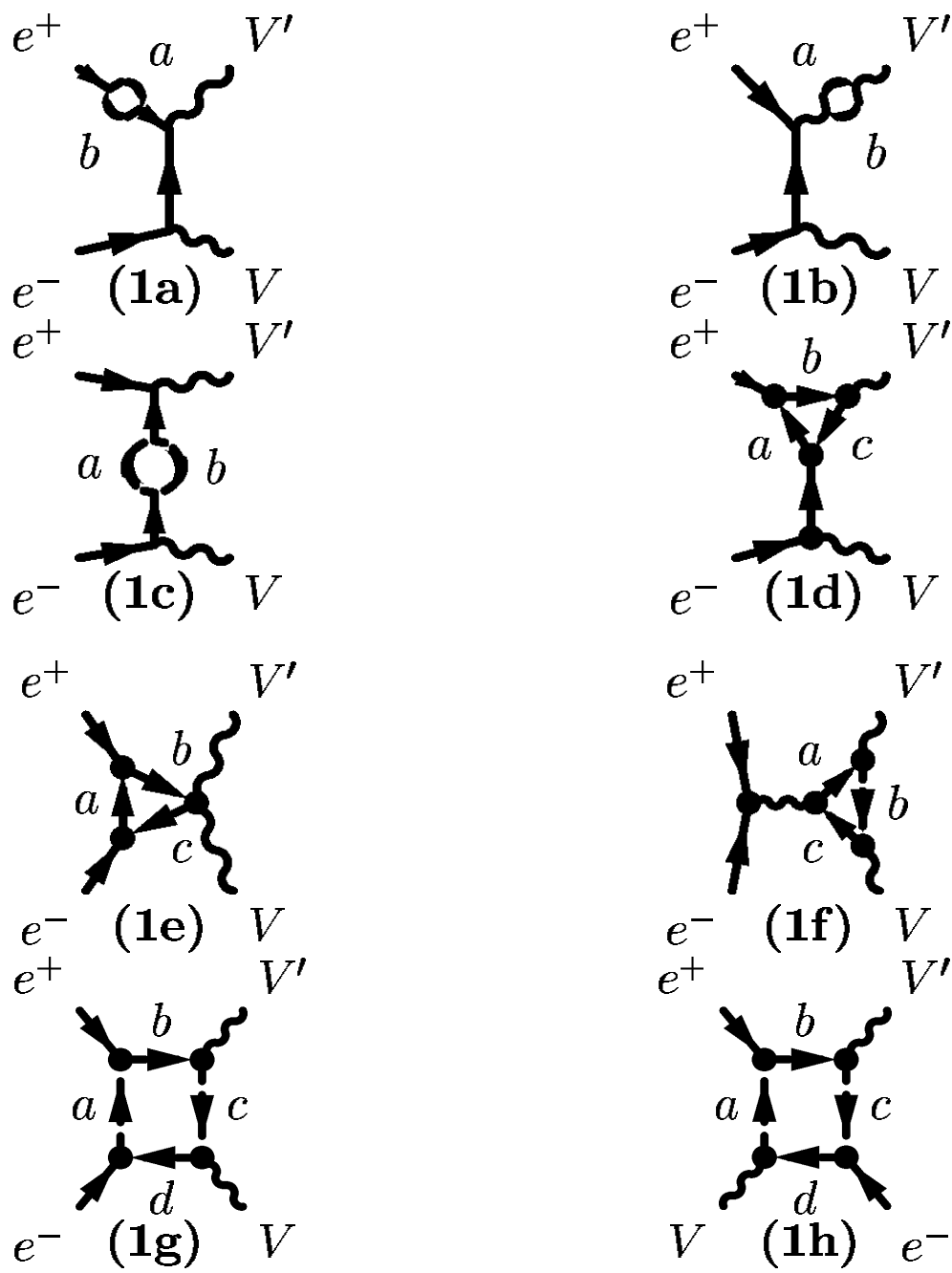


Figure 1: Diagrams at one loop

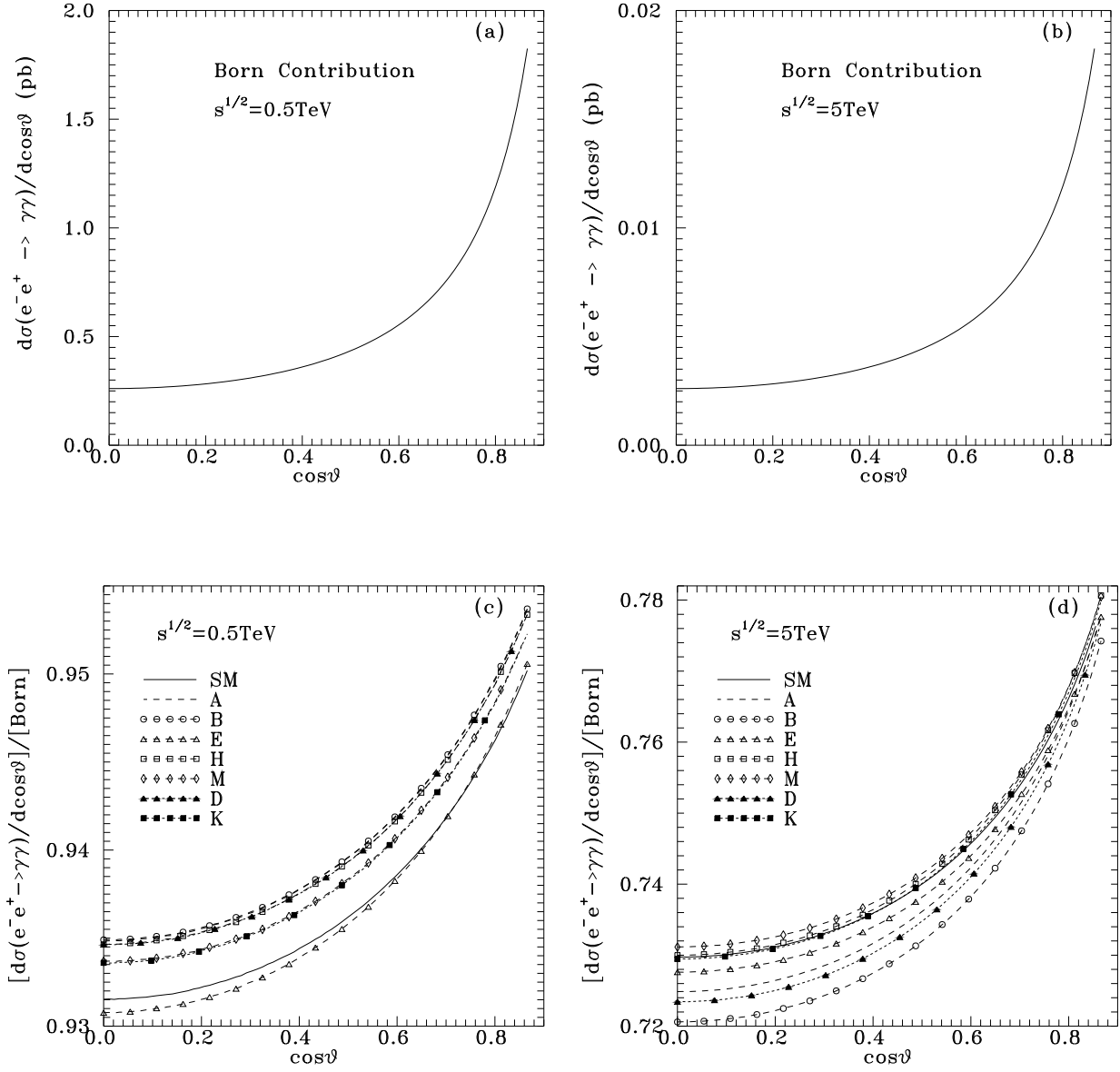


Figure 2: The unpolarized differential cross section for $e^-e^+ \rightarrow \gamma\gamma$. In (a) and (b) the Born contributions are given at 0.5TeV and 5TeV respectively; while in (c) and (d) the radiative corrections to them are respectively indicated for SM and a representative subset of the benchmark MSSM models of [22].

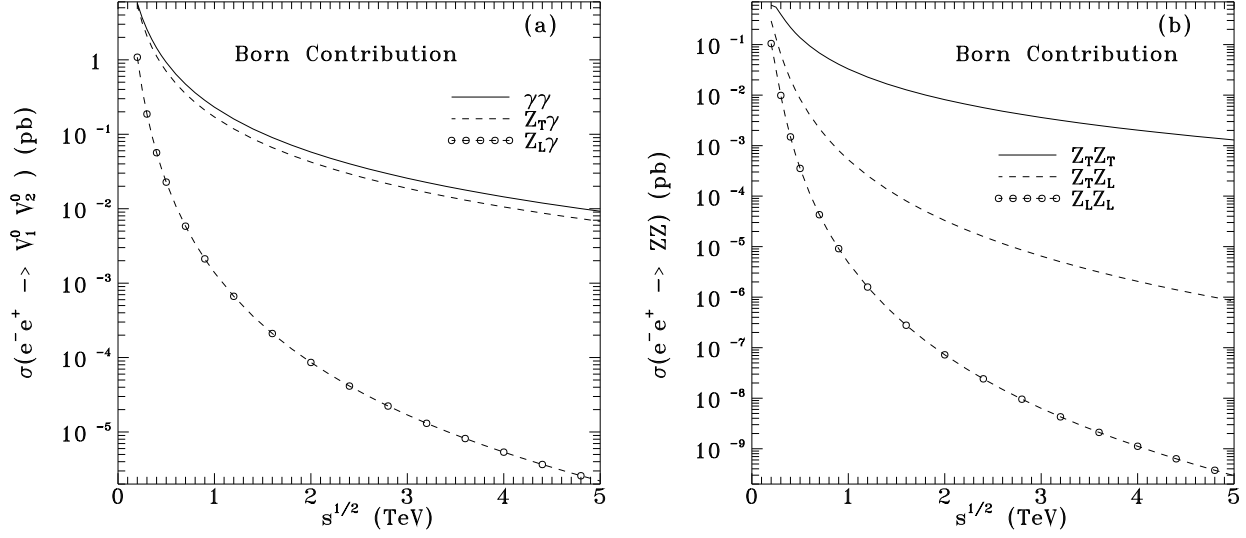


Figure 3: The integrated Born cross section in the region $30^\circ < \theta < 150^\circ$, for $e^-e^+ \rightarrow \gamma\gamma$, $Z\gamma$ (a) and $e^-e^+ \rightarrow ZZ$ (b), with transverse or longitudinal Z -states, as a function of the energy.

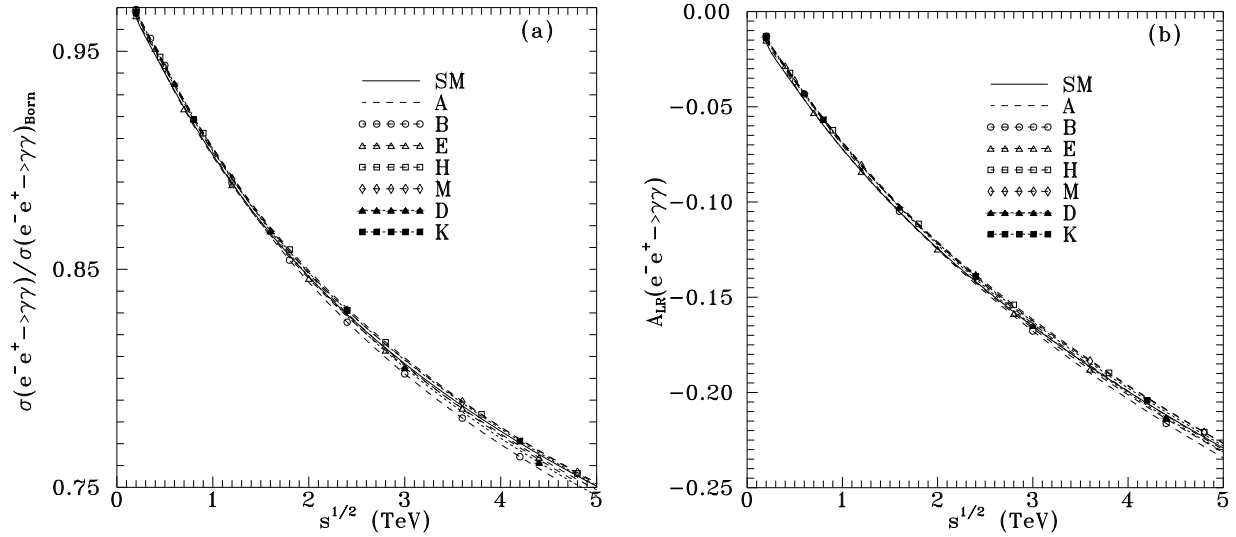


Figure 4: The ratio of the unpolarized integrated $\sigma(e^-e^+ \rightarrow \gamma\gamma)$ cross section to the Born cross section (a), and the A_{LR} asymmetry (b), as a function of the energy, for SM and a representative subset of the benchmark MSSM models of [22].

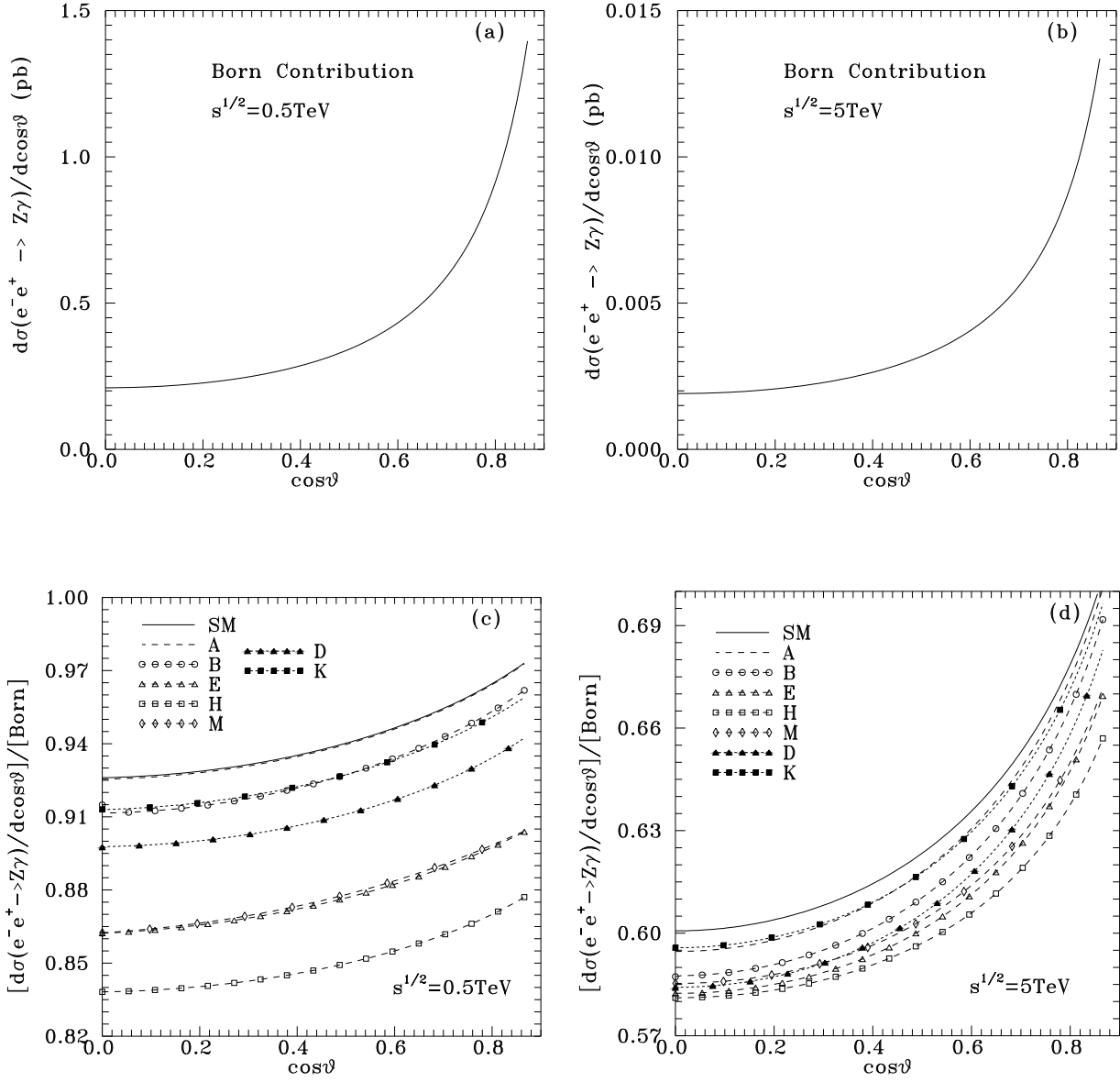


Figure 5: The unpolarized differential cross section for $e^-e^+ \rightarrow Z\gamma$. In (a) and (b) the Born contribution at 0.5TeV and 5TeV respectively are given; while in (c) and (d) the radiative corrections to it are respectively indicated for SM and a representative subset of the benchmark MSSM models of [22].

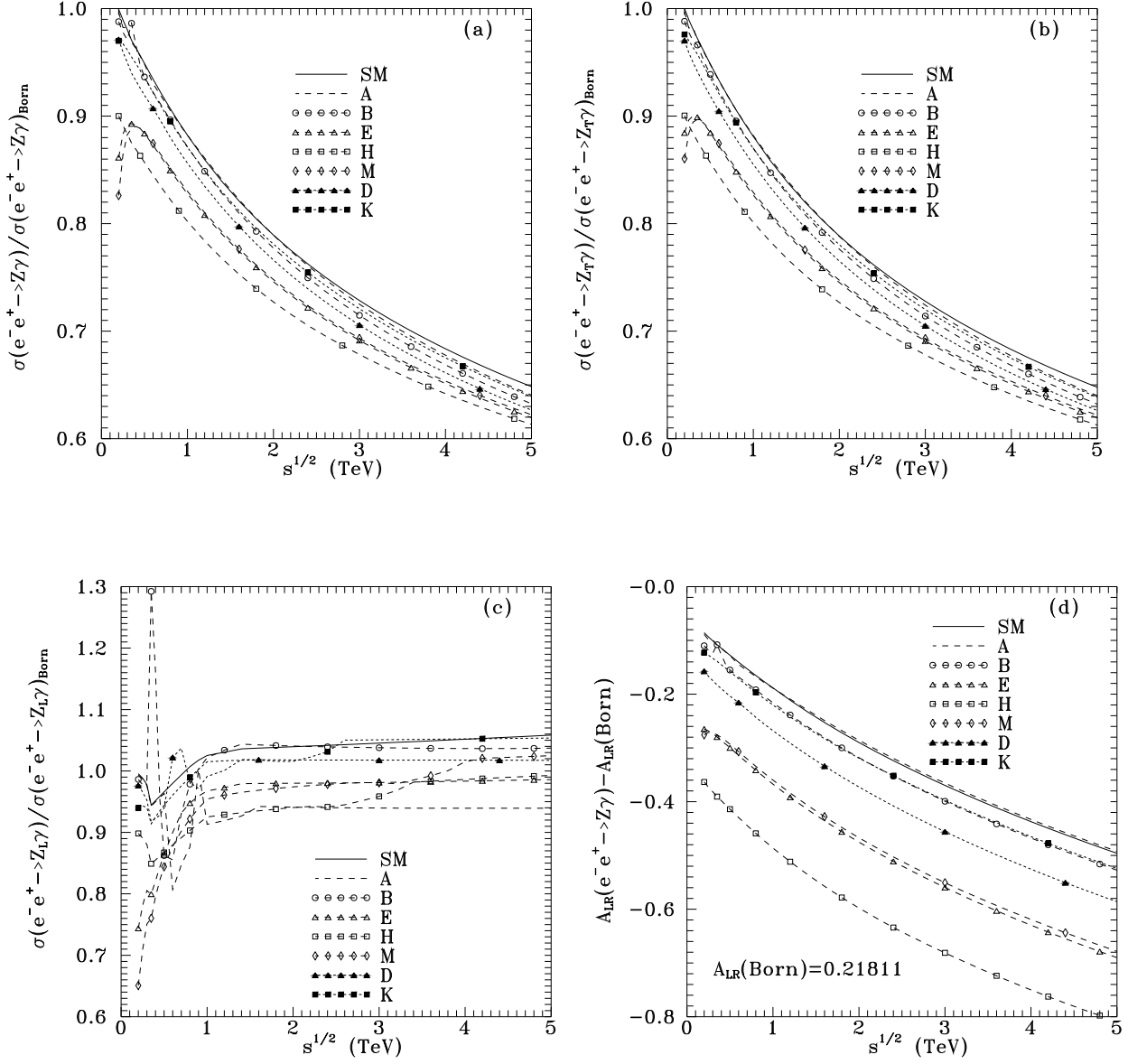


Figure 6: The radiative corrections to the integrated $\sigma(e^-e^+ \rightarrow Z\gamma)$ cross section, for unpolarized Z (a), transverse Z (b), or longitudinal Z (c) states, as a function of the energy for SM and a set MSSM models of [22]. In (d) the radiative correction to the A_{LR} asymmetry, (where all final gauge polarizations are summed over), is also given.

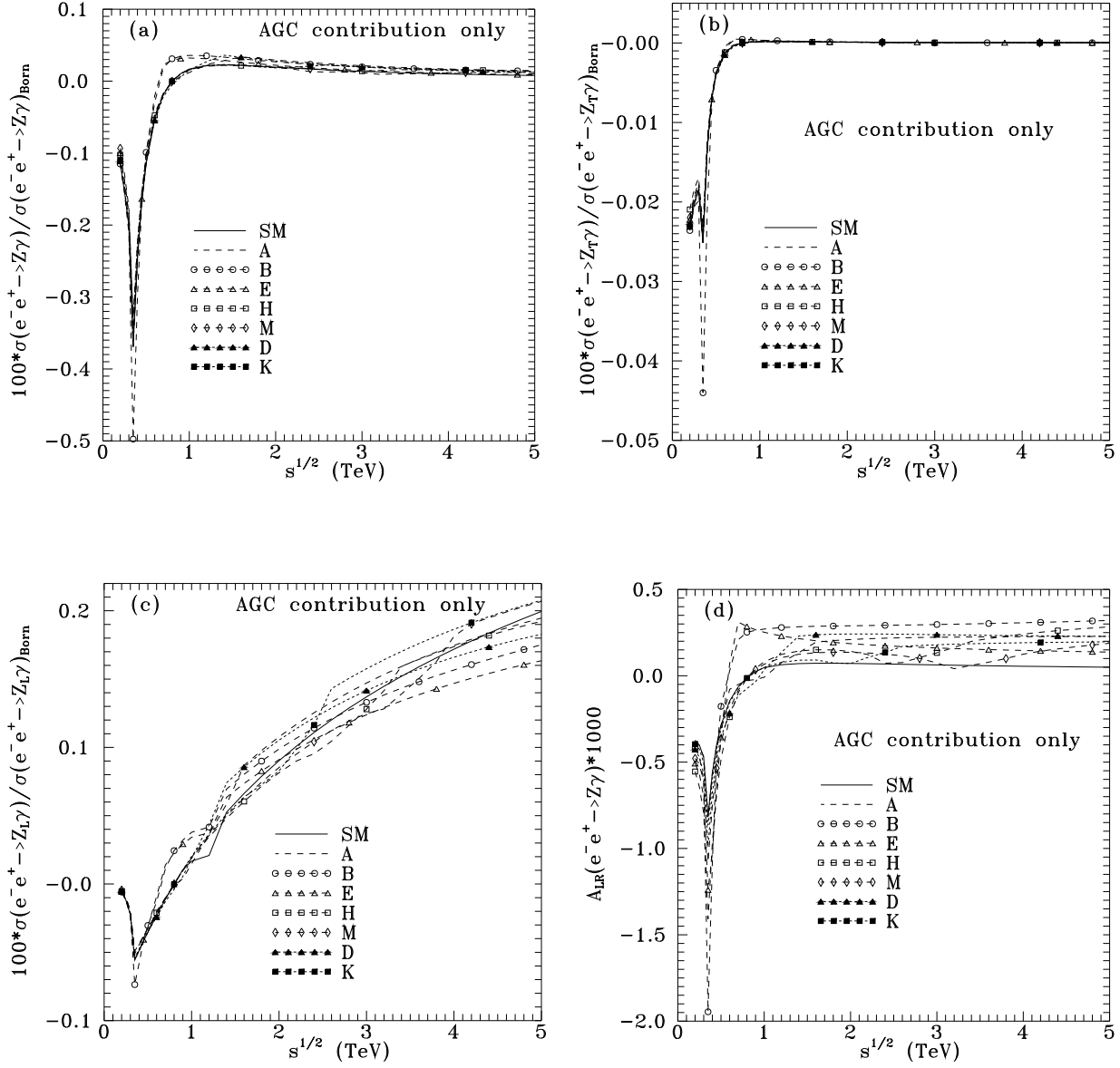


Figure 7: NAGC contributions to the unpolarized (a), TT (b), LT (c) $e^+e^- \rightarrow Z\gamma$ cross sections, and to the A_{LR} asymmetry (d), as a function of the energy.

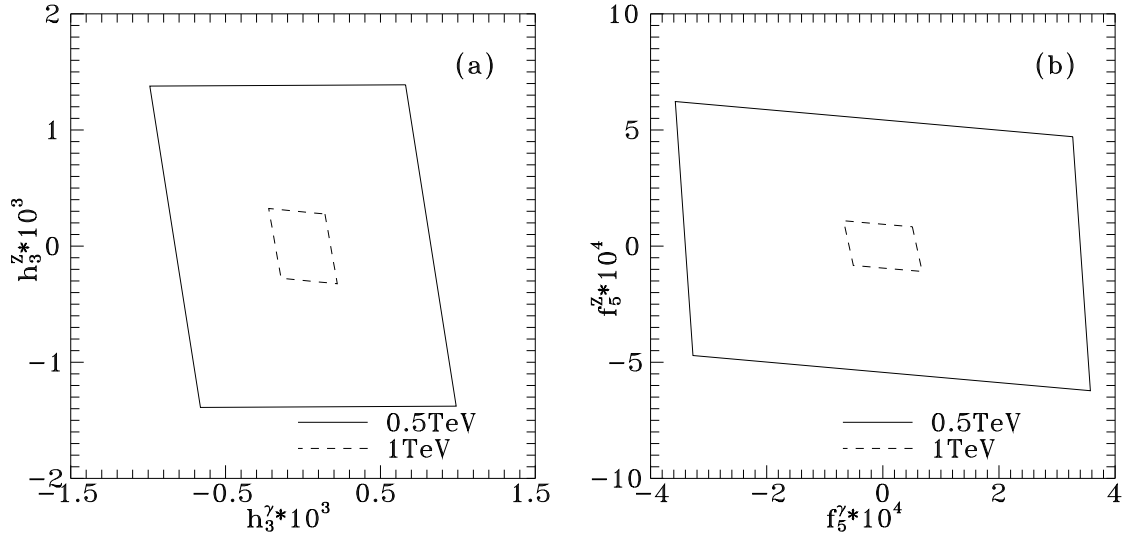


Figure 8: The NAGC limits obtained from σ_{unp} and A_{LR} in the $e^+e^- \rightarrow Z\gamma$ process (a), and in the $e^+e^- \rightarrow ZZ$ process (b), assuming an accuracy of 1% on these observables.

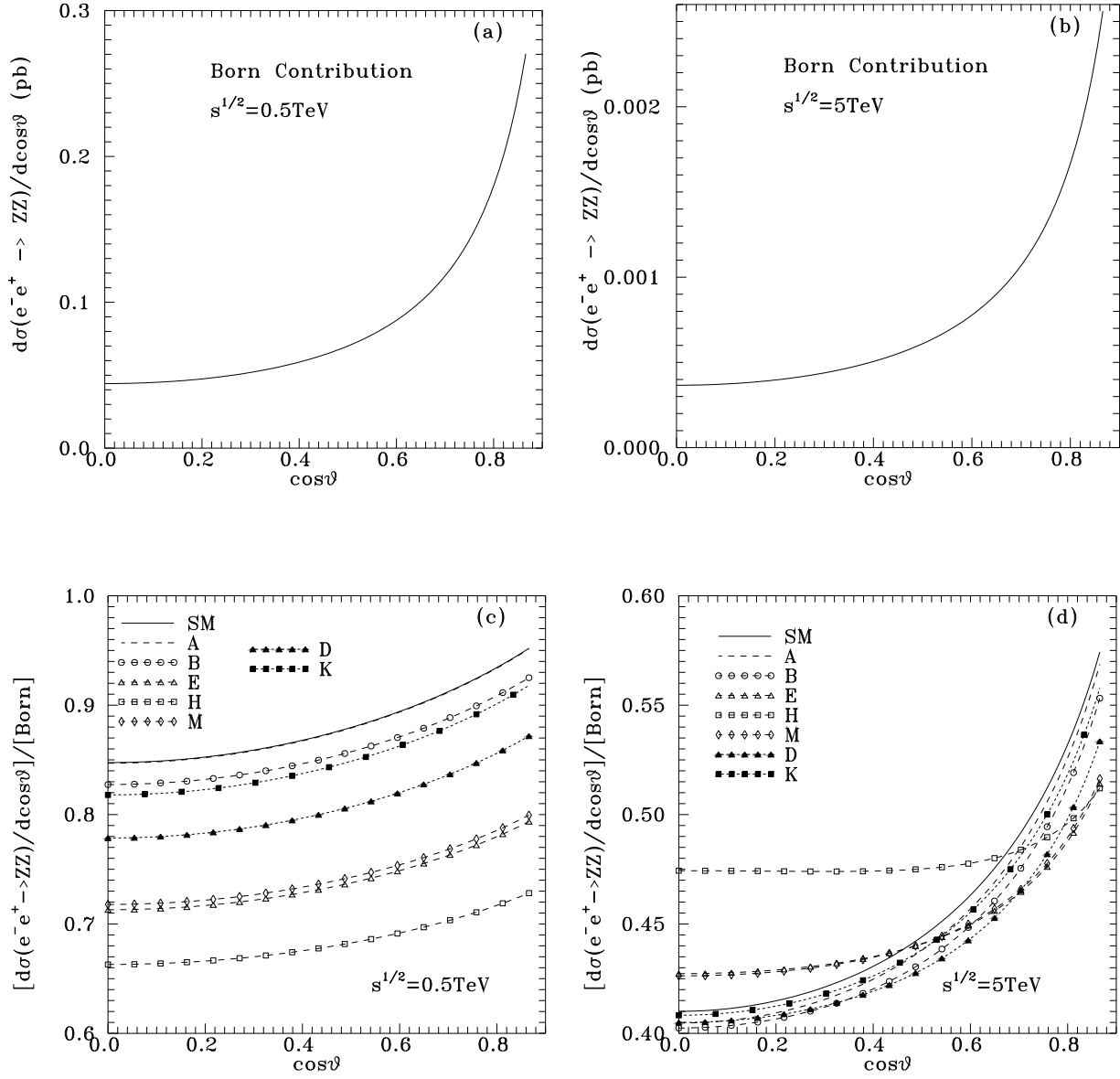


Figure 9: The unpolarized differential cross section for $e^-e^+ \rightarrow ZZ$. In (a) and (b) the Born contribution at 0.5TeV and 5TeV respectively are given; while in (c) and (d) the radiative corrections to it are respectively indicated for SM and a representative subset of the benchmark MSSM models of [22].

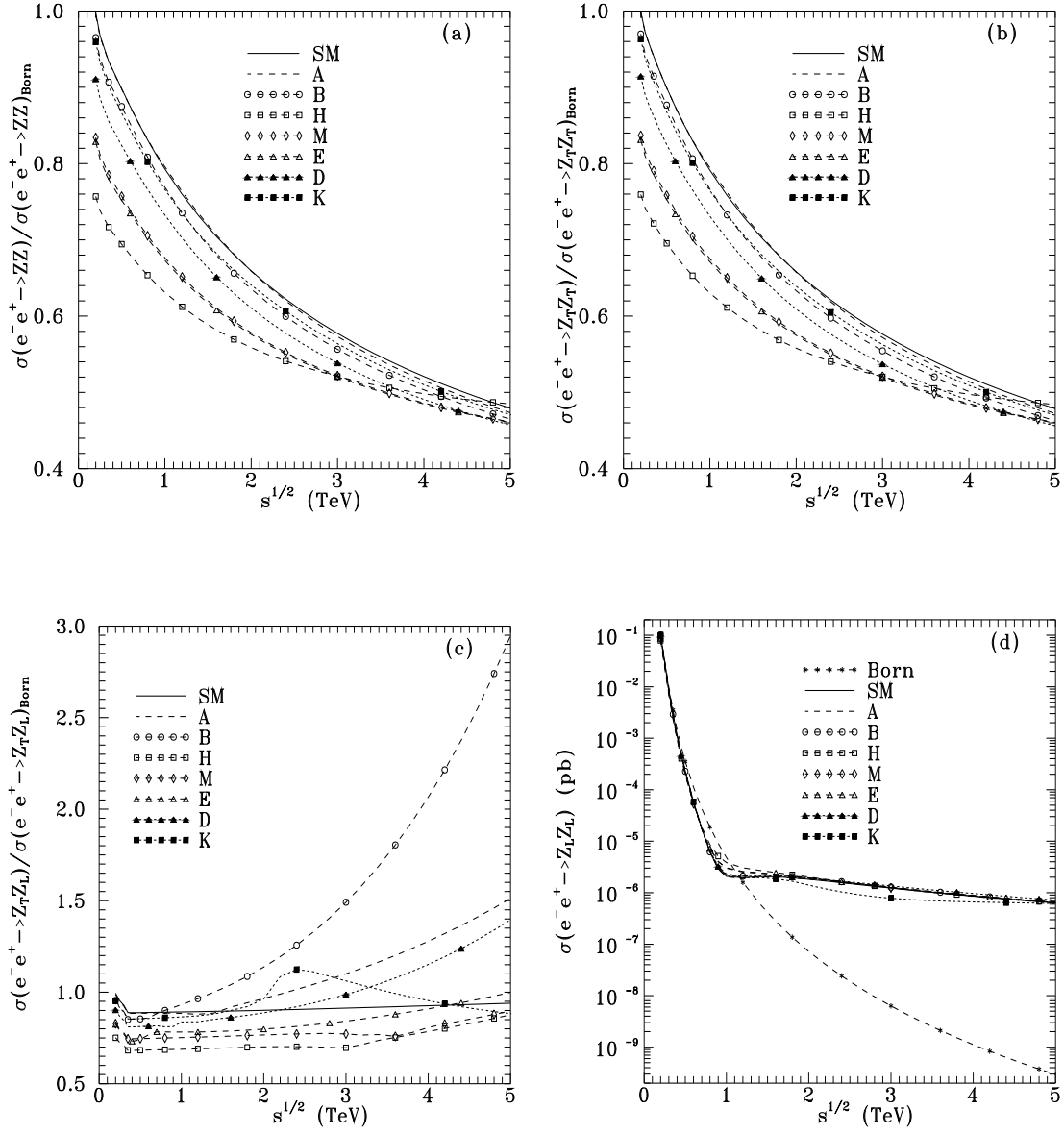


Figure 10: The ratio integrated $\sigma(e^-e^+ \rightarrow ZZ)$ to the Born cross section, for unpolarized ZZ (a), transverse $Z_T Z_T$ (b), $Z_T Z_L$ (c) final states, and the $\sigma(e^-e^+ \rightarrow Z_L Z_L)$ cross section (d) as a function of the energy. The results correspond to SM, and a representative subset of the benchmark MSSM models of [22].

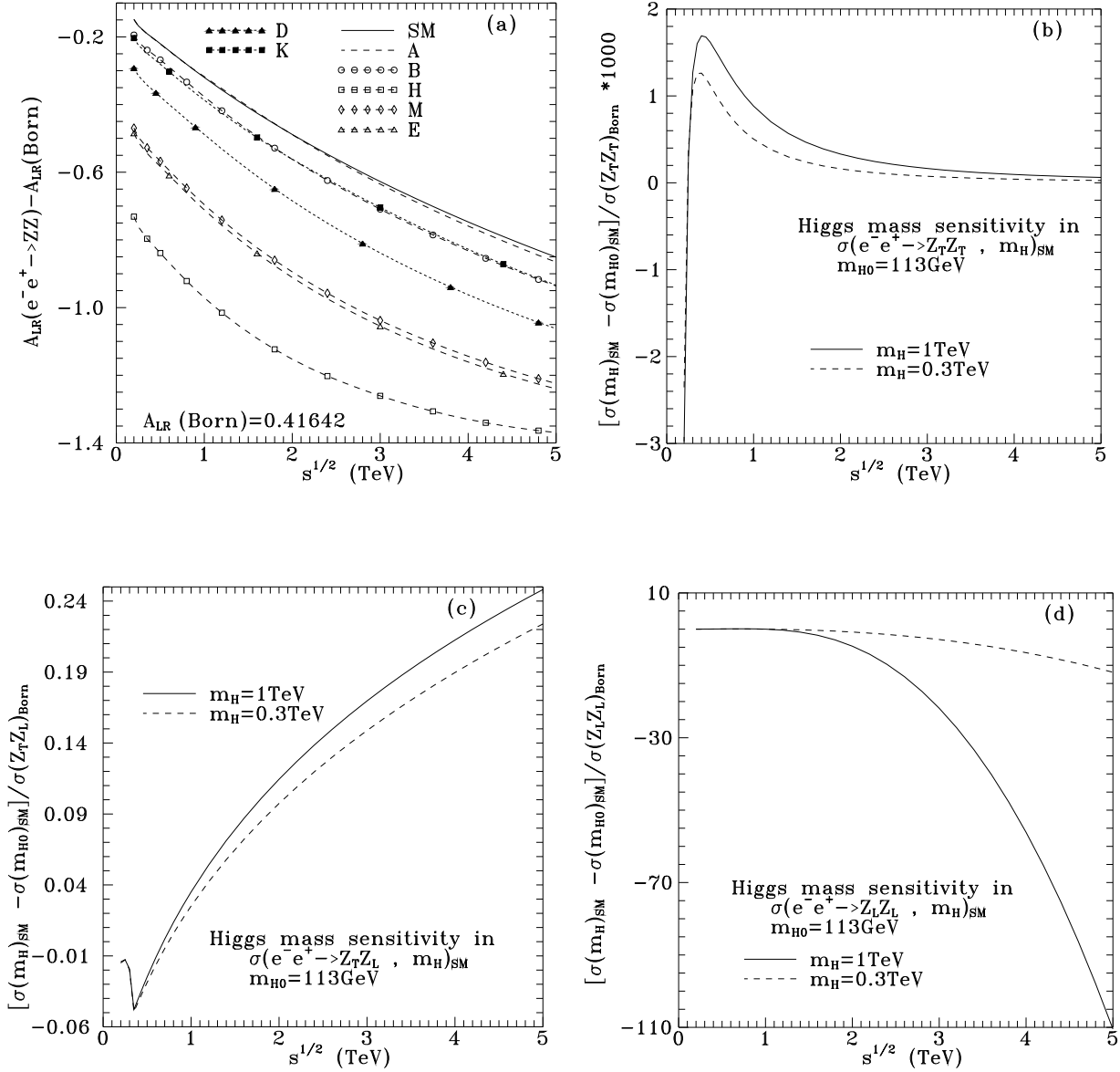


Figure 11: the A_{LR} asymmetry in $e^+e^- \rightarrow ZZ$ (a) and the Higgs box contribution to the TT (b), TL (c) and LL (d) $e^+e^- \rightarrow ZZ$ cross sections as a function of the energy.

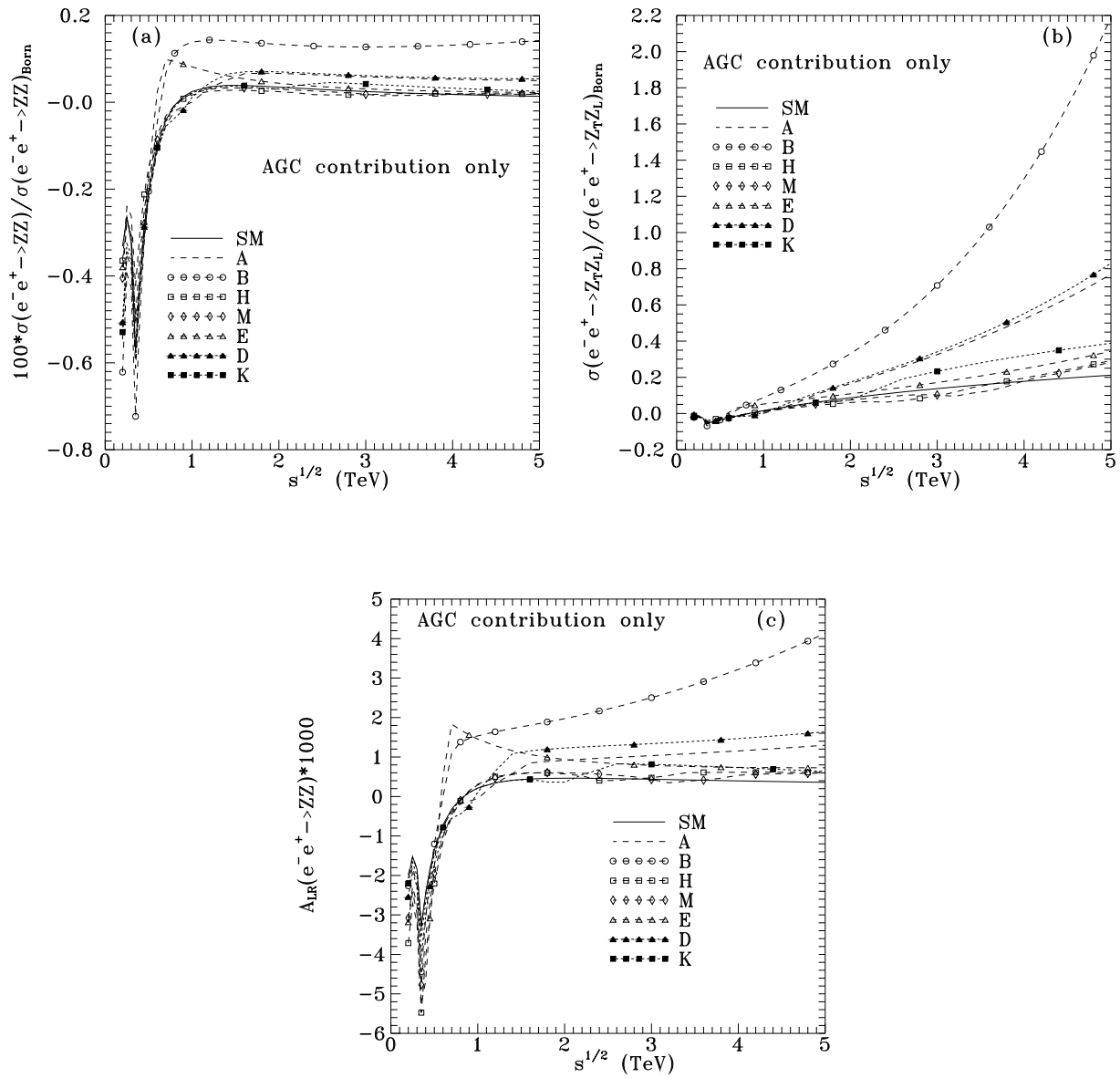


Figure 12: NAGC contributions to the unpolarized (a) and TL $e^+e^- \rightarrow ZZ$ cross sections (b), and to the A_{LR} asymmetry (c), as a function of the energy.